Nitrogen deposition and exceedances of critical loads for nitrogen in Switzerland 1990–2020

Commissioned by: Federal Office for the Environment (FOEN)

Meteotest AG
Fabrikstrasse 14
3012 Bern, Switzerland
+41 31 307 26 26
+41 31 307 26 10
office@meteotest.ch
www.meteotest.ch

Imprint

Commissioned by	Federal Office for the Environment FOEN Air Pollution Control and Chemicals Division CH-3003 Bern The FOEN is an agency of the Federal Department of the Environment, Transport, Energy and Communications (DETEC).
Contractor	Meteotest AG, Fabrikstrasse 14, CH-3012 Bern
Authors	Beat Rihm, Thomas Künzle
FOEN support	Reto Meier
Note	This report was prepared under contract to the Federal Office for the Environment (FOEN). The contractor bears sole responsibility for the content.

Bern, 13.04.2023

Summary

This report presents methods, input data and results related to atmospheric nitrogen deposition and the exceedances of critical loads for nitrogen (CLN) for the year 2020. It is an update of the reports by Rihm & Achermann 2016 and Rihm & Künzle 2019. Depositions and exceedances for the years 1990, 2000, 2005, 2010 and 2015 were also recalculated as far as improved data and methods were available.

Critical loads for nitrogen are defined as those nitrogen depositions below which harmful effects on specified sensitive receptors of the environment do not occur according to present scientific knowledge. They have been developed in the framework of the UNECE Convention on Long-Range Transboundary Air Pollution.

For Switzerland, critical loads of nitrogen were computed using two methods proposed by the Convention: (1) the simple (steady state) mass balance method (SMB) for forests; and (2) the empirical method for natural and semi-natural ecosystems such as raised bogs, fens, dry or species-rich grassland, mountain hay meadows, (sub)alpine grassland, alpine scrub habitats and alpine lakes.

The SMB balances the atmospheric depositions against the natural long-term processes that permanently immobilise nitrogen or remove it from the (eco-)system. The SMB was applied on a 1x1 km^2 grid, with 10'632 points representing productive forests, i.e. sites where harvesting is possible.

The empirical method is based on results from scientific field studies including nitrogen addition experiments, mesocosm studies, observational studies along nitrogen deposition gradients, but also on expert judgement. Swiss critical load maps were produced by assigning ecosystem specific values to national ecosystems inventories, aggregated to a 1x1 km^2 raster with a total area of 17'532 km^2 containing sensitive ecosystems.

Nitrogen deposition was mapped using a pragmatic approach that combines emission inventories, statistical dispersion models, monitoring data, spatial interpolation methods and inferential deposition models. The following compounds were considered: wet and dry deposition of nitrate (NO_3^-) and ammonium (NH_4^+) as well as gaseous deposition of ammonia (NH_3), nitrogen dioxide (NO_2) and nitric acid (HNO_3).

The resulting critical loads of nitrogen show a variation of 4 to 25 kg N ha^{-1} a^{-1}, depending on ecosystem type, soil type, altitude and other ecosystem properties. Nitrogen depositions in 2020 were in the range of 2 to 65 kg N ha^{-1} a^{-1}, the highest values occurring in the lowlands. The total deposition in Switzerland amounts to 59 kt N a^{-1} (41 kt N a^{-1} of reduced nitrogen plus 18 kt N a^{-1} of oxidised nitrogen). From 1990 to 2020 the total deposition of nitrogen compounds decreased by 26%.

At 87% of the forest sites the critical loads of nitrogen are exceeded in 2020 (Figure-S1). The critical loads for (semi-)natural ecosystems derived by the empirical method and aggregated to the 1x1 km^2 raster are exceeded on 54% of the total sensitive area. A more detailed analysis on a 100x100 m^2 raster was made for the Swiss nature reserves; Figure-S1 shows the resulting exceedances for the protected areas of raised bogs (94% of area exceeded), fens (74% of area exceeded) and species rich dry grassland TWW (42% of area exceeded).

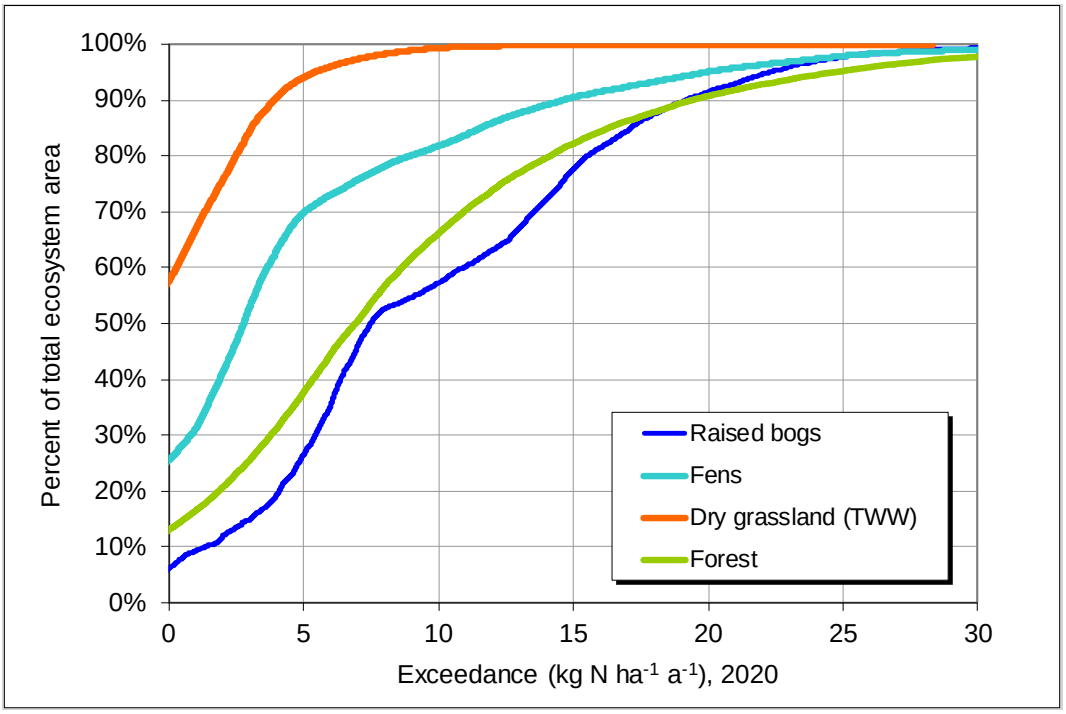

Figure-S1: Cumulative frequency distribution of the exceedances of critical loads of nutrient nitrogen for different protected ecosystems. Units: percent of total ecosystem area. Nitrogen deposition: year 2020.

Résumé

Ce rapport présente les méthodes, les données d'entrée et les résultats relatifs aux dépôts atmosphériques de composés azotés et aux dépassements des charges critiques de l'azote (CLN) pour l'année 2020. Il s'agit d'une mise à jour des rapports antérieurs de Rihm & Achermann 2016 et Rihm & Künzle 2019. Les dépôts et les dépassements pour les années 1990, 2000, 2005, 2010 et 2015 ont été recalculés dans la mesure où des données et des méthodes améliorées étaient disponibles.

Les charges critiques pour l'azote sont définies comme les dépôts d'azote en dessous desquels il n'y a pas d'effets nocifs sur des récepteurs sensibles de l'environnement, selon les connaissances scientifiques actuelles. Elles ont été élaborées dans le cadre de la Convention de la CEE-ONU sur la pollution atmosphérique transfrontière à longue distance.

Pour la Suisse, les charges critiques de l'azote ont été calculées à l'aide de deux méthodes proposées par la Convention : (1) la méthode du bilan massique simple (Simple (steady state) Mass Balance, SMB) pour les forêts ; et (2) la méthode empirique pour les écosystèmes naturels et semi-naturels tels que les tourbières, les marais, les prairies sèches ou riches en espèces, les prairies de fauche de montagne, les prairies (sub)alpines, les habitats de buissons alpins et les lacs alpins.

Le SMB équilibre les dépôts atmosphériques avec les processus naturels à long terme qui immobilisent de manière permanente l'azote ou l'éliminent du système (écologique). Le SMB a été appliqué sur une grille de 1x1 km^2, avec 10'632 points représentant des forêts productives, c'est-à-dire des sites où l'exploitation est possible.

La méthode empirique est basée sur les résultats d'études scientifiques de terrain, y compris des expériences d'ajouts d'azote, des études en mésocosme, des études d'observation le long des gradients de dépôt d'azote, mais aussi sur l'avis d'experts. Les cartes suisses des charges critiques ont été produites en attribuant des valeurs spécifiques aux écosystèmes des inventaires nationaux d'écosystèmes, agrégés sur une trame de 1x1 km^2 avec une surface totale de 17'532 km^2 contenant des écosystèmes sensibles.

Les dépôts d'azote sont cartographiés à l'aide d'une approche pragmatique combinant des inventaires d'émissions, des modèles de dispersion statistique, des données de surveillance, des méthodes d'interpolation spatiale et des modèles inférentiels de dépôt. Les composés suivants ont été pris en compte : les dépôts humides et secs de nitrate (NO_3^-) et d'ammonium (NH_4^+), ainsi que les dépôts gazeux d'ammoniac (NH_3), de dioxyde d'azote (NO_2) et d'acide nitrique (HNO_3).

Les charges critiques d'azote qui en résultent varient de 4 à 25 kg N ha^{-1} a^{-1}, en fonction du type d'écosystème, du type de sol, de l'altitude et d'autres propriétés de l'écosystème. En 2020, les dépôts d'azote étaient compris entre 2 et 65 kg N ha^{-1} a^{-1}, les valeurs les plus élevées étant observées en plaine. Les dépôts totaux en Suisse s'élèvent à 59 kt N a^{-1} (41 kt N a^{-1} sous forme d'azote réduit et 18 kt N

a^{-1} sous forme d'azote oxydé). Entre 1990 et 2020, les dépôts totaux de composés azotés ont diminué de 26%.

Dans 87% des sites forestiers, les charges critiques d'azote sont dépassées en 2020 (figure-S1). Les charges critiques pour les écosystèmes (semi-)naturels dérivées par la méthode empirique et agrégées à la trame de 1x1 km^2 sont dépassées sur 54% de la zone sensible totale. Une analyse plus détaillée sur une grille de 100x100 m^2 a été effectuée pour les réserves naturelles suisses ; la figure-S1 montre les dépassements qui en résultent pour les zones protégées de tourbières hautes (94% de la superficie dépassée), de tourbières basses (74% de la superficie dépassée) et de prairies sèches riches en espèces TWW (42% de la superficie dépassée).

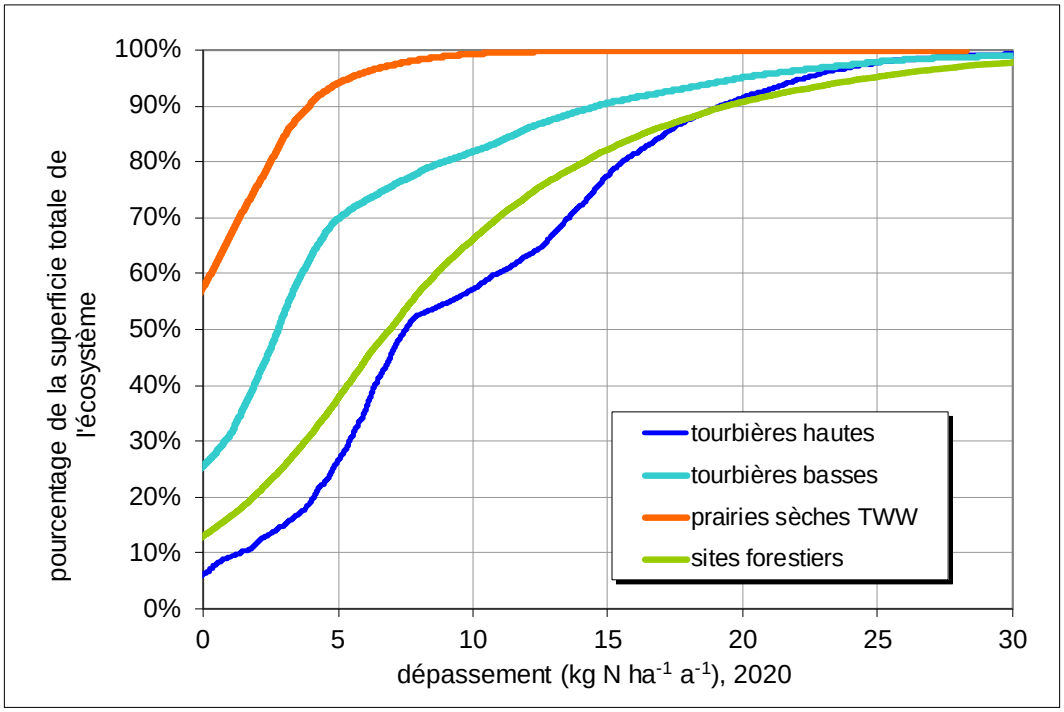

Figure-S1: Distribution de la fréquence cumulée des dépassements des charges critiques d'azote nutritif pour différents écosystèmes protégés. Unités : pourcentage de la superficie totale de l'écosystème. Dépôt d'azote: année 2020.

Zusammenfassung

Dieser Bericht beschreibt Methoden, Inputdaten und Ergebnisse in Bezug auf die atmosphärische Stickstoffdeposition und die Überschreitung der Critical Loads für Stickstoff (CLN) für das Jahr 2020. Er ist eine Aktualisierung der Berichte von Rihm & Achermann 2016 und Rihm & Künzle 2019. Die Einträge und Überschreitungen für die Jahre 1990, 2000, 2005, 2010 und 2015 wurden ebenfalls neu berechnet, soweit verbesserte Daten und Methoden verfügbar waren.

Critical Loads für Stickstoff sind definiert als jene Stickstoffdeposition, unterhalb derer nach heutigem Stand des Wissens keine schädlichen Wirkungen auf empfindliche Rezeptoren der Umwelt auftreten. Sie wurden im Rahmen des UNECE-Übereinkommens über weiträumige grenzüberschreitende Luftverunreinigung entwickelt.

Für die Schweiz wurden die kritischen Stickstofffrachten mit zwei von dieser Konvention vorgeschlagenen Methoden berechnet: (1) die einfache (stationäre) Massenbilanzmethode (SMB) für Wälder und (2) die empirische Methode für natürliche und naturnahe Ökosysteme wie Hochmoore, Flachmoore, Trockenwiesen und -weiden, montane Heuwiesen, (sub)alpines Grünland, alpine Zwergstrauchheiden und alpine Seen.

Die SMB geht von einem Gleichgewicht zwischen den atmosphärischen Einträgen und den natürlichen langfristigen Prozessen aus, die den Stickstoff dauerhaft immobilisieren oder aus dem (Öko-)System entfernen. Die SMB wurde auf einem Quadratkilometer-Raster angewendet, wovon 10'632 Punkte produktive Wälder enthalten, d.h. Standorte, an denen eine Holzernte möglich ist.

Die empirische Methode stützt sich auf Ergebnisse wissenschaftlicher Feldstudien, darunter Stickstoffadditionsversuche, Mesokosmenstudien, Beobachtungsstudien entlang von Stickstoffdepositionsgradienten, aber auch auf Expertenurteile. Schweizweite Critical Load Karten wurden mittels ökosystemspezifischer Werte erstellt, die nationalen Ökosysteminventaren zugewiesen wurden. Diese Flächen wurden auf einem Quadratkilometerraster aggregiert, woraus eine Gesamtfläche von 17'532 km^2 mit empfindliche Ökosystemen resultiert.

Die Stickstoffdeposition wurde mit Hilfe eines pragmatischen Ansatzes kartiert, welcher Emissionsinventare, statistische Ausbreitungsmodelle, Messdaten, räumliche Interpolationsmethoden und inferentielle Depositionsmodelle kombiniert. Die folgenden Verbindungen wurden berücksichtigt: die nasse und trockene Deposition von Nitrat (NO_3^-) und Ammonium (NH_4^+) sowie die gasförmige Deposition von Ammoniak (NH_3), Stickstoffdioxid (NO_2) und Salpetersäure (HNO_3).

Die resultierenden Critical Loads für Stickstoff variieren zwischen 4 und 25 kg N ha^{-1} a^{-1}, je nach Ökosystemtyp, Bodentyp, Höhenlage und anderen Ökosystemeigenschaften. Die Stickstoffdepositionen lagen im Jahr 2020 im Bereich von 2 bis 65 kg N ha^{-1} a^{-1}, wobei die höchsten Werte im Tiefland auftraten. Die Gesamtdeposition in der Schweiz beläuft sich auf 59 kt N a^{-1} (41 kt N a^{-1} reduzierter Stickstoff plus 18 kt N a^{-1} oxidierter Stickstoff). Von 1990 bis 2020 hat die Gesamtdeposition von Stickstoffverbindungen um 26% abgenommen.

Im Jahr 2020 wurden die Critical Loads für Stickstoff an 87% der Waldstandorte überschritten (Abb. S1). Die empirisch hergeleiteten Critical Loads für (halb-)natürliche Ökosysteme, aggregiert auf das Quadratkilometer-Raster, wurden auf 54% der Flächen überschritten. Eine detailliertere Analyse auf einem 100x100 m^2 Raster wurde für die schweizweit inventarisierten Schutzgebiete durchgeführt; Abbildung-S1 zeigt die daraus resultierenden Überschreitungen für die geschützten Hochmoore (94% der Fläche überschritten), Flachmoore (74% der Fläche überschritten) und artenreiche Trockenwiesen und -weiden TWW (42% der Fläche überschritten).

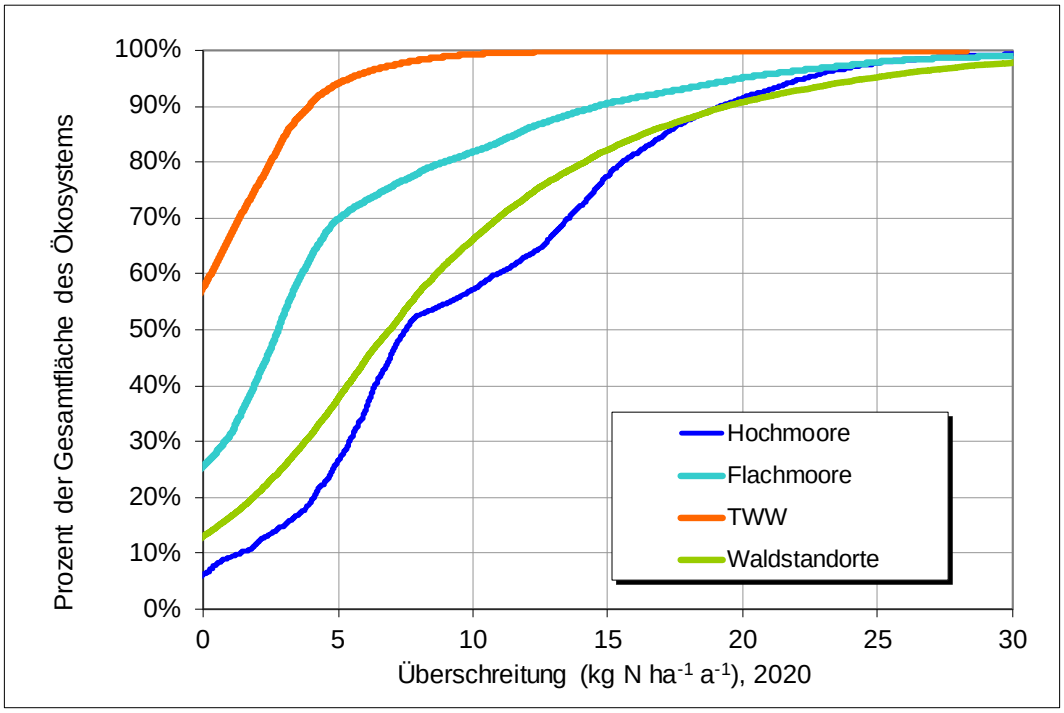

Abbildung-S1: Kumulative Häufigkeitsverteilung der Überschreitungen der kritischen Belastung durch Stickstoff für verschiedene geschützte Ökosysteme. Einheiten: Prozent der Gesamtfläche des Ökosystems. Stickstoffdeposition: Jahr 2020.

Acknowledgements

The update of the report on critical loads of nitrogen approach in Switzerland was requested and financed by the Swiss Federal Office for the Environment (FOEN), Air Pollution Control and Chemicals Division. First, we would like to thank Reto Meier (FOEN) for his encouragement and competent support. I would also like to thank Eva Seitler (FUB), Thomas Kupper (HAFL) as well as Constantin Streit (Federal Office for Agriculture) and the Federal Statistical Office for providing crucial data and information. Pleasant collaboration with Sabine Braun (Institute of Applied Plant Biology, IAP), Peter Waldner (WSL), Tobias Roth (Hintermann & Weber), Peter Kammer (PH Bern) and Sabine Augustin (FOEN), among others, was a source of good ideas and motivation.

Beat Rihm, Thomas Künzle, April 2023

Contents

Tables

Figures

1 Introduction

Critical loads are a measure of the sensitivity of ecosystems to inputs of air pollutants. They are defined as "a quantitative estimate of an exposure to one or more pollutants below which significant harmful effects on specified sensitive elements of the environment do not occur according to present knowledge" (Nilsson & Grennfelt 1988, UNECE 2012). “Sensitive elements” can be entire ecosystems or parts of them and include ecosystem development processes, structure and function (CLRTAP 2017).

Critical Loads have been developed within the UNECE Convention on Long-range Transboundary Air Pollution[1] (CLRTAP) and are regularly updated according to the current scientific knowledge. Scientific basis and guidelines for setting critical loads are given by the *Manual on Methodologies and Criteria for Modelling and Mapping Critical Loads and Levels and Air Pollution Effects, Risks and Trends* (CLRTAP 2017). Here we address critical loads for nutrient nitrogen (N) and their exceedances due to the deposition of reduced (NH_x) and oxidised (NO_y) nitrogen compounds.

National critical loads are reported to the *International Cooperative Programme on Modelling and Mapping of Critical Levels and Loads and Air Pollution Effects, Risks and Trends*[2] a scientific programme under the Convention on Long-range Transboundary Air Pollution. They are used within European-wide integrated assessment modelling[3] for developing effects-based and cost-optimized emission abatement scenarios.

Critical loads of nitrogen and their exceedances in Switzerland for the years 1990, 2000 and 2010 have been described by Rihm & Achermann (2016) and updated with data for 2015 by Rihm & Künzle 2019. The scope of this report is to provide updated results and maps for 1990 to 2020, based on the most recent input data and improved methods for calculating nationwide nitrogen deposition.

1 https://unece.org/environment-policy/air

2 https://unece.org/modelling-and-mapping

3 https://unece.org/integrated-assessment-modeling

2 Critical loads of nitrogen

For estimating and mapping critical loads of nitrogen according to chapter V of the mapping manual of the Geneva Air Convention (CLRTAP 2017) two different approaches have been applied:

- Empirical critical loads: Based on published data on observed harmful effects of N deposition to sensitive (semi-)natural ecosystems, primarily in terms of changes in the structure and functioning of the ecosystems.

- Simple Mass Balance (SMB) method: Calculation of critical loads based on long-term nitrogen mass balance considerations for specific ecosystems. The basic idea of this concept is to prevent from long-term accumulation of nitrogen. The mass balance includes consideration of nitrogen immobilization and removal processes such as plant uptake and harvest as well as losses due to denitrification and leaching, with respect to critical limits for soil functions.

The following chapters give an overview of harmful effects of increased N deposition and present the application of the two methods in Switzerland. The empirical method was used to map the sensitivity of natural and semi-natural ecosystems and the SMB method was applied to productive forests.

2.1 Adverse effects of exposure to atmospheric nitrogen compounds

The atmospheric nitrogen deposition in terrestrial and aquatic ecosystems in Switzerland as in all of Europe had increased substantially during the decades after 1950 (Schöpp et al. 2003). Since 1985 a decrease in air concentrations and wet depositions can be observed mainly for oxidized nitrogen compounds and to a lesser extent for reduced nitrogen compounds (BAFU 2022). Since 2000, the monitored concentrations of ammonia show no significant trend, however, the annual mean values in the years 2018 to 2020 were the highest since measurements began in 2000 (Seitler & Meier 2022). The main sources of reactive nitrogen in the atmosphere are emissions of NH_3 from agricultural activities and emissions of NO_x from combustion processes (FOEN 2021).

The impacts of increased nitrogen deposition and concentrations of gaseous nitrogen compounds upon biological systems are manifold, far-reaching and highly complex (Bobbink et al. 2022). The most important aspects are briefly summarized below.

2.1.1 Direct toxicity of nitrogen gases

Sensitive plant species can be damaged by the direct exposure of above-ground parts of plants to gaseous pollutants in the air. In order to protect ecosystems from those direct effects **critical levels** have been defined as the "concentration, cumulative exposure or cumulative stomatal flux of atmospheric pollutants above

which direct adverse effects on sensitive vegetation may occur according to present knowledge" (CLRTAP 2017). Critical levels were set for the nitrogen compounds nitrogen oxides (NO_x) and ammonia (NH_3) - besides sulphur dioxide (SO_2) and ozone (O_3).

The critical level for the annual mean concentration of NO_x ($NO + NO_2$, expressed as NO_2) is set at 30 µg m^{-3} for all vegetation types (CLRTAP 2017). There is also a short-term critical level for NO_x (expressed as NO_2) defined as a 24-hour mean value of 75 µg m^{-3}.

The critical level for the annual mean concentration of NH_3 is set at 3 µg m^{-3} (uncertainty range 2-4 µg m^{-3}) for higher plants, including heathland, grassland and forest ground flora. For lichens and bryophytes (including ecosystems where lichens and bryophytes are a key part of ecosystem integrity) the critical level is set at 1 µg m^{-3} (CLRTAP 2017). In March 2022, there was an expert workshop on ammonia prepared by the CCE and Germany which confirmed those critical level values (Franzaring & Kösler 2022).

2.1.2 Eutrophication of (semi-)natural ecosystems

High nitrogen deposition initially often leads to increased growth rates and biomass production followed by N-accumulation in the soil and in the biomass. The excessive nitrogen availability leads to changes in the competitive relationships between species. Nutrient-poor (semi-)natural ecosystems often show larger species diversity compared to nutrient-rich systems. Most of the plant species found in nutrient-poor conditions can only compete successfully on soils with low nitrogen availability. Under high nitrogen depositions many oligotrophic species are gradually displaced by nitrophilous species, which generally implies a loss of biodiversity and community uniqueness and a trend towards floristic homogenization. The loss of species richness in relation to elevated nitrogen deposition also applies for mycorrhiza in forest soils that are important for the nutrient uptake by the fine roots of trees.

2.1.3 Soil acidification and nutrient leaching

Soil acidification is defined as loss of acid neutralising capacity (ANC). Nitrogen deposition contributes to soil acidification due to nitrification processes and nitrate leaching, accompanied by accelerated leaching of base cations (Ca, K, Mg). As a consequence, the nutrient conditions for the plants change and can lead to nutritional imbalances. Nutritional imbalances (e.g. deficiencies of K, P, Mg, Ca, B, Mn relative to nitrogen) are concluded to be an important feature of the destabilization of sensitive ecosystems, particularly forests. Low base cation-to-aluminium ratios affect the growth rates of many tree species and other plants. These disturbances also lead to increased sensitivity to secondary stress factors such as gales, drought, insect pests and pathogens. N saturated systems also show elevated N loss in form of N_2, NO and N_2O; the latter is a potent greenhouse gas. The temporal evolution of acidifying effects depends on changes in the buffering

capacity of the soil, in base saturation and the chemical composition of the soil solution.

2.2 Empirical critical loads of nitrogen

2.2.1 The empirical method

Empirical critical loads of nitrogen ($CL_{emp}N$) for (semi-)natural ecosystems are based on results of field studies, experiments, gradient studies and on scientific expert judgement. They have been established in 1992 in the framework of the Geneva Air Convention (Grennfelt & Thörnelöf 1992) and since then repeatedly been updated according to the state of knowledge (Bobbink et al. 2011). The values from the most recent update (Bobbink et al. 2022) have been recommended for policy support within and outside of the Geneva Air Convention. The most recent values were also applied here. The empirical critical loads listed in Table 1 are an excerpt from the overview in Bobbink et al. (2022) showing only those ecosystem types that are relevant for the Swiss critical load maps.

Table 1: Overview of empirical critical loads of nitrogen ($CL_{emp}N$) for selected (semi-)natural ecosystem types (excerpt from Bobbink et al. 2022). Units are in kg N ha^{-1} a^{-1}.

Ecosystem type	**EUNIS code**	**$CL_{emp}N$ range**	**Reliability** [a)]	**Indication of exceedance**
Broadleaved deciduous forest	T1	10-15	##	Changes in soil processes; nutrient imbalance; altered composition mycorrhiza and ground vegetation
Coniferous forests	T3	3-15	##	Changes in soil processes; nutrient imbalance; altered composition mycorrhiza and ground vegetation; increase in mortality with drought
Arctic and (sub-)alpine scrub habitats	S2	5-10 [d)]	#	Decline in lichens, bryophytes and evergreen shrubs
semi-dry perennial calcareous grassland (meadow steppe)	R1A	10-20	##	Increase in tall grasses; decline in diversity; change in species composition; increased mineralization; N leaching; surface acidification
Moist or wet mesotrophic to eutrophic hay meadow	R35	15-25	(#)	Increase in tall graminoids; decreased diversity; decrease in bryophytes
Mountain hay meadows	R23	10-15	(#)	Increase in nitrophilous graminoids, changes in diversity; decline of typical species
Temperate acidophilous alpine grassland	R43	5-10	#	Changes in species composition; increase in plant production
Arctic-alpine calcareous grassland	R44	5-10	#	Changes in species composition; increase in plant production
Permanent oligotrophic lakes, ponds and pools	C1.1	2-10 [b)]	##	Increased algal productivity and a shift in nutrient limitation of phytoplankton from N to P; shifts in macrophyte community
Alpine and sub-Arctic clear water lakes	C1.1	2-4	##	Increased algal productivity and a shift in nutrient limitation of phytoplankton from N to P
Raised and blanket bogs	Q1	5-10	##	Increase in vascular plants; decrease in bryophytes; altered growth and species composition of bryophytes; increased N in peat and peat water
Valley mires, poor fens and transition mires	Q2	5-15	#	Increase in sedges and vascular plants; negative effects on bryophytes
Rich fens	Q41-Q44	15-25	#	Increase in tall vascular plants (especially graminoids); decrease in bryophytes

[a)] The reliability is indicated by ## reliable; # quite reliable and (#) expert judgement.

[b)] This CLempN should only be applied to oligotrophic waters with low alkalinity and with no significant agricultural or other human inputs. Apply the lower end of the range to

clear-water sub-Arctic and alpine lakes, the middle range to boreal lakes and the higher end of the range to Atlantic soft waters.
[d)] Use towards high end of range if phosphorus limited, and towards lower end if phosphorus is not limiting.

For each ecosystem type the critical load is given as a range reflecting (1) the real intra-ecosystem variation within the ecosystem type, (2) the range of experimental treatments where an effect was observed or not observed and (3) uncertainties in estimated total atmospheric deposition values, where critical loads are based on field observations. The table also lists the indications of exceedance, i.e. the harmful changes in ecosystems to be expected when the critical load is exceeded in the long term. The reliability of the given critical load values is indicated as follows:

- ## reliable: when several geographically separated studies showed similar results, or when experimental studies were supported by gradient studies
- # quite reliable: when one or two studies supported the range given;
- (#) expert judgement: when results from experimental studies were lacking for this type of ecosystem. The critical load is then based upon knowledge of ecosystems which are likely to be comparable with this ecosystem.

2.2.2 Mapping empirical critical loads for ecosystems in Switzerland

For the purpose of applying the empirical critical loads approach, countries have to identify those receptors or ecosystems of maximum sensitivity relating to their individual priorities to protect the environment. Table 2 and Table 3 present the ecosystems for which the empirical critical load approach was applied in Switzerland. Table 3 specifically addresses dry grassland (TWW).

The selection of sensitive ecosystems to be protected by applying the empirical method is based on ecosystem and vegetation data compiled from various sources described below. All of the selected ecosystems are of high conservation importance with respect to biodiversity, landscape quality and ecosystem services. They include natural as well as semi-natural ecosystem types. Overall, 45 sensitive ecosystem types according to EUNIS classes were identified and included in the critical load data set:

- 21 various so-called “types of vegetation worthy of protection” from the vegetation atlas by Hegg et al. (1993) including rare and species-rich forest types, alpine heaths, grasslands and surface waters. The atlas contains distribution maps for 97 vegetation types with a resolution of 1x1 km^2. 21 vegetation types sensitive to eutrophication were selected (see Table 2).

- 1 type of mountain hay meadow (see Table 2) in montane to sub-alpine altitudinal zones with more than 35 species per 10 m^2 (Roth et al. 2013). This applies to 122 sites of the Swiss Biodiversity Monitoring[4] (BDM, indicator Z9).

- 1 type of raised bog from the Federal Inventory of Raised and Transitional Bogs of National Importance (Appendix to Swiss Confederation 1991) (see Table 2). This data set[5] is available in vector format at a scale of 1:25'000. The version used for mapping is from 2017. The inventory contains only bogs with relevant occurrences of *sphagnion fusci*.

- 2 types of poor fens and 2 types of rich fens from the Federal Inventory of Fenlands of National Importance (Appendix to Swiss Confederation 1994, Hunziker 2022) (see Table 2). This data set is available in vector format at a scale of 1:25'000.

- 1 type of oligotrophic alpine lakes (see Table 2). The catchments of 100 lakes in Southern Switzerland at altitudes between 1650 m and 2700 m (average 2200 m) were mapped by Posch et al. 2007. To a large extent the selected catchments consist of crystalline bedrock and are therefore sensitive to acidification and eutrophication.

- 18 types of dry grassland (TWW) from the National Inventory of Dry Grasslands of National Importance (Eggenberg et al. 2001, Hunziker 2022) (see Table 3). This data set is available in vector format at a scale of 1:25'000. Many of those grasslands are extensively managed as hay meadows. They also include alpine and subalpine grassland.

For most of the selected ecosystems a value in the middle of the proposed range was chosen as the critical load. Only in the case of fens and several grassland types the critical load value was set near the lower end of the range because the respective ecosystems are considered to be more sensitive than the average, since they are nutrient poor or located in relatively high altitudes with short vegetation periods.

Raised bogs, oligotrophic ponds, alpine grassland, alpine heaths and most of the selected forest types are (semi-)natural ecosystems, i.e. they are not managed or only poorly managed.

Fens and species-rich grassland below the alpine level are semi-natural systems, in general. They developed under permanent traditional management over centuries. When these extensive forms of management change, the ecosystems generally decrease in biodiversity.

---

4 http://www.biodiversitymonitoring.ch

5 https://www.bafu.admin.ch/bafu/de/home/themen/biodiversitaet/fachinformationen/oekologische-infrastruktur/biotope-von-nationaler-bedeutung/moore.html

The TWW data set complements well the grassland types mapped by Hegg et al. (1993). It contains 18 vegetation groups, which partially also occur in the inventory of Hegg. The two inventories are used here in a complementary way, because they answer different purposes: The atlas by Hegg gives an overview of the occurrence of selected vegetation types, while TWW focuses on the precise description of sites with national importance.

For the data and maps used under the Convention on Long-range Transboundary Air Pollution and submitted to the Coordination Centre for Effects (FOEN 2017) and for the national maps presented in this report, the outlines of all ecosystem-specific polygons (in vector format) were converted to a 1x1 km^2 grid (present/absent criterion). If more than one ecosystem type occurs within a 1x1 km^2 grid-cell, the lowest value of $CL_{emp}N$ was selected for this cell. The spatial distribution of the selected ecosystem types and their $CL_{emp}N$ according to Table 2 and Table 3 are shown on the maps in Figure 1 to Figure 5.

Table 2: Selected ecosystems for the application of empirical critical loads, $CL_{emp}N$, applied in Switzerland. Units are kg N ha^{-1} a^{-1}.

Ecosystem type	**$CL_{emp}N$ range**	**Relevant vegetation types in Switzerland**	**EUNIS code**	**$CL_{emp}N$**
Broadleaved deciduous forest (EUNIS T1)	10-15	Quercion robori-petraeae *(Traubeneichen-wald)* Quercion pubescentis *(Flaumeichenwald)* Fraxino orno-Ostryon *(Mannaeschen-Hopfenbuchwald)*	T1912 T1911 T193	12 12 12
Coniferous forests (EUNIS T3)	3-15	Molinio-Pinetum *(Pfeifengras-Föhrenwald)* Ononido-Pinion *(Hauhechel-Föhrenwald)* Cytiso-Pinion *(Geissklee-Föhrenwald)* Calluno-Pinetum *(Heidekraut-Föhrenwald)* Erico-Pinion mugi (Ca) *(Erika-Bergföhrenwald auf Kalk)* Erico-Pinion sylvestris *(Erika-Föhrenwald)*	T35 T353 T35 T35 T348 T354	12 12 12 10 12 12
Arctic and (sub)-alpine scrub habitats (EUNIS S2)	5-10	Juniperion nanae *(Zwergwacholderheiden)* Loiseleurio-Vaccinion *(Alpenazaleenheiden)*	S2311 S2211	7 7
semi-dry perennial calcareous grassland (meadow steppe)	10-20	Mesobromion (erecti) *(Trespen-Halbtrockenrasen)*	R1A	15
Molinia caerulea meadows	15-25	Molinion (caeruleae) *(Pfeifengrasrieder)*	R371	15
Mountain hay meadows	10-15	Grassland types 4.5.1-4.5.4 (Delarze et al. 2008)	R23	12
(sub)-alpine grassland	5-10	Chrysopogonetum grylli *(Goldbart-Halbtrockenrasen)* Seslerio-Bromion (Koelerio-Seslerion) *(Blaugras-Trespen-Halbtrockenrasen)* Stipo-Poion molinerii *(Engadiner Steppenrasen)*, sub-alpine Elynion *(Nacktriedrasen)*, alpine	R43 R4431 R44 R4421	10 10 10 7
Permanent oligotrophic lakes, ponds and pools	2-10	Littorellion *(Strandling-Gesellschaften)*	C1.1	7
Alpine and sub-Arctic clear water lakes	2-4	Sensitive alpine lakes in Southern Switzerland	C1.1	4
Raised and blanket bogs	5-10	Sphagnion fusci *(Hochmoor)*	Q11	7

Valley mires, poor fens and transition mires	5-15	Scheuchzerietalia *(Scheuchzergras)*, occurence of raised bog vegetation Caricion fuscae *(Braunseggenried)*	Q22 Q22	10 12
Rich fens	15-25	Caricion davallianae *(Davallsseggenried)*, Molinion Other fens: Phragmition,Magnocaricon, Calthion/ Filipendulion	Q41 Q43	15 20

Table 3: Empirical critical loads for nitrogen, $CL_{emp}N$, assigned to the vegetation types of the National Inventory of Dry Grasslands (TWW), in kg N ha^{-1} a^{-1}.

TWW-code		Vegetation type	EUNIS	Remarks	$CL_{emp}N$
1	CA	Caricion austro-alpinae *(Südalpine Blaugrashalde)*	R44	(sub-)alpine grassland	7
2	CB	Cirsio-Brachypodion *(Subkontinentaler Trockenrasen)*	R1A	similar to TWW 18 (Mesobromion), also used as hay meadow	12
3	FP	Festucion paniculatae *(Goldschwingelhalde)*	R4321	similar to TWW 13 (Festucion variae); also mapped by Hegg et al.	7
4	LL	low diversity, low altitude grassland *(artenarme Trockenrasen der tieferen Lagen)*	R1A	contains different types, promising diversity when mown	15
5	AI	Agropyrion intermedia *(Halbruderaler Trockenrasen)*	R1	transitional type	15
6	SP	Stipo-Poion *(Steppenartiger Trockenrasen)*	R1B3	pastures/fallows in large inner-alpine valleys; $CL_{emp}N$ based on national expert-judgment (Hegg et al. 1993)	10
7	MB SP	Mesobromion / Stipo-Poion *(Steppenartiger Halbtrockenrasen)*	R1A32	pastures, slightly more nutrient-rich than Mesobromion (TWW18)	15
8	XB	Xerobromion *(Subatlantischer Trockenrasen)*	R1A42	meadows/pastures/fallows in large inner-alpine valleys; $CL_{emp}N$ based on national expert-judgment (Hegg et al. 1993)	12
9	MB XB	Mesobromion / Xerobromion *(Trockener Halbtrockenrasen)*	R1A32	similar to TWW 18 (Mesobromion)	12
10	LH	low diversity, high altitude grassland *(artenarme Trockenrasen der höheren Lagen)*	R1A	contains different types of dry grassland at high altitude	12
11	CF	Caricion ferrugineae *(Rostseggenhalde)*	R4412	(sub-)alpine grassland; also mapped by Hegg et al.	7
12	AE	Arrhenatherion elatioris *(Trockene artenreiche Fettwiese)*	R23	often used as meadows, lower range chosen as it occurs at all altitude levels	12
13	FV	Festucion variae *(Buntschwingelhalde)*	R432	(sub-)alpine grassland, middle of the range chosen	7
14	SV	Seslerion variae *(Blaugrashalde)*	R4431	alpine grassland, middle of the range chosen; also mapped by Hegg et al.	7
15	NS	Nardion strictae *(Borstgrasrasen)*	R431	meadows, subalpine	12
16	OR	Origanietalia *(Trockene Saumgesellschaft)*	R23	meadows/fallows	15
17	MB AE	Mesobromion / Arrhenatherion *(Nährstoffreicher Halbtrockenrasen)*	R1A3	slightly more nutrient-rich than Mesobromion (TWW18)	15
18	MB	Mesobromion *(Echter Halbrockenrasen)*	R1A32	genuine semi-dry grassland	12

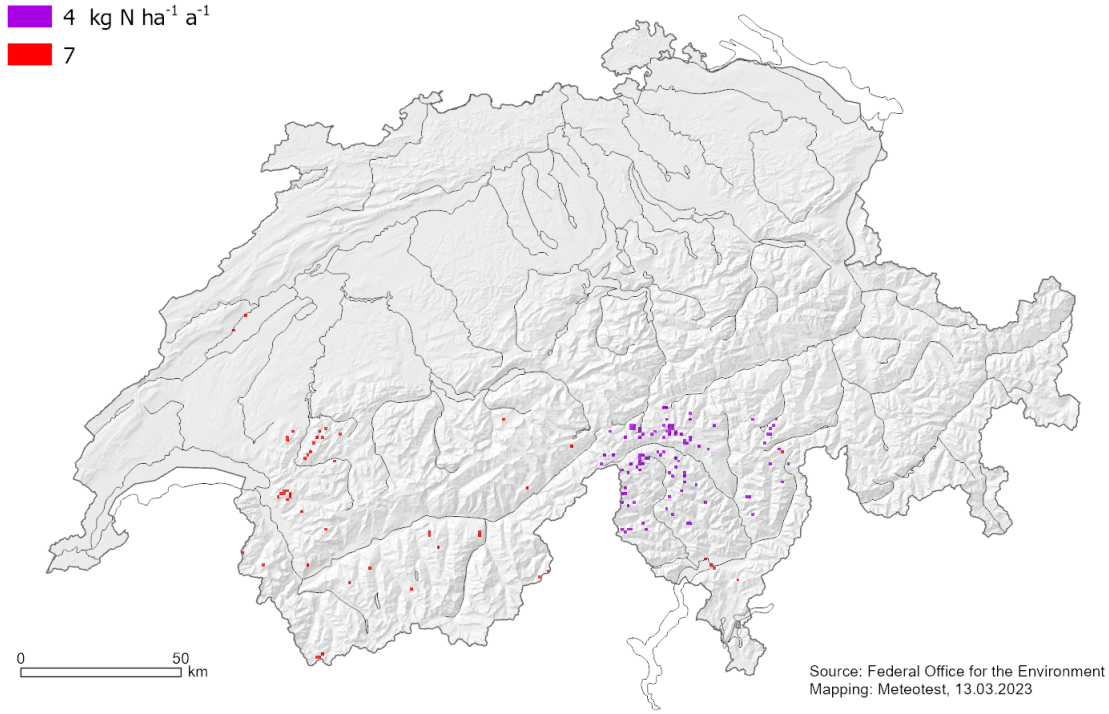

Figure 1: $CL_{emp}N$ for oligotrophic surface waters (EUNIS code C1.1). Sources: Hegg et al. 1993, Posch et al. 2007.

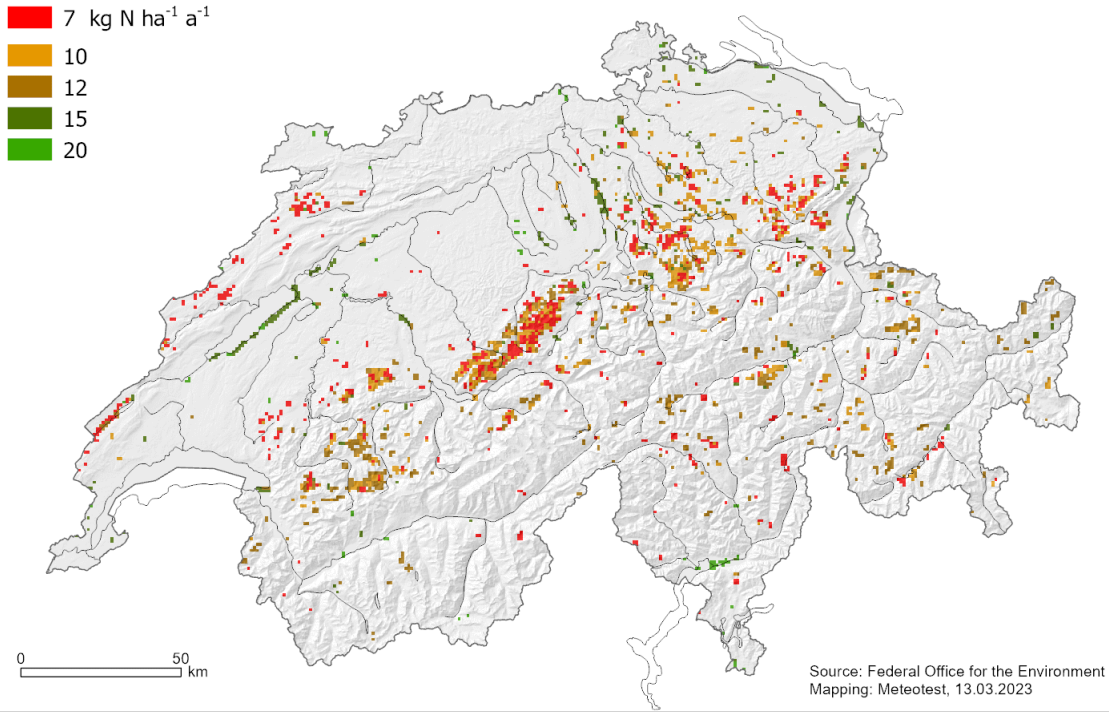

Figure 2: $CL_{emp}N$ for raised bogs and fens (EUNIS codes Q1, Q2, Q4). Sources: Swiss Confederation 1991 and 1994.

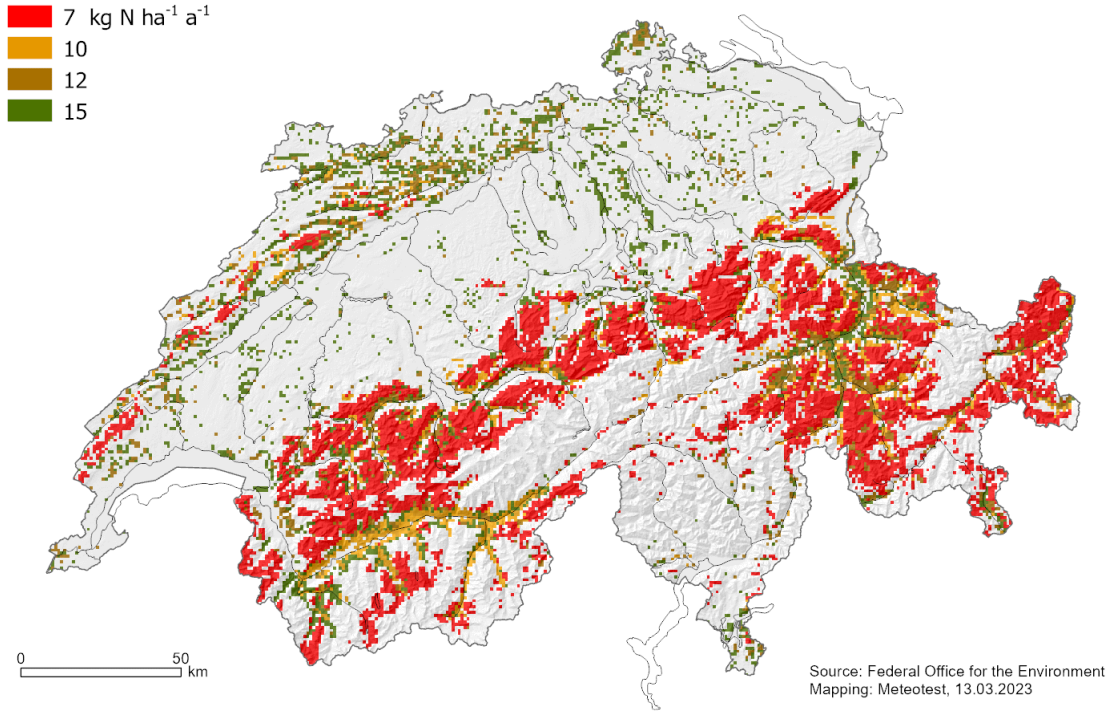

Figure 3: $CL_{emp}N$ for selected grassland types (EUNIS code R1-R4). Sources: Hegg et al. 1993, TWW, BDM.

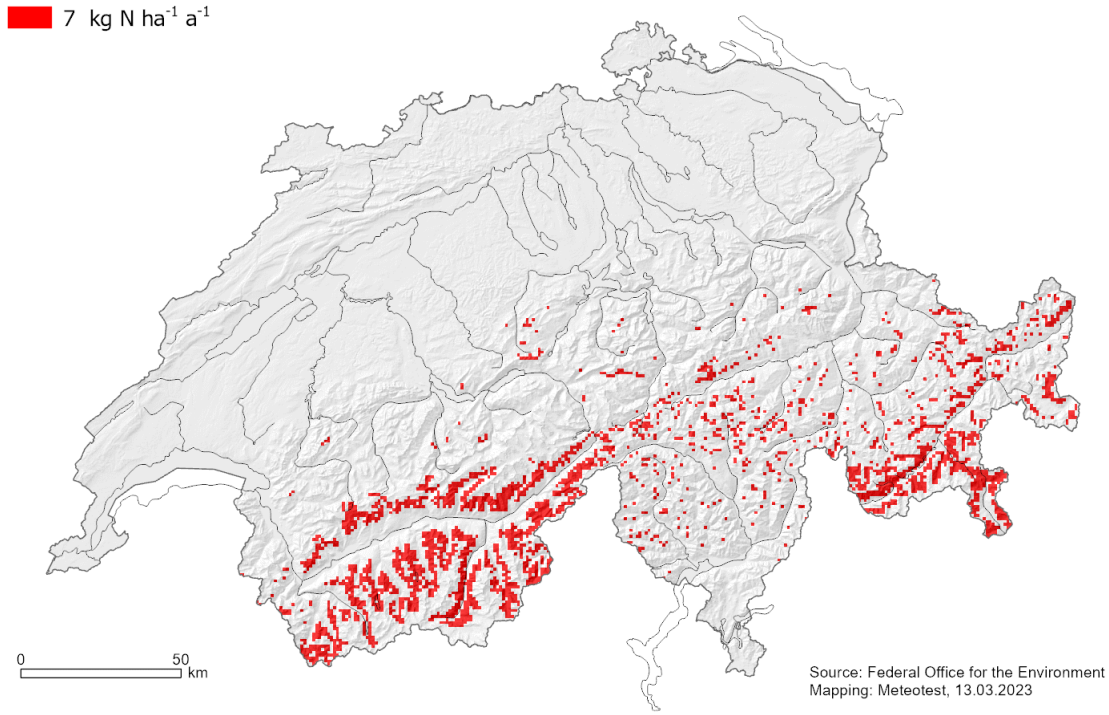

Figure 4: $CL_{emp}N$ for selected alpine scrub habitats (EUNIS code S2). Source: Hegg et al. 1993.

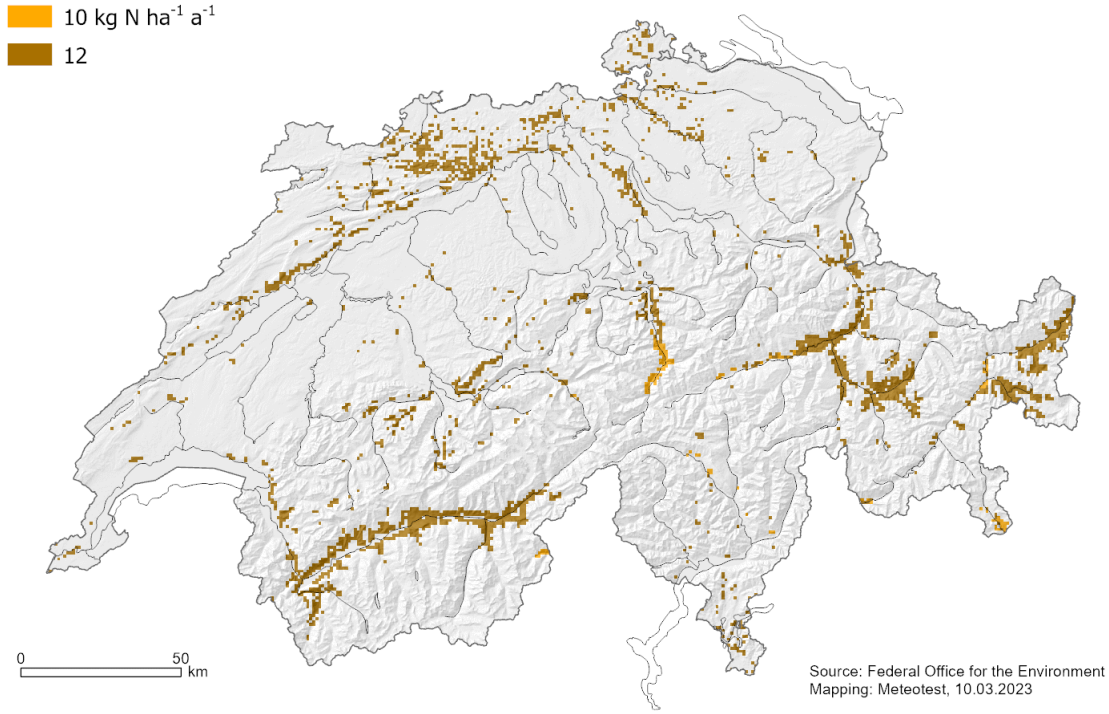

Figure 5: $CL_{emp}N$ for selected forest types (EUNIS code T). Source: Hegg et al. 1993.

2.3 The simple mass balance method (SMB)

In Switzerland, the SMB method was applied for productive forest ecosystems, i.e. sites where wood harvesting is possible. The method was not changed since 2015 (see Rihm & Achermann 2016).

2.3.1 The calculation method

The SMB method for calculating critical loads of nutrient nitrogen is a steady-state model based on the nitrogen saturation concept. There are several definitions of N saturation. In this context it is understood as follows: The atmospheric nitrogen deposition must not lead to a situation where the availability of inorganic nitrogen is in excess of the total combined plant and microbial nutritional demand. I.e. the inputs should not be larger than the natural sinks plus outputs.

The basic principle of the SMB method is to identify the long-term average sources and sinks of inorganic nitrogen in the system, and to determine the maximum tolerable nitrogen input that will protect the system from nitrogen saturation. The nitrogen cycling within the ecosystems is mainly regulated by biological processes that depend on the following factors: (1) the ecosystem type, (2) former and present land use and management, (3) environmental conditions, especially

those influencing the nitrification rate and the immobilization rate. Consequently, these factors are important for calculating and setting critical loads of nutrient nitrogen.

In the mapping manual (CLRTAP 2017) a simplified SMB equation is formulated as follows:

$$CL_{nut}N = N_i + N_u + N_{de} + N_{le(acc)} \quad (2.1)$$

Where:

- $CL_{nut}N$ = critical load of nutrient nitrogen [kg N ha^{-1} a^{-1}].
- N_i = acceptable immobilization rate of N in soil organic matter (including forest floor) at N inputs equal to critical load, at which adverse ecosystem change will not take place [kg N ha^{-1} a^{-1}].
- N_u = nitrogen uptake; net removal of nitrogen in vegetation at critical load [kg N ha^{-1} a^{-1}]. This is the amount of nitrogen which is removed from the system by (wood) harvesting.
- N_{de} = denitrification rate [kg N ha^{-1} a^{-1}]. This is the flux to the atmosphere of gaseous compounds (N_2, N_2O and NO) produced by microorganisms (mainly under anaerobic conditions) in the soil.
- $N_{le(acc)}$ = acceptable total nitrogen leaching from the rooting zone at which no damage occurs in the terrestrial or linked ecosystem plus any enhanced leaching following forest harvesting [kg N ha^{-1} a^{-1}]. This is the N removed from the soil by the vertically percolating water flux.

The equation is based on the following assumptions:

- All rates and fluxes of the involved processes are represented by annual means.
- Temporal variations in Nu as a function of forest age and management are not included, i.e. the temporal scale of the investigation is longer than one rotation period (>100 years).
- Nitrogen losses by natural fires, erosion and ammonia volatilisation as well as biological N fixation are negligible in most Swiss forests.

Equation 2.1 as such is not operational, as N_{de} strongly depends on nitrogen deposition. The mapping manual proposes to use linear or non-linear functions to calculate N_{de}. For the application in Switzerland the constant function is used:

$$N_{de} = f_{de} \cdot (N_{dep} - N_u - N_i) \quad \text{if } N_{dep} > N_u + N_i \quad (2.2)$$
$$N_{de} = 0 \quad \text{otherwise}$$

Where:

- f_{de} = denitrification fraction
- N_{dep} = nitrogen deposition [kg N ha^{-1} a^{-1}].

This formulation implicitly assumes that immobilization and uptake are faster processes than denitrification. Under critical load conditions N_{dep} is equal to $CL_{nut}N$. By inserting equation 2.2 into 2.1 the critical load becomes:

$$CL_{nut}N = N_i + N_u + N_{le(acc)} / (1 - f_{de}) \quad (2.3)$$

Maps of critical loads to be used under the Convention on LRTAP were produced in two steps:

In a first step, equation 2.3 was applied for 10'331 sites of the National Forest Inventory NFI (WSL 1990/92, EAFV 1988) located on a 1x1 km^2 raster, and for 301 forest sites used for dynamic models (Achermann et al. 2015). Thereby, only NFI-sites with a defined mixing ratio of deciduous and coniferous trees are included. This corresponds approximately to the productive forest area as unproductive and unmanaged woodlands such as brush forests and inaccessible forests are excluded.

In a second step, the lower limit of $CL_{nut}N$ calculated by the SMB was set to 10 kg N ha^{-1} a^{-1} (corresponding to the lower limit of $CL_{emp}N$ used for forests in Switzerland). This means, all values of $CL_{nut}N$ below 10 kg N ha^{-1} a^{-1} were set to 10. This was done with respect to the fact that so far no empirically observed harmful effects in forest ecosystems were published for depositions lower than 10 kg N ha^{-1} a^{-1} and for latitudes and altitudes typical for Switzerland. Therefore, the critical loads calculated with the SMB method were adjusted to empirically confirmed values.

2.3.2 Quantification of the input parameters

Table 4 gives a summary of the input parameter values applied for the national maps.

Table 4: Ranges of input parameters used for calculating $CL_{nut}(N)$ with the SMB method.

Parameter	Values	Comment
$N_{le(acc)}$	4 kg N ha^{-1} a^{-1} at 500 m a.s.l., 2 kg N ha^{-1} a^{-1} at 2000 m a.s.l., linear interpolation in-between	Acceptable N leaching. Leaching mainly occurs by management (after cutting), which is more intense at lower altitudes.
N_i	1.5 kg N ha^{-1} a^{-1} at 500 m a.s.l., 2.5 kg N ha^{-1} a^{-1} at 1500 m a.s.l., linear interpolation in-between	N immobilization in the soil. At low temperature (correlated with high altitude) the decomposition of organic matter slows down and therefore the accumulation rates of N are naturally higher.
N_u	0.5 – 14.7 kg N ha^{-1} a^{-1}	N uptake calculated on the basis of long-term harvesting rates in managed forest ecosystems.
f_{de}	0.2 – 0.7 depending on the wetness of the soil	Denitrification fraction. For sites of the National Forest Inventory (NFI), information on wetness originates from soil map 1:200'000. For sites with application of dynamic models (DM-sites) it is a classification according to the depth of the water-logged horizon.

a) Nitrogen immobilization

According to the mapping manual (CLRTAP 2017) there is no full consensus yet on long-term sustainable immobilization rates. E.g. in Swedish forest soils the annual N immobilisation since the last glaciation was estimated at 0.2–0.5 kg N ha^{-1} a^{-1} (Rosén et al. 1992). Considering that immobilization of N is probably higher in warmer climates, the mapping manual states that values up to 1 kg N ha^{-1} a^{-1} could be used without causing unsustainable accumulation of N in the soil and that even higher values were used for critical load calculations. Considering these uncertainties, the following (relatively high) values are used for the Swiss critical load map:

N_i = 1.5 kg N ha^{-1} a^{-1} at low altitudes (<500 m a.s.l.)
N_i = 2.5 kg N ha^{-1} a^{-1} at high altitudes (>1500 m a.s.l.)

At altitudes in-between N_i is calculated by linear interpolation (see Figure 6). The reason for the altitude dependency is the retarded decomposition of organic matter at lower temperatures and/or higher precipitation; therefore, the accumulation rates of soil organic matter (including N and carbon) are naturally higher at high altitudes. The general increase of the carbon content in the soil with altitude for large parts of Switzerland was shown on modelled maps by Nussbaum & Burgos (2021).

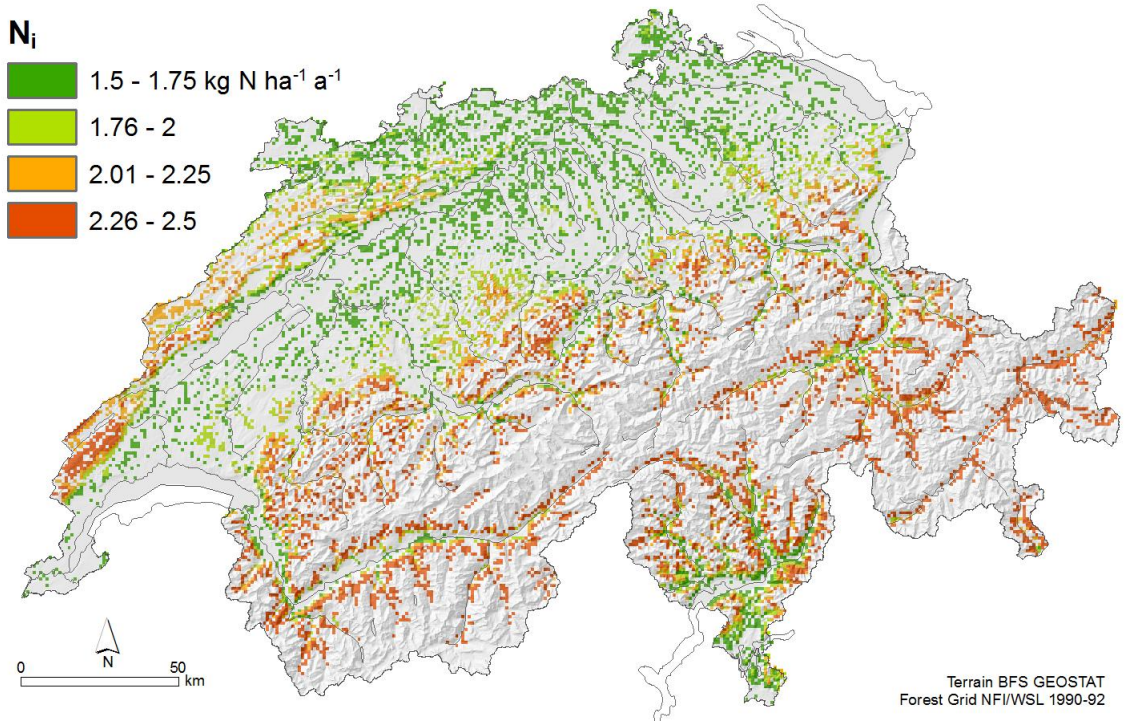

Figure 6: Nitrogen immobilization values for forest soils used for the SMB method on the 1x1 km^2 raster.

b) Nitrogen uptake

Nitrogen and base cations (Ca, Mg, K, Na) are taken up by trees and used for biomass production. In unmanaged forests at steady state, the net uptake will be zero since biomass production is in balance with biomass decomposition. In a managed forest, the net uptake rate is obtained by multiplying the long-term net growth (harvesting) rate with nitrogen and cation contents of the wood.

For the 301 sites used in dynamic modelling (DM-sites), Kurz & Posch (2015) modelled net-uptake fluxes with MakeDep (Alveteg et al., 2002) using biomass data from the third National Forest Inventory (NFI, WSL 2013), tree genera-specific logistic growth curves, site productivity index, nutrient contents in the various compartments of the tree, and average annual harvesting rates (FOEN 2013). MakeDep is able to consider the mutual dependence of deposition, forest canopy growth/size and nutrient demand of the growing forest.

Harvesting rates were stratified according to the five NFI-regions: Jura, Central Plateau, Pre-Alps, Alps and Southern Alps. The harvesting rates before 2000 add up to 4.5 million m^3 stem wood, which is in the range of the typical annual harvest in Switzerland (in years without heavy storms); after 2000, the harvest of energy wood slightly increased and the average harvest was around 5.0 million m^3 (FOEN 2013).

The nitrogen uptake for the forest sites on the 1x1 km^2 raster was derived from the results at the DM-sites by linear regressions with altitude (z); the regression analysis was stratified according to the five NFI-regions (Table 5, Figure 7). In the Jura and Central Plateau regions, the average harvesting rates reach the long-term gross growth, but in the mountainous and southern parts of Switzerland it is much lower than gross growth. The resulting uptake values are in the range from 1.0 to 8.8 kg N $ha^{-1}a^{-1}$ (see Figure 7).

Table 5: Net nitrogen uptake (N_u) in the five NFI-regions (kg N ha^{-1} a^{-1}).

Region	**Average**	**Function of altitude z (m a.s.l.)**
1. Jura	5.3	6.99 - 0.00300 z
2. Central Plateau	8.5	8.5
3. Pre-Alps	4.3	7.60 - 0.00322 z
4. Alps	2.9	3.58 - 0.00064 z
5. Southern Alps	1.6	2.29 - 0.00056 z
Average CH	4.4	--

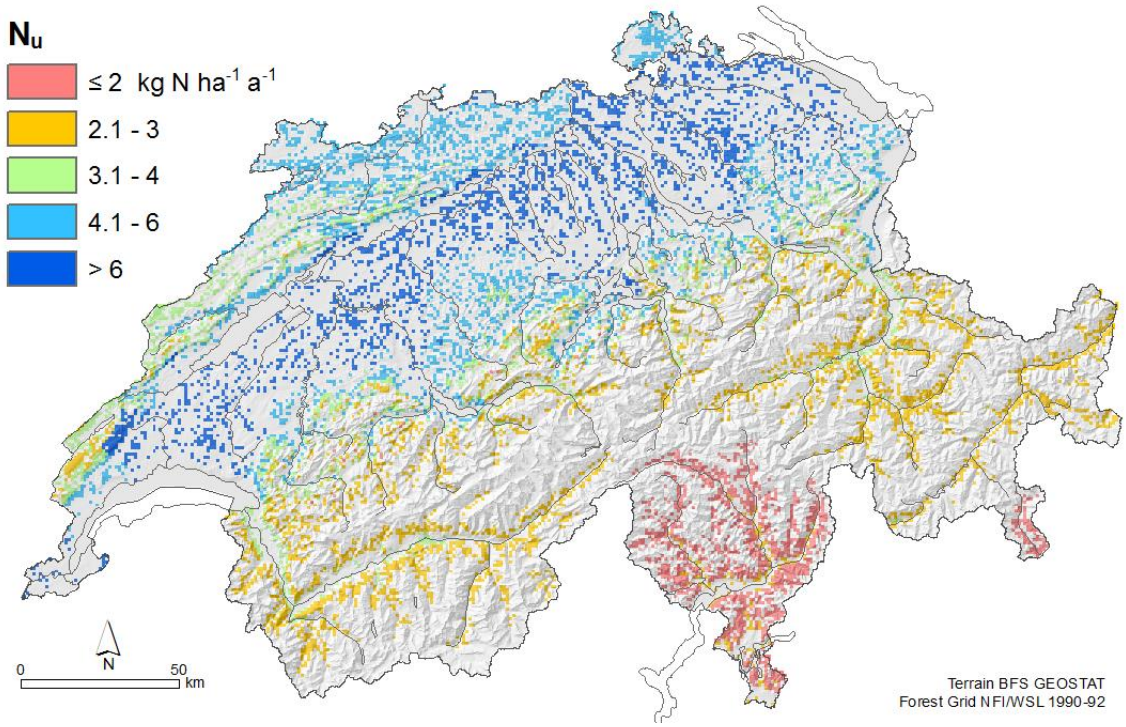

Figure 7: Net nitrogen uptake (N_u) of managed forest ecosystems used for the SMB method on the 1x1 km^2 raster.

c) Nitrogen leaching

Limit values for acceptable leaching of inorganic nitrogen were chosen as total annual nitrogen leaching according to the Mapping Manual (LRTAP 2017, chapter V.3.1.2):

$N_{le(acc)}$ = 4 kg N ha^{-1} a^{-1} at low altitudes (<500 m a.s.l.)
$N_{le(acc)}$ = 2 kg N ha^{-1} a^{-1} at high altitudes (>2000 m a.s.l.)

At altitudes between, $N_{le(acc)}$ is calculated by linear interpolation. The rationale for this procedure is that the productive forest areas are managed and the (acceptable) leaching mainly occurs after disturbances by management (cutting), which is more intense at lower altitudes. The resulting map is shown in Figure 8.

The use of concentration-based limit values has previously been evaluated and rejected because it led to implausible high N leaching and $CL_{nut}N$, mainly in high precipitation areas (see Achermann et al. 2007). High N leaching is accompanied by substantial losses of base cations and thus leading to a gradual decrease of the base saturation and can therefore not be accepted for critical load calculations (see chapter 2.1.3).

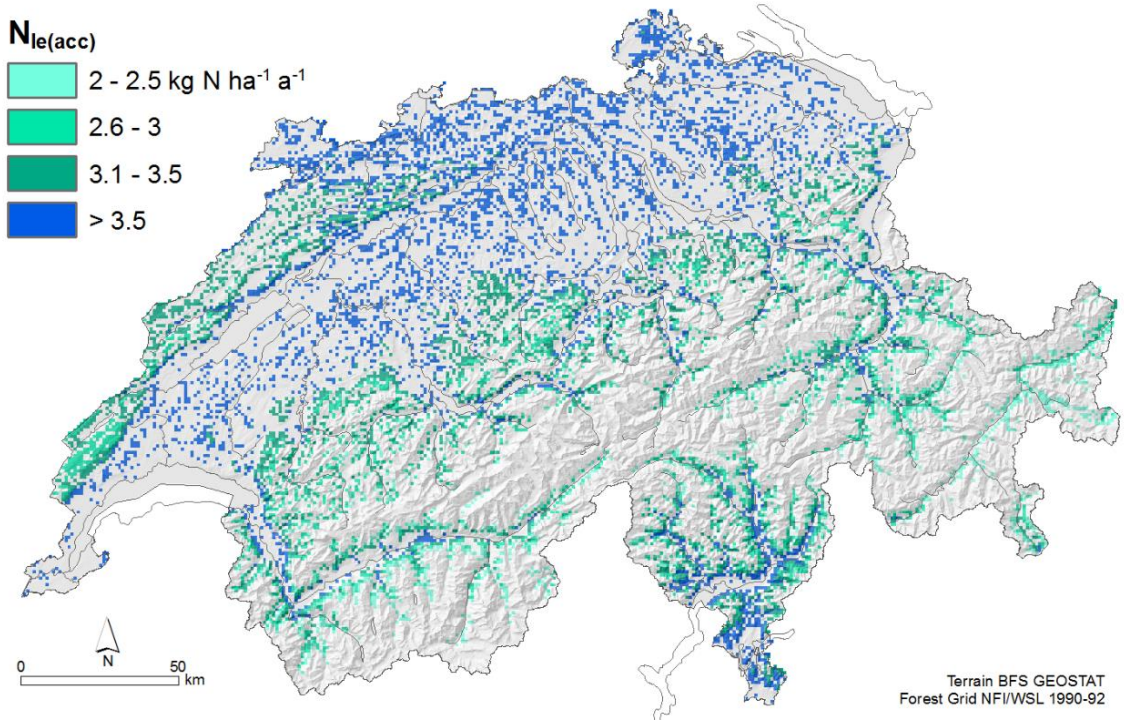

Figure 8: Acceptable nitrogen leaching values of forest ecosystems used for the SMB method on the 1x1 km^2 raster.

d) Denitrification fraction

The f_{de} values proposed in the mapping manual (LRTAP 2017) are between 0.0 and 0.8. There are two proposals for relating f_{de} values to different soil properties:

- Soil types: for sandy soils without gleyic features or loess a value of 0.0-0.1, for sandy soils with gleyic features 0.5, for clay soils 0.7, for peat soils 0.8.
- Soil drainage status: excessive 0.0, good 0.1, moderate 0.2, imperfect 0.4, poor 0.7, very poor 0.8.

For calculating $CL_{nut}N$ at the 1x1 km^2 raster of the National Forest Inventory), f_{de} was determined according to wetness information from the digital soil map BEK (SFSO 2000) as shown in Table 6 and Figure 9.

Table 6: Values of f_{de} selected for different classes of soil wetness.

Wetness class BEK	Description	Depth of water logged horizon	f_{de}
0	Unknown	--	0.2
1	No groundwater	--	0.2
2	Moist	below 90 cm, but capillary rise	0.3
3	Slightly wet	60-90 cm	0.4
4	Wet	30-60 cm	0.6
5	Very wet (not occurring on the digital map)	<30 cm	0.7

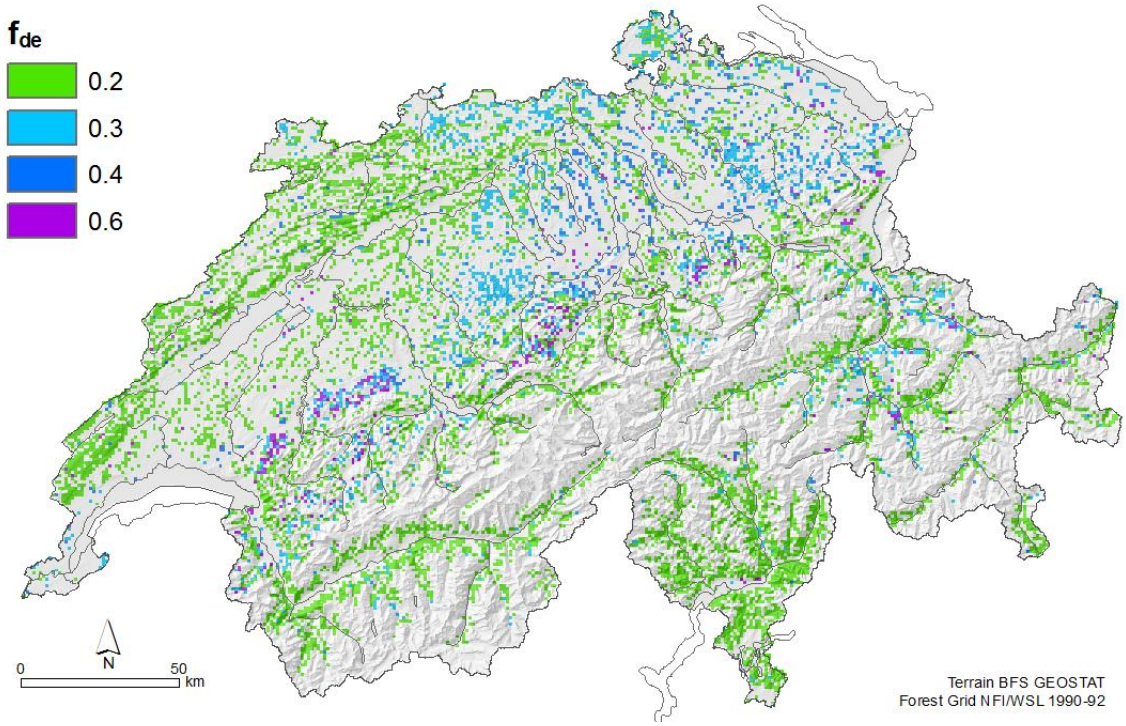

Figure 9: Denitrification fraction values used for forest sites for the SMB method applied on the 1x1 km^2 raster.

3 Mapping nitrogen deposition

3.1 Modelling approach

The general approach for modelling and mapping nitrogen deposition was adopted from Rihm & Achermann (2016) including methodical improvements from Rihm & Künzle (2019). Maps of emissions, concentrations and depositions were calculated for the years 1990, 2000, 2005, 2010, 2015 and newly 2020.

Nitrogen **deposition** (N_{dep}) is defined as the sum of reduced (NH_x) and oxidised (NO_y) nitrogen compounds that are deposited by atmospheric processes to a specified receptor of the environment in a specified time period.

Accordingly, nitrogen deposition is used to compute the **exceedance** of critical loads for nitrogen i.e., of empirical critical loads ($Ex_{emp}N$) as well as of critical loads calculated with the SMB method ($Ex_{nut}N$):

$$Ex_{emp}N = N_{dep} - CL_{emp}N \quad (3.1)$$

$$Ex_{nut}N = N_{dep} - CL_{nut}N \quad (3.2)$$

So far, it is not possible to define separate critical loads for the deposition of NH_x-N and NO_y-N. Therefore, a total N deposition is used for the calculation of exceedances. The exceedance is time-dependent as it is related to the reference period of the deposition. On the other hand, the critical loads are assumed to be time-invariant.

While the critical load computations (see chapter 2) are based on methods described in detail in the UNECE mapping manual, the methods for computing depositions were developed specifically for Switzerland. Corresponding proposals in the mapping manual are more on a conceptual level (CLRTAP 2017, chapter II).

Transboundary air pollutant transport and depositions, which are required for modelling abatement scenarios for the UNECE region, are calculated at the European level with a resolution of 0.1°x0.1° longitude latitude[6].

For national maps, the aim was to estimate ecosystem-specific depositions for the whole area of Switzerland with a high spatial resolution (1x1 km^2 grid or finer), thus, also accounting for the influence of local emission sources. Atmospheric nitrogen deposition was mapped using a pragmatic approach that combines emission inventories, statistical dispersion models, monitoring data, spatial interpolation methods and inferential deposition models. The following nitrogen compounds and deposition paths were considered in the model:

- wet deposition of nitrate (NO_3^-) and ammonium (NH_4^+);

[6] https://emep.int/mscw/emep_grid.html

- dry deposition of gaseous ammonia (NH_3), nitrogen dioxide (NO_2) and nitric acid (HNO_3);

- dry deposition of particulate nitrate and ammonium (secondary aerosols).

As shown in Figure 10, concentrations of the primary gaseous pollutants (NH_3 and NO_2) are modelled by means of emission maps and statistical dispersion models with a resolution of 100x100 m^2 or 200x200 m^2. Thus, the high spatial variability of these pollutants nearby emission sources can be reflected in the models. The concentrations of secondary pollutants (aerosols, HNO_3) as well as the concentrations of N in precipitation are derived from field monitoring results by applying geo-statistical interpolation methods.

Wet deposition is calculated by combining the concentration field of N compounds in rainwater with the precipitation amount (4- or 5-year-averages), see chapter 3.2.

“Inferential” models are used for assessing the dry deposition of gases and aerosols: The concentration maps are multiplied with effective deposition velocities (V_{dep}), which depend on the reactivity of the pollutant, the surface roughness and climatic parameters (Chapter 3.3). Values of V_{dep} were taken from literature. 'Occult' deposition through cloud water or fog is not taken into account.

Maps of nitrogen deposition were calculated for the years 1990, 2000, 2005, 2010, 2015 and 2020, as consistently as possible. For 2000, 2005 and 2010 identical methods were used, i.e. it is a homogenous time series. For the year 1990, a somewhat modified method adapted to the limited availability of ammonia emission data was applied. For the years 2015 and 2020, additional data and refined methods were used for mapping emissions and concentrations of ammonia.

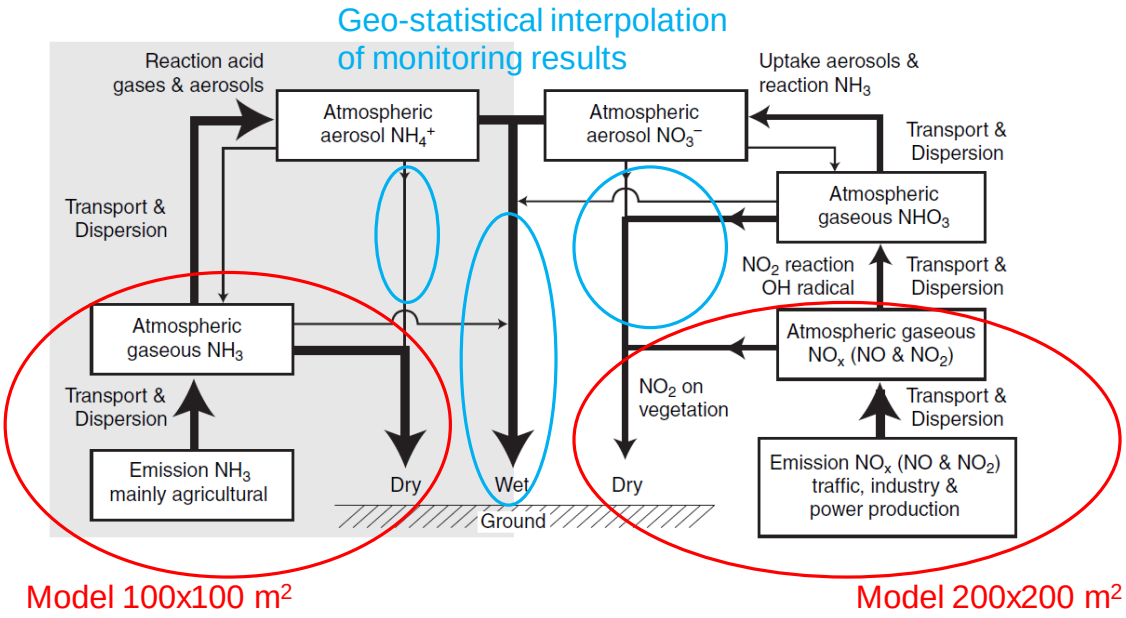

Figure 10: Deposition modelling scheme, based on a figure by Ole Hertel (pers. comm., Hertel et al. 2006).

3.2 Wet Deposition

Wet deposition was obtained by multiplying the annual precipitation rate with mean concentrations of soluble inorganic N compounds in precipitation. For precipitation and concentrations, a 4-year-average (2018–2021) was used. Maps with interpolated precipitation amounts were supplied by MeteoSwiss (2022, see Figure 11). In regions with high precipitation, the calculated deposition can be overestimated as the scavenging effect (wash-out of gases and particles by rain) gets smaller. Therefore, precipitation was limited to maximum of 1'800 mm a^{-1} in the deposition computation.

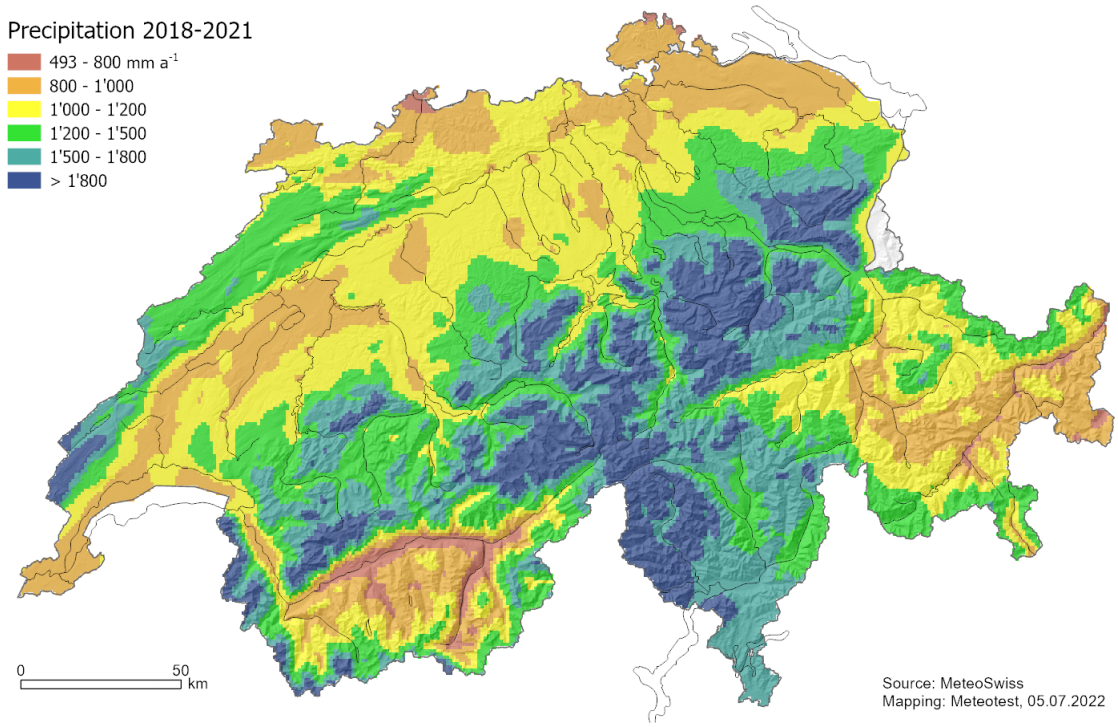

Figure 11: Precipitation, average 2018–2021, 1x1 km² raster.

For mapping concentrations of ammonia (NH_4^+) and nitrate (NO_3^-) in rain water, different approaches are used in Northern and Southern Switzerland.

In Northern Switzerland (including the Alps), data of the National Air Pollution Monitoring Network (NABEL 2022) on wet deposition imply that the concentrations are highest in Central Switzerland (monitoring station Dübendorf) and that they are lower in the Western part of Switzerland (station Payerne). Therefore, the concentrations of Dübendorf and Payerne were interpolated along the west-east axis for altitudes below 800 m. At higher altitudes the concentrations are lower as can be seen in the differences between Payerne (489 m) and Chaumont (1136 m) as well as between Dübendorf (432 m) and Rigi (1031 m). Additional data from bulk measurements made at higher altitudes (Seitler et al. 2021) indicate a decrease in concentration above 800 m. Based on this information we applied a linear decrease of 80% between 800 and 2’500 m altitude and again a constant concentration above 2’500 m.

In Southern Switzerland, the wet-only monitoring network is relatively dense. Besides the NABEL site at Magadino, the Canton Ticino also measures wet deposition at several sites at different altitudes. Concentrations in rainwater and deposition maps were calculated by regression models considering longitude, latitude and altitude. They were initially developed by Barbieri & Pozzi (2001) and updated most recently by Steingruber (2018, 2022). For the period 2018–2021, ammonium and nitrate concentrations in precipitation can be calculated for the region of the Canton Ticino as follows (Steingruber 2022):

$$C_{wet}(NH_4^+) = 29.1 + 0.00004307 \cdot x - 0.0001915 \cdot y - 0.007215 \cdot z$$
$$C_{wet}(NO_3^-) = -21.7 + 0.00007864 \cdot x - 0.00009808 \cdot y - 0.002519 \cdot z$$

where:

$C_{wet}(N)$ = concentration of N-compound in rain water [meq m^{-3}]
x, y = longitude/latitude in Swiss projection LV03[7] (m)
z = altitude (m)

For the nitrate concentrations, a smooth transition from the region of Southern Switzerland to the northern region was applied: the concentrations were reduced between latitude 142'000–152'000 m by 50%.

The resulting rainwater concentration maps are shown in Figure 12.

[7] https://www.swisstopo.admin.ch/en/knowledge-facts/surveying-geodesy/reference-frames/local.html [22.09.2022]

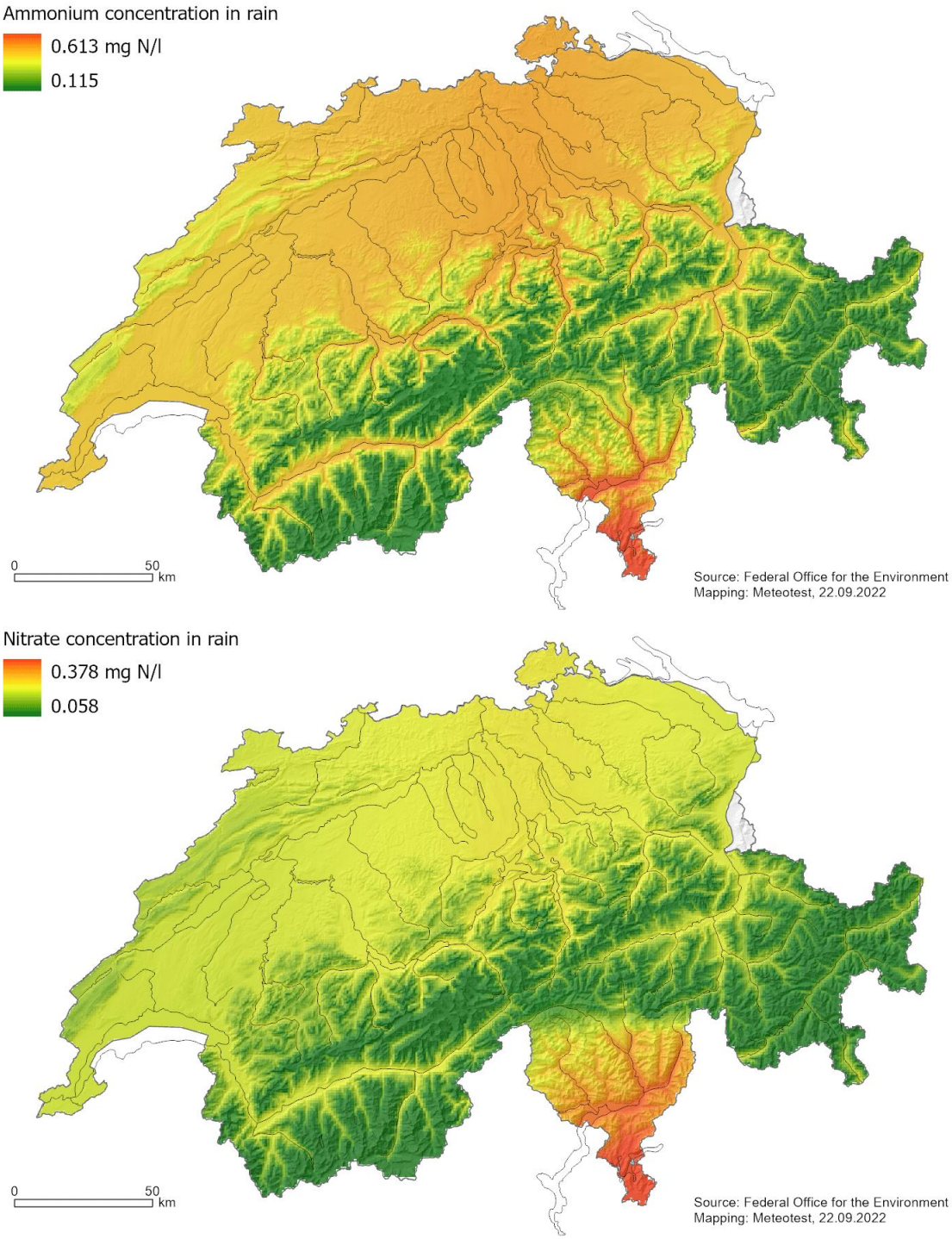

Figure 12: Concentration in rainwater of ammonium (above) and nitrate (below), average 2018–2021, 1x1 km² raster.

3.3 Dry Deposition of Gases

Dry deposition of NH_3, NO_2 and HNO_3 gases was calculated on the basis of modelled air concentrations (annual means) and average deposition velocities (V_{dep}) applying small-scale “inferential models” (CLRTAP 2017, Chapter II). Dry deposition is inferred by multiplying the concentration with the deposition velocity of the component of interest. V_{dep} can be calculated using a resistance model in which the vertical transport to the ground and the absorption of the component by the surface is described.

For NH_3 and NO_2 the air concentrations were calculated applying an emission-dispersion approach (see Figure 10). Emissions, dispersion and concentrations of NH_3 were mapped on a grid of 100x100 m^2. The NH_3 model is presented in detail in Chapter 3.5.

The NO_2 concentration for the period 2018–2021 was available on a 200x200 m^2 raster from the Federal Office for the Environment[8], see Figure 13. They were calculated on the basis of a comprehensive emission inventory for transport, industry, households/commerce and agriculture/forestry (Heldstab et al. 2020) including monitoring results from the specified period.

[8] https://www.bafu.admin.ch/bafu/en/home/topics/air/state/data/historical-data/maps-of-annual-values.html [22.09.2022]

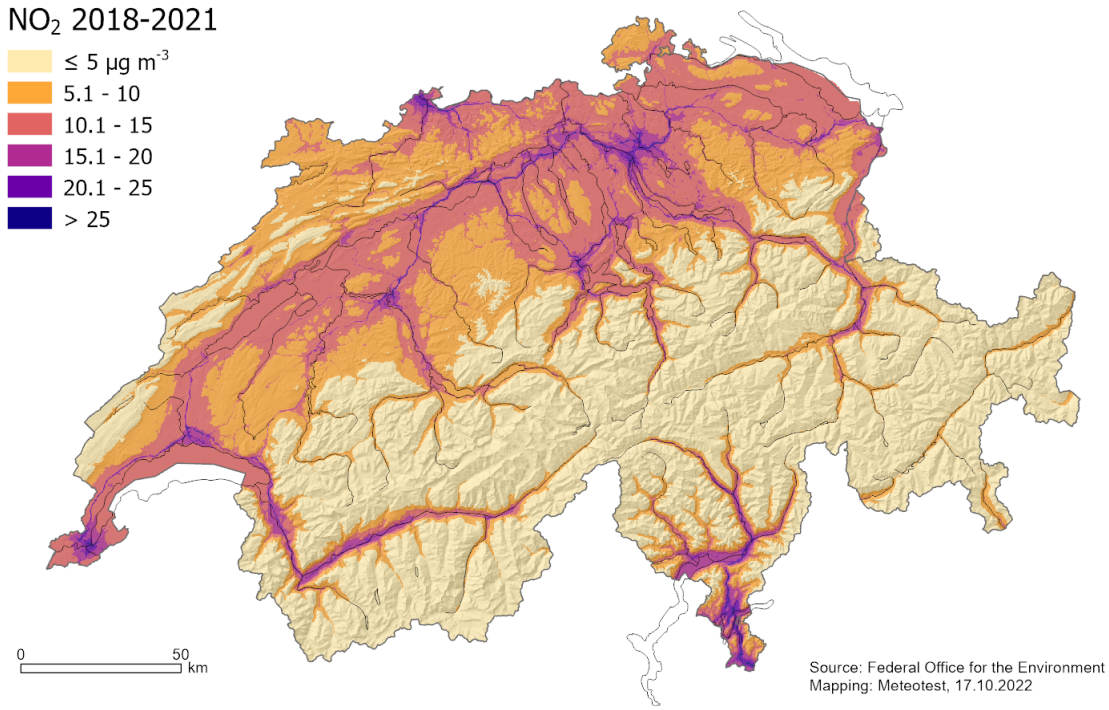

Figure 13: NO_2 concentration, mean 2018–2021, 200x200 m^2 raster.

Measurements of HNO_3 are very rare. Therefore, a basic concentration map for HNO_3 was derived (Rihm & Künzle 2019) from existing maps of air humidity, temperature, ozone concentrations and NO_2 concentrations applying an empirical relationship developed by ICP Materials (UNECE 2005):

$$HNO_3 = 516\ e^{-3400\ /\ (T+273)}\ (Rh\ [O_3]\ [NO_2])^{0.5} \qquad (3.5)$$

Where:

T = temperature in °C, annual mean
Rh = relative humidity in percent, annual mean
$[O_3]$ = ozone concentration in µg m^{-3}, annual mean
$[NO_2]$ = nitrogen dioxide concentration in µg m^{-3}, annual mean

The input maps for temperature, humidity and ozone were produced for the modelling of corrosion rates (Reiss et al. 2004) with a resolution of 250x250 m^2 using geo-statistical interpolation methods. The resulting annual mean concentrations of HNO_3 on this basic map were between 0 and 1.2 µg m^{-3}. In 2014, HNO_3 concentrations were measured at 17 sites in Switzerland (Seitler et al. 2016). They were used to improve the map by fitting with a change factor method. The resulting HNO_3 concentrations are in the range 0–2.5 µg m^{-3} (Figure 14). In 2019, the measurements of HNO_3 concentrations were repeated with similar results as in 2014 (Seitler et al. 2021).

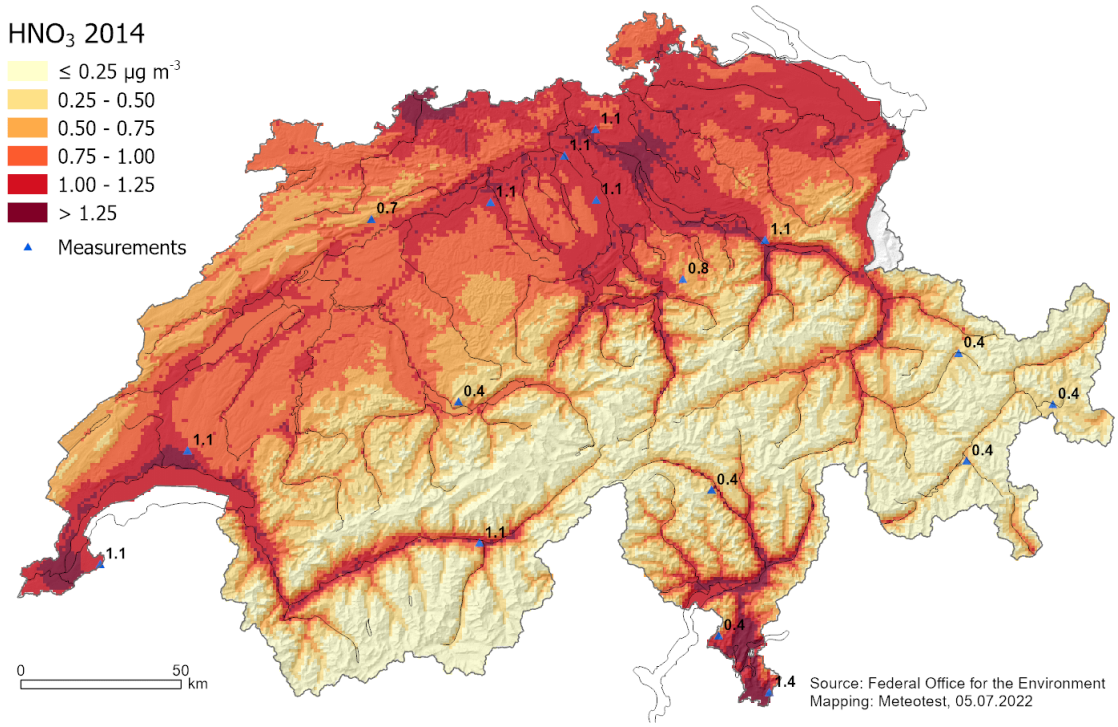

Figure 14: HNO_3 concentrations 2014, 250x250 m^2 raster and monitoring results.

Deposition velocities (V_{dep}) can be calculated using resistance models in which the vertical transport to the ground and the absorption of the component by the surface is parametrised, e.g. the DEPAC modul (van Zanten et al. 2010). Or, they can be measured by micrometeorological measurement techniques (e.g. Brümmer et al. 2022). Both approaches are highly complex and many scientific questions are still open. Flechard et al. (2011) compared several dry deposition models and found differences between models reaching a factor 2–3. Generally, forests have higher V_{dep} than low vegetation (due to higher aerodynamic roughness) and fertilised (agricultural) land has lower V_{dep} than unfertilised (semi-)natural land. The latter is a consequence of elevated ammonia emissions from fertilized land leading to a compensation point (ammonia concentration within the vegetation) above the atmospheric concentration, thus reducing the effective V_{dep}.

For calculating the Swiss deposition maps, average values of V_{dep} from literature were used representing typical conditions for different pollutants and land-use types (Table 7). These values are meant to represent effective annual mean deposition velocities in order that they can be multiplied with annual mean concentrations to calculate annual depositions.

For NH_3, typical values of V_{dep} were optained from literature reviews (Sutton et al. 1994, Loubet et al. 2009, Staelens et al. 2012, Schrader & Brümmer 2014), modelling exercises within the NitroEurope Network (Fléchard et al. 2011, Fléchard et al. 2020), the CAMx model for Switzerland (Aksoyoglu & Tinguely 2018) and recent flux measurements at a German forest site (Brümmer et al. 2020). For Switzerland the following values were used (see Table 7):

- 18–25 mm s^{-1} for forests. Coniferous forests have generally a rougher surface and no needle loss in winter which implicates higher annual V_{dep} in comparison with deciduous forests.

- 12–15 mm s^{-1} for natural or extensively managed low vegetation. Ammonia is absorbed faster by wet surfaces than under dry conditions. Therefore, unproductive vegetation mainly consisting of wetlands and shrubs has a higher V_{dep} than dry grassland.

- 4–10 mm s^{-1} for fertilised areas such as intensively managed cropland and grassland. The effective V_{dep} can be interpreted as an annual net deposition velocity. After the application of nitrogen fertilizers (especially manure) the compensation point is high and the areas are an emission source, while they act as a sink during the rest of the year. Therefore, V_{dep} was set to a lower value of 4 mm s^{-1} if the emission on the site is more than 40 kg NH_3-N ha^{-1} a^{-1}, and to a value of 10 mm s^{-1} if the emission on the site is less than 5 kg NH_3-N ha^{-1} a^{-1} (with linear interpolation in-between).

- 5–8 mm s^{-1} for other areas with no or little vegetation.

Table 7: Effective deposition velocities (V_{dep}) of gaseous pollutant compounds used for the calculation of annual deposition in Switzerland (mm s^{-1}).

Land use ID	**Land use description**	**V_{dep} NH_3**	**V_{dep} NO_2**	**V_{dep} HNO_3**
11	Coniferous forest, >90% coniferous trees	25	4	25
12	Mixed forest, 11–90% coniferous trees	20	3.5	20
13	Deciduous forest, >90% deciduous trees	18	3	18
21	Cropland and grassland (fertilised)	*4-10*	1.5	15
22	Perennial crops (vineyards, fruit trees)	12	1.5	15
31	Pastures, meadows (alps, dry grassland TWW)	12	1.5	15
41	Unproductive vegetation (wetlands, scrub forest)	15	1.5	15
51	Settlements	8	1.5	15
61	Bare land (rocks, glaciers)	5	1	15
62	Surface water (lakes, streams)	8	1	15

V_{dep} for NO_2 are lower than for NH_3. On the basis of values indicated by Lövblad & Erisman (1992), Hornung et al. (1994), Duyzer & Fowler (1994), Hesterberg et al. (1996) and Aksoyoglu & Tinguely (2018), values between 1.5 and 4.0 mm s^{-1} were applied (see Table 7).

For HNO_3 the deposition velocity was set to 15 mm s^{-1} for all non-forest land use types. For forest, the same values as for NH_3 were used (see Table 7). This V_{dep} is based on values listed by Riedmann & Hertz (1991), Lövblad & Erisman (1992), Wesley & Hicks (2000), and Aksoyoglu & Tinguely (2018). According to Duyzer & Fowler (1994) the canopy resistance to uptake of HNO_3 is negligible, thus leading to a very efficient deposition to the cuticle and to a dominant stomatal uptake.

The land-use types shown in Table 7 are defined on the basis of the Swiss Land-use Statistics (SFSO 2021, survey 2014/2018, hectare raster) and two raster data sets indicating the forest type (forest mix rate of coniferous and deciduous trees): Primarily, a new data set with 10 m resolution is used (BAFU/WSL 2021); where data are missing in the new data set the information from a former data set (SFSO 2004) is included.

3.4 Dry Deposition of Aerosols

Dry deposition of aerosols includes (1) the gravitational sedimentation of aerosols not bound to precipitation, and (2) the interception, which is the filtering effect of the vegetation through horizontal impact of aerosols. Sedimentation and interception are treated together since they both depend on wind speed and surface properties of the vegetation layer. The dry deposition is calculated by multiplying the concentration in the air with altitude- and receptor-dependent deposition velocities.

The concentrations of particulate ammonium and nitrate (secondary aerosols) were modelled for the year 2020 by Heldstab et al. (2020) as shown in Figure 15. According to chemical analysis of PM10 at sites on the Central Plateau, the mean concentration was approximately 1.1 µg NH_4^+ m^{-3} and 2.4 µg NO_3^- m^{-3} (Hüglin & Grange 2021). The concentrations decrease clearly with altitude.

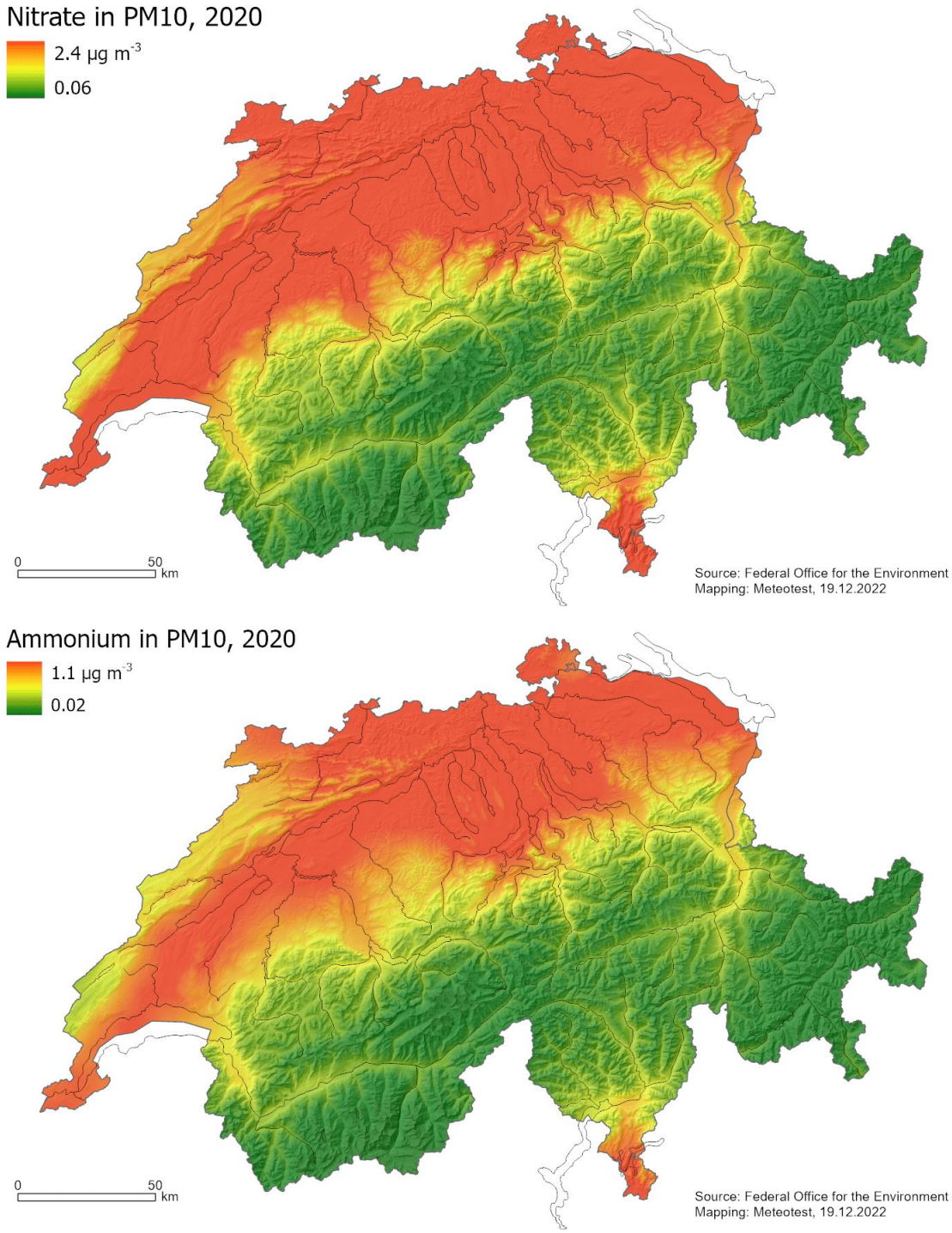

Figure 15: Concentration in aerosols (PM10) of ammonium (above) and nitrate (below), modelled for the year 2020, 100x100 m² raster (Heldstab et al. 2020).

V_{dep} are average values obtained from literature (e.g. Lövblad & Erisman 1992, Asman & van Jaarsveld 1992, Lövblad et al. 1993; Duyzer (1994), Fangmeier et al. 1994, Hesterberg et al. 1996, Loubet et al. 2009). An estimate of the altitude

dependence of V_{dep} for Switzerland was observed by Riedmann & Hertz (1991) as follows (see Table 8):

$$V_{dep}(900m) = 2 \cdot V_{dep}(450m) \quad (3.6)$$

The increase of V_{dep} with altitude can be explained by the fact that the average wind speed also increases strongly, rising from 450m to 900m a.s.l in the Central Plateau. Thereby the filtering effect of vegetation is reinforced. Between 900 m and 2000 m an increase also exists, although this is smaller.

The additional filtering effect of forests is taken into account by using deposition velocities that are 1.5–2.5 times higher than for open fields (see Table 8).

Table 8: Effective deposition velocities (V_{dep}) of aerosols containing ammonium and nitrate depending on altitude and land use.

Altitude	**Land-use ID, description**	**V_{dep} mm s^{-1}**
≤ 400 m	11: coniferous forest	2.5
	12: mixed forest	2.0
	13: deciduous forest	1.5
	21–62: non-forest	1.0
≥ 800 m	11: coniferous forest	5.0
	12: mixed forest	4.0
	13: deciduous forest	3.0
	21–62: non-forest	2.0
400–800 m	linear interpolation	

3.5 Mapping Ammonia

3.5.1 Emissions of Ammonia

a) Overview

The emissions of ammonia were modelled based on livestock census 2020 (SFSO 2021b), livestock emission factors for the year 2020 (Kupper et al. 2022), the national inventory of air pollutants (FOEN 2021) and model results for emissions from road transportation (Heldstab et al. 2021). Foreign emissions within a distance of 50 km to the Swiss border were taken from the EMEP dataset for the year 2019[9], which has a resolution of approximately 7 by 10 km^2.

[9] Download from https://www.ceip.at/the-emep-grid/gridded-emissions/nh3 [05.04.2022]

Table 9 shows a summary of the total emissions in Switzerland: agriculture is the main source of NH_3 accounting for about 93% of total ammonia emissions, other anthropogenic sources account for 6% and natural sources for 1%.

The emission maps were calculated with a resolution of 100x100 m^2. Figure 16 shows the map of total NH_3 emissions in 2020. The following sections show the mapping methods in more detail.

Table 9: Swiss ammonia emissions for different source categories in 2020 modelled with 100x100 m^2 resolution[1].

Source category	Emission (kt NH_3-N a^{-1})	Percent
Housing/hardstandings	13.81	30.8%
Storage of manure	6.80	15.2%
Application of manure	16.89	37.7%
Grazing	1.17	2.6%
Total livestock	**38.68**	**86.3%**
Mineral fertilizers	2.05	4.6%
Organic recycling fertilizers	0.78	1.8%
Cropland, grassland, alpine pastures	-	0.0%
Total plant production	**2.83**	**6.3%**
Total agriculture	**41.51**	**92.7%**
Commerce and industry	0.41	0.9%
Transport	0.75	1.7%
Households	0.79	1.8%
Waste treatment	0.74	1.6%
Total non-agriculture	**2.68**	**6.0%**
Natural sources	**0.60**	**1.3%**
Total emission	**44.79**	**100.0%**

[1] The values are slightly different from the totals by Kupper et al. (2022) due to the rasterization process and some generalizations in cattle categories.

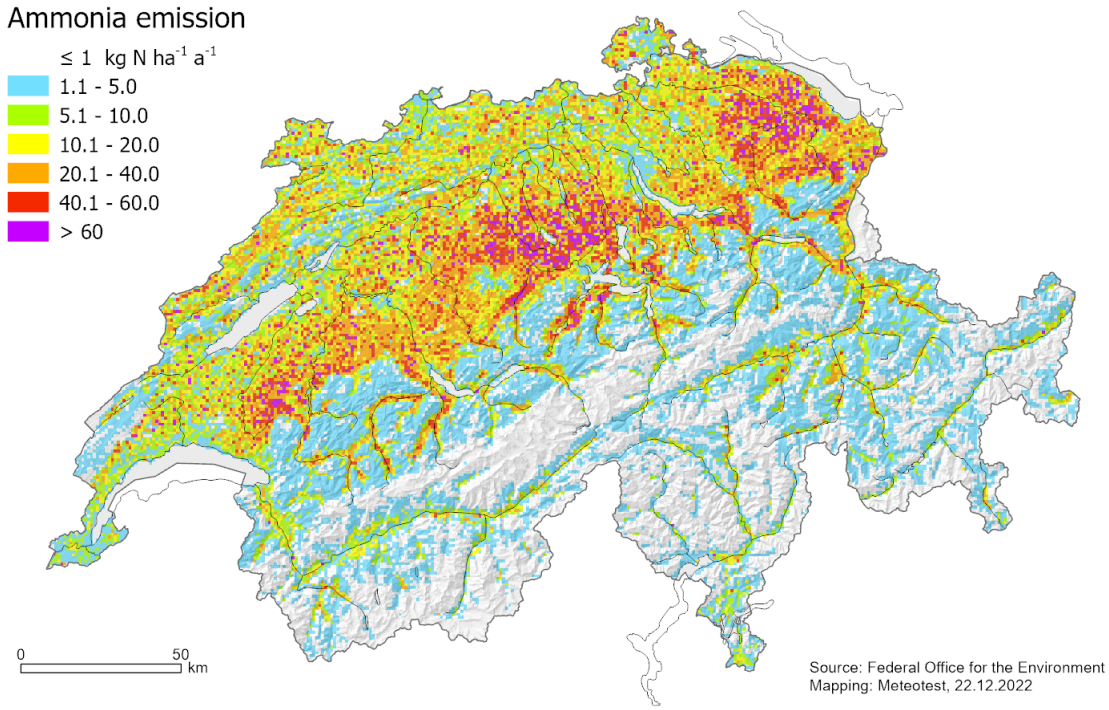

Figure 16: Ammonia emissions 2020, modelled on 100x100 m² raster.

The emissions from animal husbandry were modelled with livestock statistics of the year 2020 (SFSO 2021b) using a 'bottom-up' approach (i.e. with georeferenced activity data and emission factors). The emissions from traffic were also modelled 'bottom-up'. The other emission categories (crop farming, industries, households, waste treatment and natural sources) were spatially allocated in a top-down approach to the relevant categories of a land-use map. The procedure is summarised in the following sections.

b) Emissions from livestock/animal production

The SFSO (2021b) supplied the livestock per farm as well the locations of 49'289 farms (coordinates rounded to hectometres). Livestock data included the number of animals at the reference date (January 1st) as well as the number of animals that had spent the summertime on summering pastures in the Alps or in the Jura mountains. Therefore, the NH_3-emissions occurring during the summering period were subtracted from the total emissions and mapped separately (see chapter 3.5.1 d).

In 2020, there were 41'378 farms reporting livestock data. Hence, the emissions from animal husbandry were calculated for each of these farm (f) as:

$$E(f)_s = \sum_a (N(f)_a \cdot EF_{acs}) \qquad \text{(Equation 3.1)}$$

where:

$E(f)_s$	=	NH_3-emissions on the farm f at the emission stage s [kg NH_3-N a^{-1}].
s	=	emission stage (housing, manure storage, manure application, grazing)
$N(f)_a$	=	number of animals in category a on the farm f.
a	=	animal category (see Table 10).
EF_{acs}	=	emission factor of animal category a in farm class c at the emission stage s [kg NH_3-N a^{-1} $animal^{-1}$].
c	=	farm class; combines geographic region, altitude zone and production type.

For each farm, the livestock numbers were multiplied with emission factors that are stratified into 24 animal categories, 6 emission stages ("Stufen") and 40 farm classes ('Schichten'). The fully stratified emission factors (not shown) were calculated with the Agrammon model by Kupper & Häni (2021). Farm classes account for the differences in production techniques in various regions of the country, also reflecting the implementation of emission reduction measures. It is derived by combining three geographic regions (Central, Eastern and Western/Southern Switzerland), three altitude zones (valley, hill and mountain) and five production types (arable farms, cattle farms, pig/poultry farms, mixed farms and other farms) as shown by Kupper et al. (2022).

Table 10 presents an overview of the total animal numbers in Switzerland, the mean emission factors (emission per animal) for four emission stages (housing/exercise yards, storage of liquid and solid manure, application of liquid and solid manure, grazing) and the resulting total emissions from animal husbandry. The mean emission factors per animal and stage were calculated by dividing the total emission of all farms by the total number of animals.

The total mapped emission in Switzerland from animal production amounts to 38.7 kt NH_3-N. This is 0.7% more than the results given by Kupper et al. (2022) for the year 2020. The difference is due to the use of a simplified method for transforming the cattle categories of the census (SFSO 2021b) to the animal categories used in the Agrammon model (Table 10).

Table 10: Emission factors, number of animals and total NH_3-emissions for the 24 animal categories used in the mapping process for the year 2020.

Code	2020 Animal category	Emission factor (kg NH_3-N/a per animal) Housing, exercise yards	Storage manure	Application manure	Grazing	Total	Number of animals	Emission (kt NH_3-N/a)
DC	Dairy cows	9.44	6.26	17.45	0.86	34.01	546'479	18.58
H1	Dairy followers <1 year	2.49	1.39	3.14	0.27	7.27	202'465	1.47
H2	Dairy followers 1–2 years	3.41	1.91	4.58	0.62	10.52	202'628	2.13
H3	Dairy followers >2 years	4.79	2.76	6.87	0.77	15.19	105'302	1.60
SC	Suckling cows	8.64	4.29	9.43	1.20	23.57	131'384	3.10
CS	Pre beef-fattening calves	2.28	1.13	2.23	0.33	5.97	88'863	0.53
BC	Beef cattle	3.78	2.49	5.55	0.16	11.98	157'262	1.88
FC	Beef calves	2.02	1.42	2.64	0.01	6.10	80'709	0.49
PD	Dry sows	6.97	1.11	2.62	0.00	10.70	80'972	0.87
PN	Farrowing sows	8.06	2.37	5.25	0.00	15.69	26'326	0.41
PP	Piglets <25 kg	0.66	0.19	0.42	0.00	1.27	284'881	0.36
PE	Boars	3.99	0.63	1.54	0.02	6.18	2'378	0.01
PF	Fattening pigs	2.94	0.57	1.42	0.00	4.93	807'849	3.98
PG	Poultry growers	0.04	0.01	0.02	0.00	0.08	1'149'653	0.10
PL	Laying hens	0.11	0.04	0.08	0.02	0.24	3'854'017	0.94
PB	Broilers	0.04	0.01	0.04	0.00	0.09	10'083'364	0.95
PT	Turkeys	0.18	0.03	0.13	0.02	0.36	88'373	0.03
PO	Other poultry	0.08	0.05	0.05	0.01	0.19	24'011	0.00
HU	Horses >3 years	4.42	2.42	1.25	0.50	8.59	43'921	0.38
HL	Horses <3 years	3.55	1.78	1.13	0.73	7.19	3'059	0.02
OA	Ponies, donkeys, mules	1.62	0.89	0.55	0.16	3.21	33'092	0.11
OS	Sheep	1.04	0.64	0.32	0.33	2.32	206'257	0.48
OM	Milk sheep	1.91	1.16	0.42	0.27	3.76	13'816	0.05
OG	Goats	1.41	0.74	0.54	0.29	2.97	60'364	0.18
	Total							38.68

For spatial attribution of emissions, it was assumed that the emissions from housing, exercise yards and manure storage are located in the same hectare-cell as the farm buildings (total 20.6 kt NH_3-N a^{-1}, see Table 9). The emissions from manure application and grazing (total 16.9 and 1.2 kt NH_3-N a^{-1}, respectively, see Table 9) were distributed over the agricultural areas within the corresponding municipalities.

Municipality boundaries (version 2006) were used as a proxy for the land managed by the farms as the information which parcels belong to a specific farm was not available in this project. The municipality areas are available in digital form at swisstopo (2006). The size of the 2'827 municipalities varies from about 3 km^2 in the Plateau to more than 100 km^2 in alpine regions (average 14 km^2). Inside each municipality, the land use-map (SFSO 2021, nomenclature NOAS04, survey 2014–2018) with a resolution of one hectare and 72 categories was used to en-

hance the accuracy of the spatial emission pattern. For the emissions from manure application, this was done by weighting the land-use categories as follows (land-use code in parenthesis):

- Weight = 1.00: meadows (42)
- Weight = 0.75: field fruit trees (38), arable land (41)
- Weight = 0.50: orchards (37), horticulture (40), farm pastures (43)
- Weight = 0.25: vineyards (39), brush meadows/farm pastures (44), and - if not in the summering pasture region (see FOAG 2021) - alpine meadows (45) and favourable alpine pastures (46). These categories are assumed to emit much less ammonia than arable land and regular meadows because fertilization is less intense.

For the emissions from grazing the following weighting was used:

- Weight = 1.00: farm pastures (43)
- Weight = 0.50: favourable alpine pastures (46), if not in the summering pasture region (see FOAG 2021)
- Weight = 0.25: field fruit trees (38), meadows (42), brush meadows/farm pastures (44)

All other land-use categories were excluded from the area sources. Furthermore, all areas protected by the Federal Inventories of Raised and Transitional Bogs, of Fenland and of Dry Grassland (see chapter 2) were excluded as fertilizing is generally not allowed.

c) Accounting for manure transport (HODUFLU)

Swiss farmers are obligated to register each transport of manure from and to their farm in a central database named HODUFLU (*Hofdüngerflüsse*). The database is hosted by the Federal Office for Agriculture (FOAG)[10]. Besides manure, it includes also transport of recycling fertilizers as well as transport to biogas or composting facilities. Obviously, this translocation of manure influences the spatial distribution of ammonia emissions from manure application. Therefore, the registered shipments of the year 2020 were used to account for this effect in the emission map.

The HODUFLU data were processed by Hutchings (2021) in the MODIFFUS project (Hürdler et al. 2015, Hutchings et al. 2023). The Federal Office for Agriculture (FOAG) provided anonymized records of manure shipments in 2020 containing

[10] https://www.blw.admin.ch/blw/de/home/politik/datenmanagement/agate/hoduflu.html [20.12.2022]

15.0 kt N. Spatial evaluation of the transport routes were inferred based on the zip-codes of the sender and the recipient (Figure 17). Coordinates and GIS-data of the zip-codes are supplied by the Geodesy and Federal Directorate of Cadastral Surveying[11].

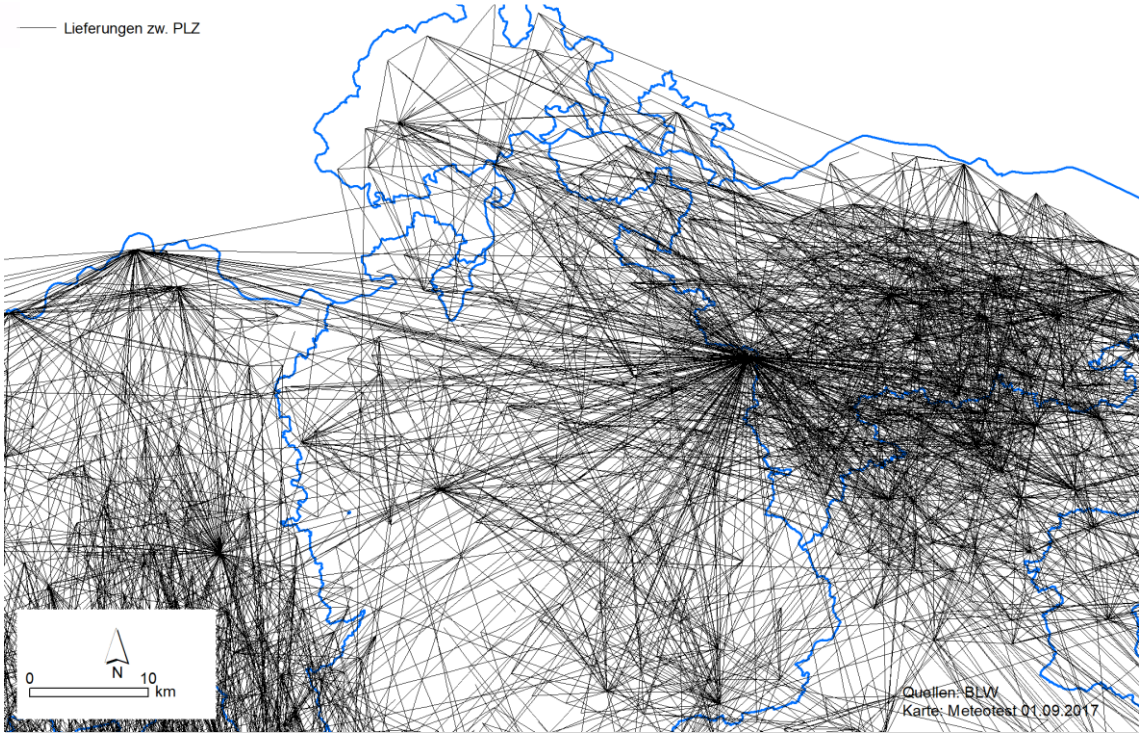

Figure 17: Transportations of manure defined by linking the zip-codes of the sender and the receiver (example of the year 2015, FOAG 2017a). The map shows North-eastern Switzerland. Large clusters can indicate major biogas/composting facilities or companies involved in manure transport. Blue lines: cantonal borders.

In addition to the zip-codes and the amount of total N (N_{ges}), the transportation receipts indicate the type of sender, the type of receiver and the product specification. The types of sender/receiver are: biogas facilities, composting facilities and farms. With this information, the deliveries that are relevant for the ammonia emissions can be extracted and their net balance for each zip-code can be calculated. Table 11 shows a summary of the nitrogen amounts transferred between the different sender/receiver types and the product categories in 2020 (Hutchings 2021). The following transfers are relevant for the emissions from manure application:

- Deliveries from farms to farms (all products) cause lower emissions at the sender and higher emissions at the receiver (highlighted in blue, Table 11).

[11] https://www.cadastre.ch/en/services/service/registry/plz.html [21.12.2022]

- Deliveries from farms to biogas/composting (all products) cause lower emissions at the sending farms (highlighted in green, Table 11).

- Deliveries from biogas or composting facilities to farms cause higher emissions at the receiving farms (highlighted in red, Table 11).

The sum of the relevant fluxes is 15.0 kt N. Manure and recycling fertilizers cannot be strictly separated if biogas or composting facilities are involved in the transfers. However, the data in Table 11 show a net nitrogen input to farms of around 3.2 kt N coming from non-agricultural biomass. Assuming a mean emission rate of 21%, this net input corresponds to an ammonia emission of 0.66 kt NH_3-N, which is comparable to the emission amount for recycling fertilizers in Table 9.

Table 11: Transfers of nitrogen between biogas/composting facilities and agriculture (farms) for different products in 2020 (Hutchings 2021, FOAG/HODUFLU). The highlighted transfers are related to emissions of manure application on farms (see text).

Type of transfer	Product	t N
From farm to farm	**Total**	**5'217**
	Crop residues	0
	Liquid manure	3'666
	Solid manure	1'550
From farm to biogas/compost facility	**Total**	**3'296**
	Crop residues	215
	Liquid manure	1'418
	Solid manure	1'664
From biogas/compost facility to farm	**Total**	**6'454**
	Industrial biogas facilities	**2'373**
	Solid digestate	417
	Liquid digestate	1'937
	Unspecified digestate	19
	Agricultural biogas facilities	**2'565**
	Thin liquid manure	760
	Liquid manure	1'704
	Solid manure	100
	Composting facilities	**1'516**
	Compost	1'516
All transfers		**14'967**

By summing up all relevant transports, the net balance of the fluxes can be calculated per zip-code. Figure 18 shows a map of the net nitrogen fluxes per zip-code area.

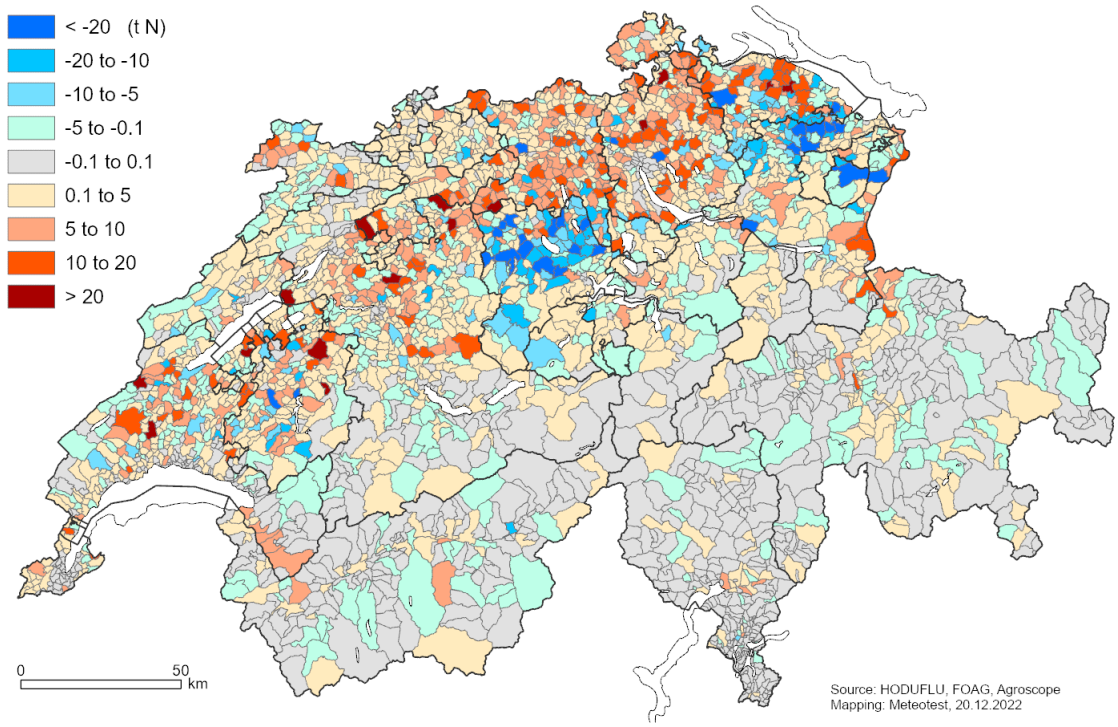

Figure 18: Net nitrogen fluxes per zip-code caused by manure transports in 2020. Negative values indicate net export (blue-green colours), positive values mean net import (orange-red colours). Data source: Hutchings 2021, Federal Office for Agriculture (FOAG), HODUFLU data base.

There are several zip-code areas with very high exports or imports (see Figure 18) that can be explained by large biogas/composting facilities or transportation companies located at these sites. Such highly frequented nodes can also be seen in Figure 17. It can be assumed that those high net fluxes are not related directly to manure application but are rather due to effects of the high storage capacities at those facilities such as inter-annual shifts.

For adjusting the NH_3-emisson map from manure application, the transported amount of nitrogen was converted to the respective emission of NH_3-N by a factor of 21%. This value was derived from results of the Agrammon model supplied by Bonjour & Kupper (2017); along with emission factors (EF, see Table 10) they calculated average fluxes of nitrogen fed to manure storage for different animal categories. The factor was calculated as: (EF of application) / (N to application) for dairy cows and fattening pigs and by weighting with the frequency of the farm class.

The influence of manure transport on ammonia emissions from manure application calculated per zip-code was spatially transferred to the agricultural areas where manure is applied (i.e. meadows, arable land, field fruit trees, orchards, horticulture, farm pastures, see chapter 3.5.1 b) using a GIS-density function with a radius of 4 km. The resulting map in Figure 19 confirms that ammonia emissions are generally translocated from areas with very high livestock densities to

areas with lower densities. The total amounts of reductions and additions are 0.66 kt NH_3-N, corresponding to the net input of non-agricultural biomass by recycling fertilizers.

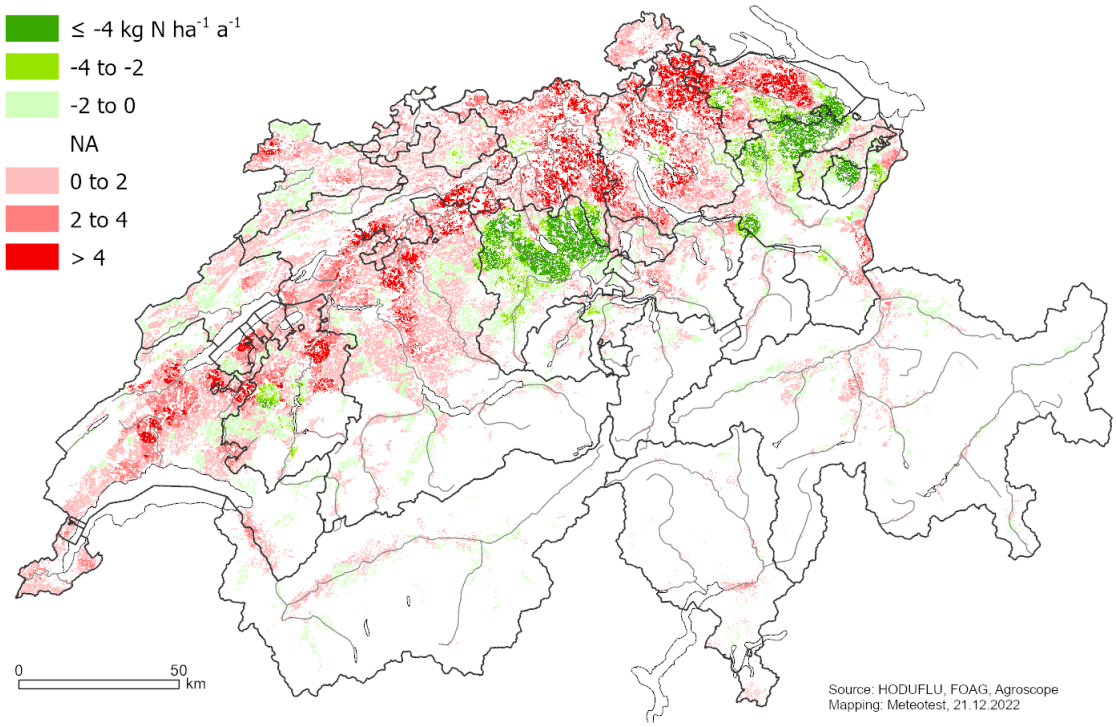

Figure 19: Reductions and additions of the ammonia emissions from manure and recycling fertilizers caused by fertilizer transports according to the HODUFLU database 2020 (FOAG, Hutchings 2021).

d) Summering of animals on alpine pastures

For each farm, the livestock statistics (SFSO 2021b) also provided the number of cattle, horses, sheep and goats spending the summer up on the alps. The summering period is defined to last 100 days. In 2020, there were 20'428 farms reporting summering of animals. The emissions of those animals during summering were calculated with the stratified emission factors (Kupper & Häni 2021) for the stages housing, manure application and grazing by considering the relative length of the summering period (factor 100/365). As a best guess, it was assumed that the emissions by manure storage are not altered or relocated by summering.

The emissions by summering were subtracted from the yearly emissions of each farm reporting summering of animals; for further processing see chapter 3.5.1b. The total emission by summering in 2020 amounted to 1.801 kt NH_3-N. Most of the summered animals come from farms in the mountain valleys of the Alps and Jura. But also in large parts of the Swiss Plateau, there are farms sending animals to the alps. As an example, Figure 20 shows the origin of summered animals and corresponding emission subtractions.

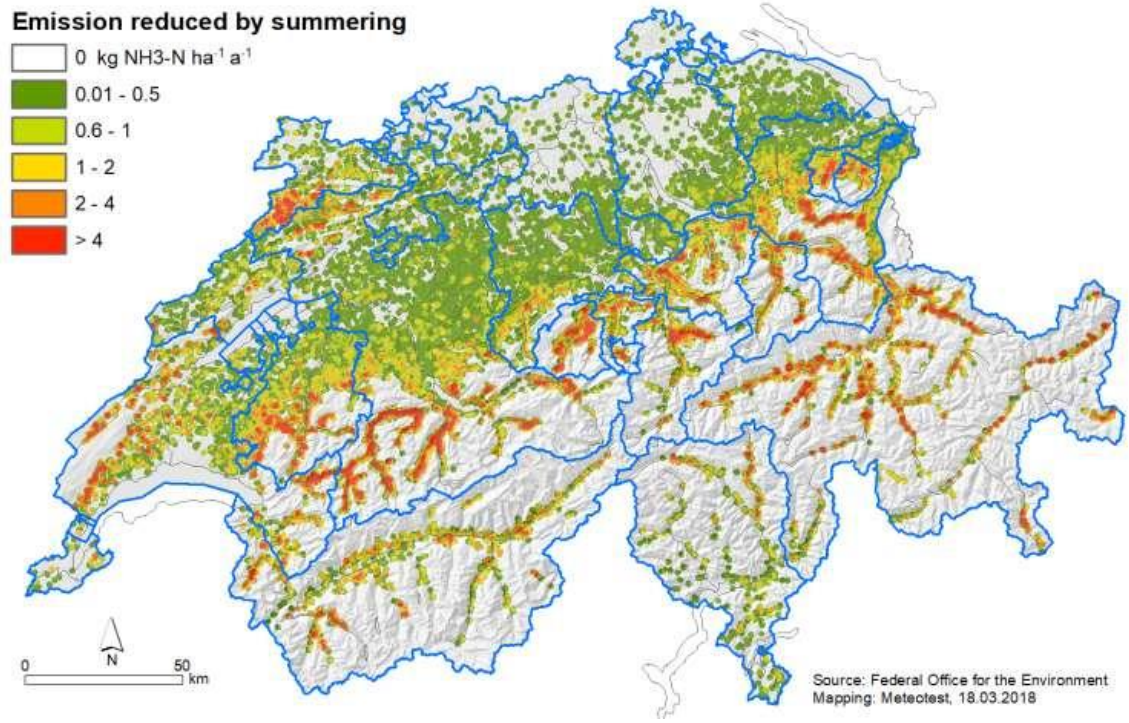

Figure 20: The emissions of summered animals are subtracted from the yearly emissions on each farm sending animals. The map shows these emission reductions in 2015; for better display a GIS-density function (radius 2 km) was applied. Data source: SFSO 2017. Blue lines: cantonal borders.

As there was no explicit information where the summered animals exactly go to, further auxiliary data were used for mapping the summering emissions. We assumed that the summering emissions (1.801 kt NH_3-N) occur on the land-use category "alpine agricultural areas" (NOAS04 codes 45–49, SFSO 2021). The emission rates on those areas were weighted according to the expected intensity of summering activities.

For estimating the summering intensity, the database of the Swiss summering farms (*Sömmerungsbetriebe,* farms in operation only seasonally) was used as well (FOAG 2017b). The database contains the location of the summering farm (alp) and its regular carrying capacity expressed as NST (*Normalstoss*); NST is defined as one livestock unit (LSU, *Grossvieheinheiten GVE*) summered for 100 days. As can be seen in Figure 21, the database is quite heterogenous and data are missing for several cantons[12]; the map presents the result of a GIS-density function spreading the NST of each alp within a radius of 2 km (units NST/ha).

[12] A further database (not considered at the time of modelling) with detailed information on summering farms has been published by SAB (*Schweizerische Arbeitsgemeinschaft für Berggebiete*): http://www.alporama.ch/gv2/get/get_ov_Kanton.asp

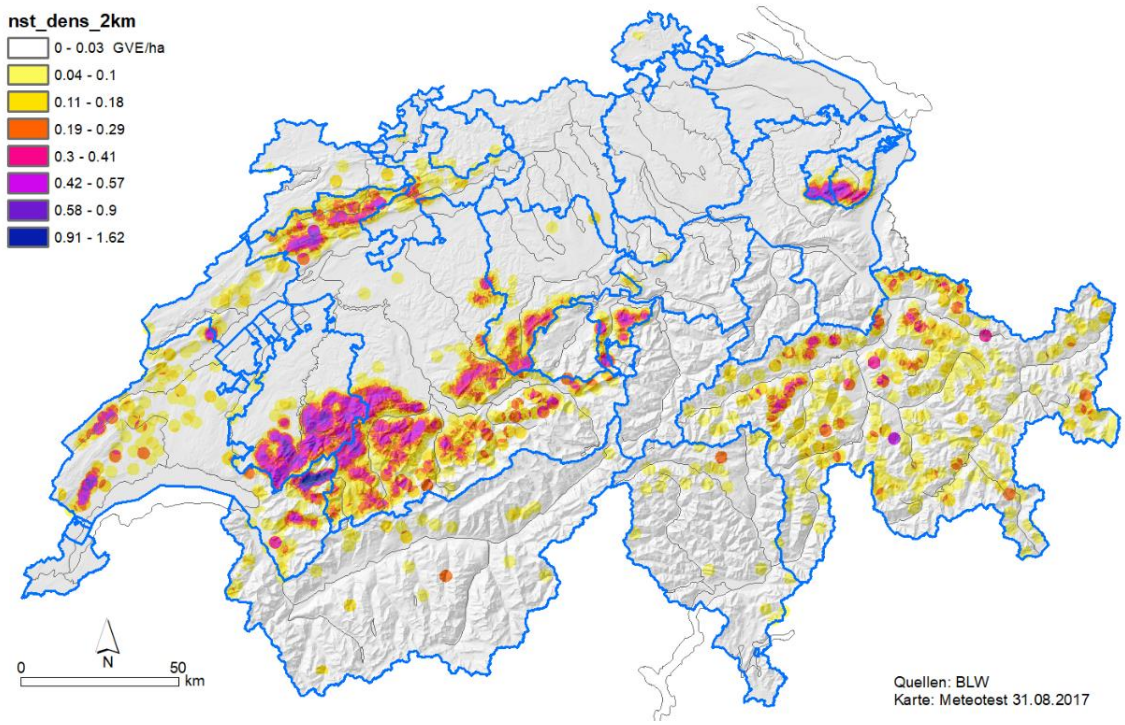

Figure 21: Carrying capacity of the summering farms (alps) provided by FOAG (2017b). The number of livestock units (LSU) per site were transformed to LSU/ha by a GIS-density function with radius 2 km. Blue lines: cantonal borders.

As the summering farm data were quite incomplete, further information on the possible weighting of alpine pastures was derived from the calculated emissions of the "sending" farms (see Figure 20): The summering-related emissions on the "sending" farms were dispersed by a density function within a radius of 8 km (units kg NH_3-N/ha). The result is shown in Figure 22 (weight sending farms); regions with a density of more than 0.4 kg NH_3-N/ha are highlighted.

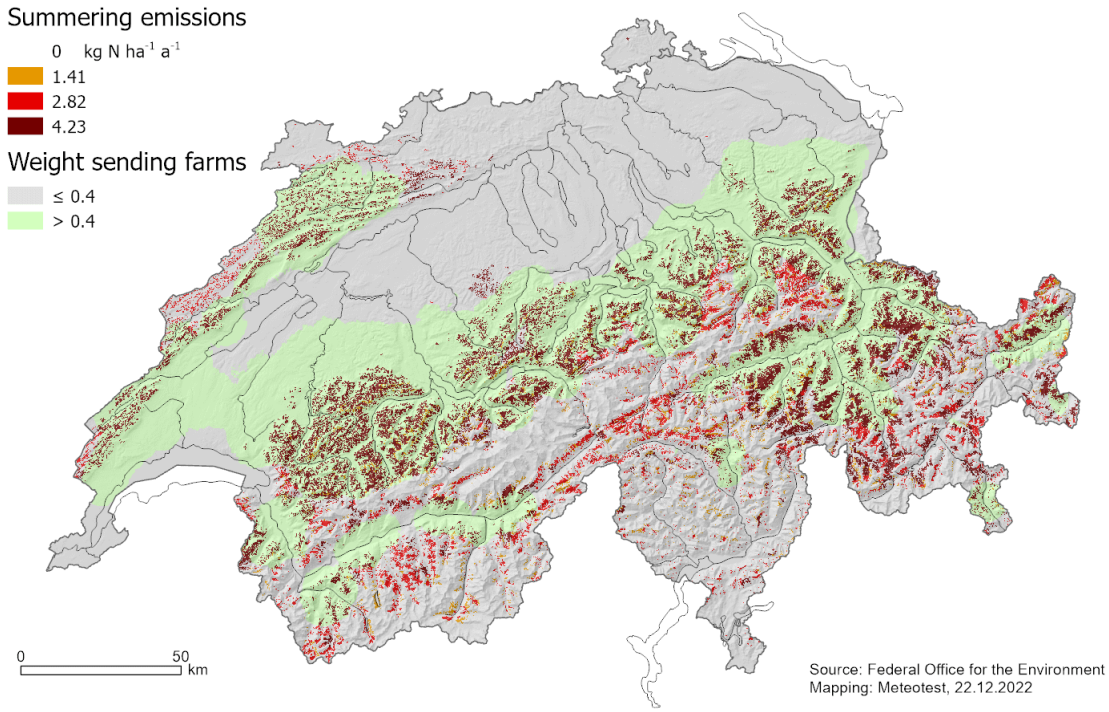

Figure 22: (1) Weight of farms sending the summering livestock calculated from the respective ammonia emissions by a density function with radius 8 km. (2) Ammonia emissions from alpine agricultural areas due to summering.

Finally, the alpine agricultural areas were weighted, with regard to ammonia emissions by summering, as follows (land-use codes in parenthesis):

- Weight = 0.33: sheep pastures (49).
- Weight = 0.66: remote areas that are covered by alpine meadows (45), favourable alpine pastures (46), brush alpine pastures (47) or rocky alpine pastures (48).
- Weight = 1.00: accessible areas that are covered alpine meadows (45), favourable alpine pastures (46), brush alpine pastures (47) or rocky alpine pastures (48).

The accessible areas were defined by a carrying capacity of the summering farms greater than 0.03 LSU/ha (Figure 21) or by a weight of the sending farm greater than 0.4 kg NH_3-N/ha (Figure 22). All other areas were considered as remote areas.

With the total summering emissions of 1. 801 kt NH_3-N, the resulting emission rate for an area with a weight 1.00 is 4.23 kg NH_3-N/ha as shown on Figure 22.

e) Emissions from plant production

Emissions from the application of mineral fertilizer and organic recycling fertilizer are 2.05 and 0.78 kt NH_3-N a^{-1}, respectively (see Table 9). By accounting for the fertilizer transport (see chapter 3.5.1 c), 0.66 kt NH_3-N a^{-1} from recycling fertilizer were already included and subtracted here. The remaining emissions were distributed top-down over the following land-use categories using the land-use map by SFSO (2021):

- Weight = 1.00: golf courses (33), orchards (37), field fruit trees (38), vineyards (39), horticulture (40), arable land (41), farm pastures (43)
- Weight = 0.50: meadows (42). It is assumed that meadows are fertilized preferably by manure.

Further emissions on agricultural land arising from decomposition of plant material were reported until 2017 (FOEN 2017b). In more recent emission inventories this category (NFR code 3Db) has been omitted.

f) Non-agriculture emissions

Emissions from commerce and industry (0.41 kt NH_3-N a^{-1}, see Table 9, adopted from FOEN 2021) were distributed over the land-use categories 'industrial and commercial areas' (SFSO 2021, codes 1 and 2).

The ammonia emissions from road transportation (0.71 kt NH_3-N a^{-1}, see Table 9) were mapped by a bottom-up approach based on a traffic model for the year 2020 using methods and emission factors as described by Heldstab et al. (2021). The traffic model includes the main road-networks and zonal traffic. The emissions on the road-links were converted to a hectare raster. The zonal emissions were allocated to a ha-raster according to population density and settlement areas.

Emissions from households (0.79 kt NH_3-N a^{-1}, see Table 9, adopted from FOEN 2021) were distributed over the land-use categories (SFSO 2021) for residential areas (codes 3–8), agricultural building areas (codes 11 and 12) and garden allotments (code 35).

Emissions from waste treatment (0.74 kt NH_3-N a^{-1}, see Table 9, adopted from FOEN 2021) were distributed over the land-use categories 'waste water treatment plants' and dumps (codes 25 and 27).

Natural emissions (0.60 kt NH_3-N a^{-1}, see Table 9, adopted from Kupper et al. 2013) originate from soil processes on natural grassland as well as from wild animals. They were distributed over the land-use categories wooded areas (codes 50–60) and unproductive vegetation (codes 64–67).

The total non-agricultural emissions (3.28 kt NH_3-N a^{-1}) are shown in Figure 23.

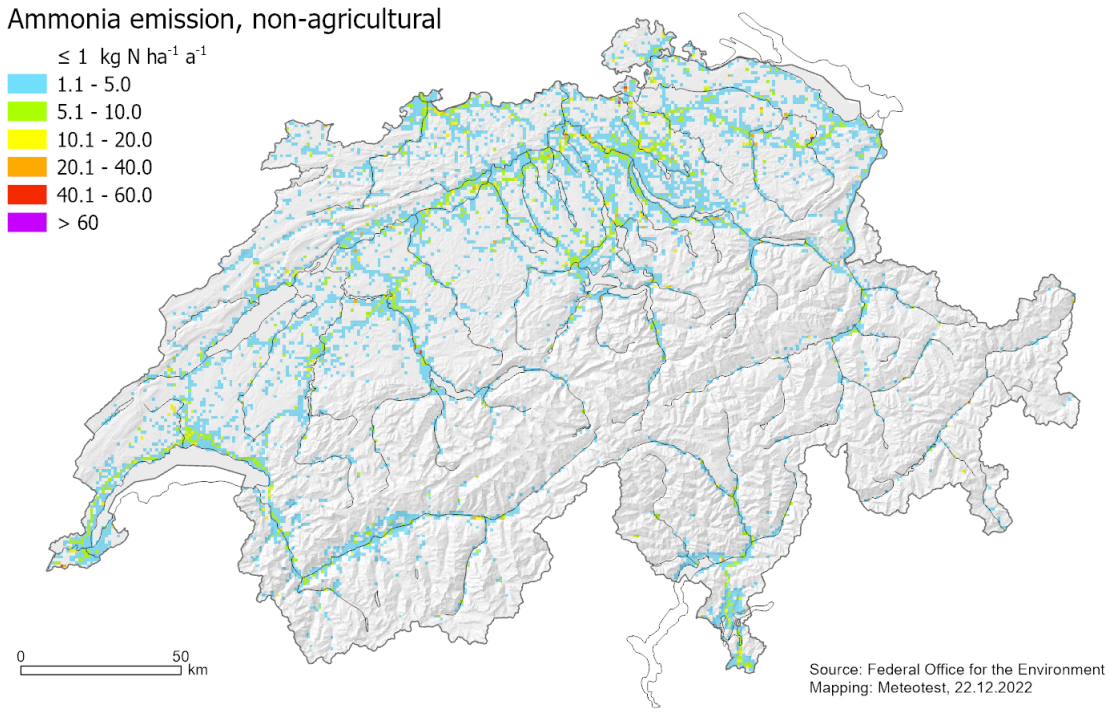

Figure 23: Non-agricultural ammonia emission 2020.

3.5.2 Ammonia Concentration

A statistical dispersion model with a resolution of 100x100 m^2 (ha-raster) was applied to calculate annual mean concentrations of ammonia in the air. It includes all emission sources at a maximum distance of 50 km. The model was set up as follows:

- The calculations are split in a local part and a regional part. The local part includes the ammonia sources within a maximum distance of 4 km to the receptor point; it is calculated on a ha-raster. The regional part represents the background concentration induced by the sources between 4 and 50 km distance to the receptor point; it is calculated on a 1x1 km^2-raster.

- Normalised mean transfer functions were established; they provide the annual mean concentration (µg m^{-3}) induced by a standard source of one kg NH_3 a^{-1} depending on the distance and direction to the source; the functions are derived for different wind regions.

- The transfer functions are applied to all cells of the emission map to calculate an intermediate concentration map.

- The intermediate ammonia concentrations were compared with measured concentrations. The comparison showed a systematic effect of (relative) elevation which was included for calculating the final concentration map.

The method used to calculate the concentration C (µg m^{-3}) induced by the emissions from surrounding sources can be formulated as:

$$C = \sum_i \left(\frac{17}{14} \cdot E_i \cdot p(D_i, R_i) \right) \qquad \text{(eq. 3.1)}$$

where:

i	=	denotes all sources (raster-cells) within a radius of 50 km
E_i	=	NH_3-emission from raster-cell i (kg NH_3-N a^{-1}), see chapter 3.5.1
17/14	=	conversion from [kg NH_3-N] to [kg NH_3].
D_i	=	Distance to source i (m).
R_i	=	Direction to source i (azimuth).
p(D, R)	=	average transfer function; concentration as a function of D and R.

If the same frequency is assumed for all wind directions the transfer function depends on distance alone (p(D), see Figure 25, left). This type of function was calculated by Asman & Jaarsveld (1990) using an atmospheric transport model. The model was applied and tested in several countries (The Netherlands, United Kingdom, Belgium, Denmark and Sweden) and in Europe (Asman & Jaarsveld 1992). In Switzerland, the integrated distance-function shown in Figure 24 and Equation 3.1 was used the first time by Rihm & Kurz (2001) to calculate NH_3-concentration maps; the comparison with measured NH_3-concentrations was promisingly good. Thus, the method was further developed and used for mapping NH_3 in Switzerland for EKL (2014), Rihm & Achermann (2016) and Rihm & Künzle (2019).

The function p(D) integrates effects of several atmospheric processes such as dilution by turbulence, deposition on the ground and chemical transformation of ammonia to ammonium. It is related to a point source at a height of 3 m above ground and the resulting concentrations are given for a reference height of 1 m above ground. In the present study, it was assumed that the sources and the receptor points are situated in the centre of the 100x100 m^2 cells. For calculating the concentration in a raster-cell induced by the emission of the same cell (where D = 0 m), a distance of 50 m was used in p(D).

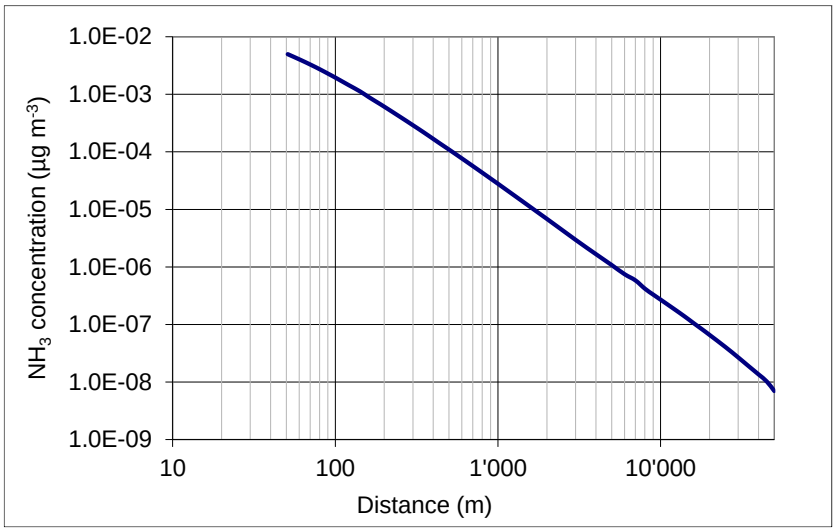

Figure 24: NH_3 concentration as a function of the distance to a source emitting 1 kg NH_3 a^{-1} for distances between 50 m and 50 km (by Asman & Jaarsveld 1990).

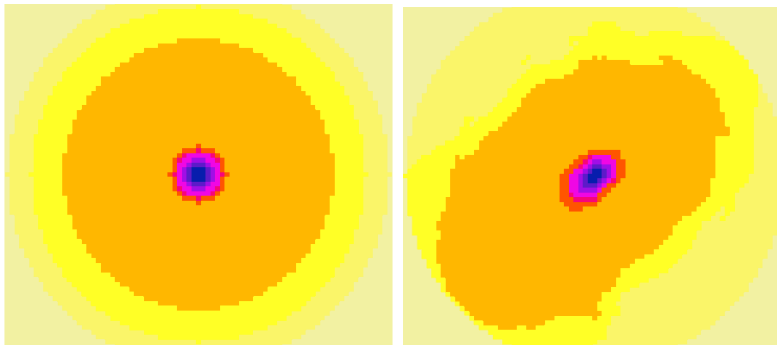

Figure 25: Schematic distance-functions. Left: rotation-symmetric use of p(D) in the Alps. Right: modified p(D, R) function according to prevailing wind directions in the Jura/Plateau region.

Furthermore, twelve different climatic regions were defined for the calculation of distances below 4 km (see Figure 26):

- In Northern Switzerland (covering the Jura Mountains and the Swiss Plateau) the p(D) function was modified according to prevailing wind directions in this area (Figure 25, right); i.e. the concentration is calculated as a function of distance and direction between source and receptor. The modification was based on the specific dispersion profiles of NO_x developed for different climate regions (FOEN 2011).
- At higher altitudes in the Alps and Southern Switzerland, the function p(D) was applied rotation-symmetrically (Figure 25, left).
- In the Alpine valleys, the distance-function was adjusted to the prevailing canalised wind directions as shown in Figure 26.

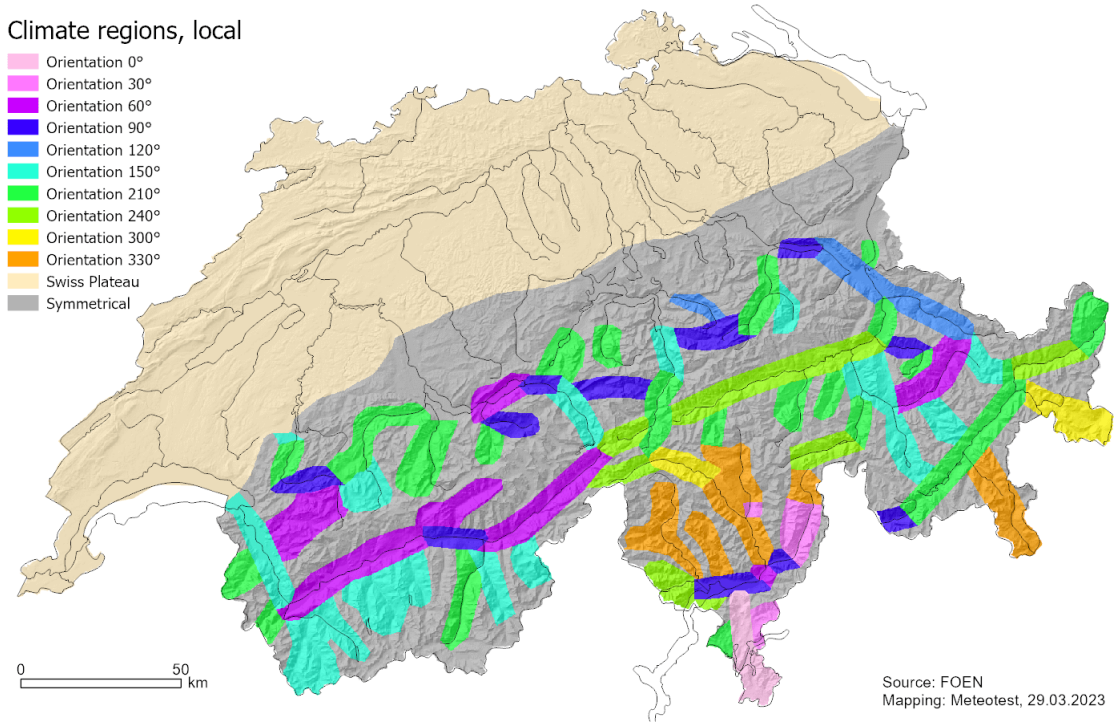

Figure 26: The twelve wind regions used for the local dispersion modelling (0–4 km distance from sources) with their prevailing wind directions (orientation).

For the regional modelling, four different climatic regions were defined as shown in Figure 27: Plateau/Jura, Basle, Alps and Southern Switzerland. The regional transfer functions were based on the Asman-Jaarsveld distance function (Figure 24) and modified using transfer functions that were developed for PM10 (FOEN 2013).

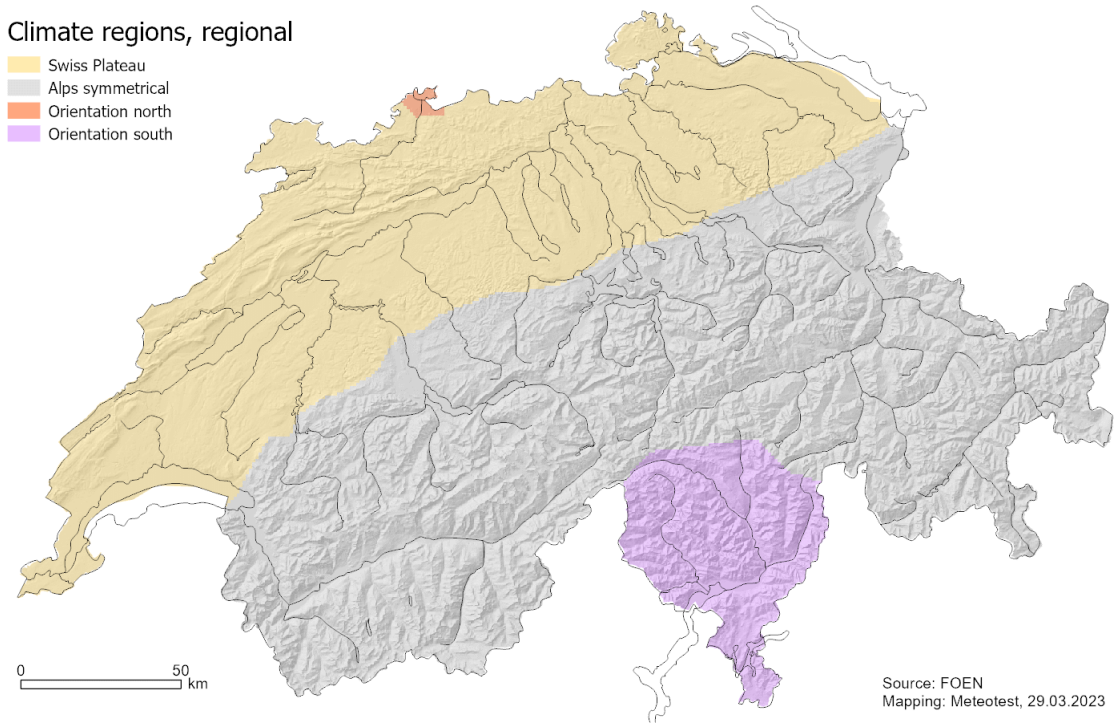

Figure 27: The four climatic regions used for the regional dispersion modelling (4–50 km distance from sources).

There are 112 sites in Switzerland where ammonia concentrations were measured in the period 2018–2021 (Seitler 2022, Seitler & Meier 2022). For the comparison with the raw model results, the average concentration 2018–2021 at each measurement location was used. However, 32 sites were excluded in the comparison for the following reasons: Their distance to the nearest farm is below 150 m (comparison is difficult as the location of the farms in the model is rasterized to 100x100 m^2); they are situated in a forest or on a tower. Furthermore, the sites of local monitoring clusters were thinned out by excluding the sites closest to farms.

In the comparison of the raw modelled data and measured ammonia concentrations, the residuals showed a systematic influence by topography. For further examination of the effect, the relative elevation (Hrel2) was used. Hrel2 was calculated as: elevation minus the minimum elevation within a radius of 2 km. In flat terrain, Hrel2 is 0 while in very steep topographic situation it can reach values over 1'000 m (Figure 28).

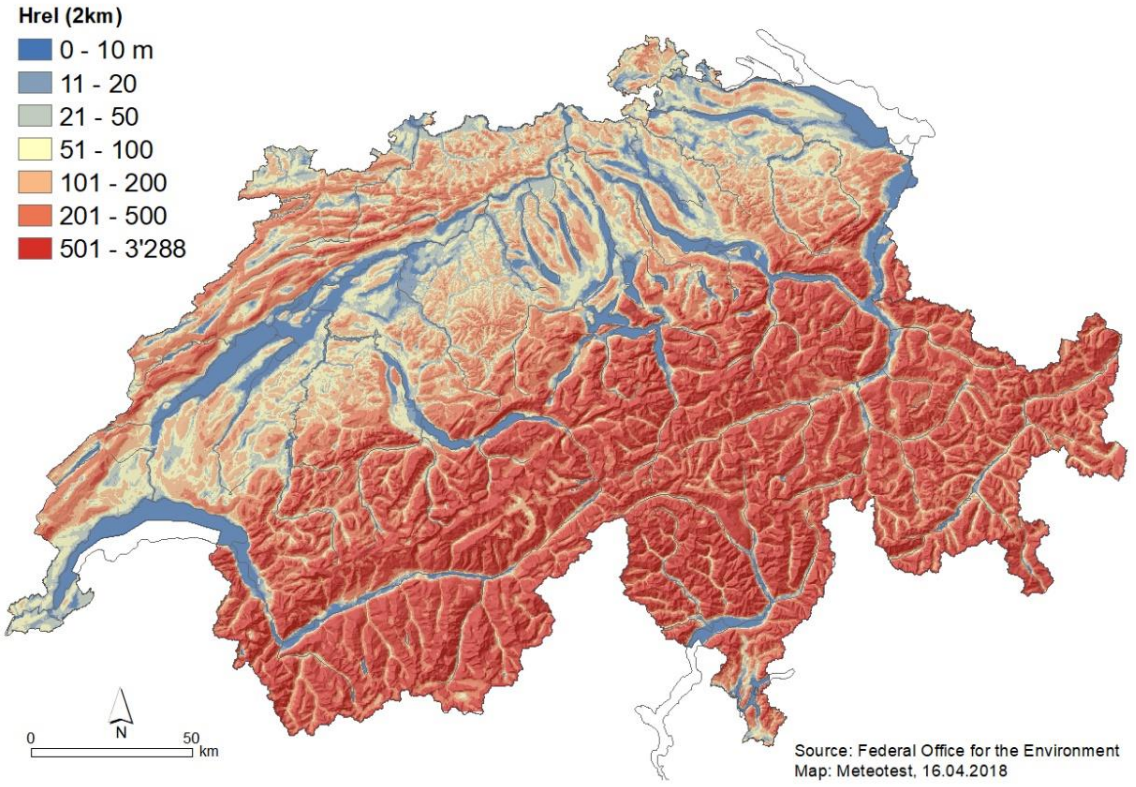

Figure 28: Relative elevation Hrel2 (elevation minus minimum elevation within a radius of 2 km).

Figure 29 shows the relationship between the residuals (expressed as ratio modelled to measured) and Hrel2: In flat terrain, the model underestimates the concentrations and in steep terrain, the model is close to the measured ammonia levels. This relation can be reasonably explained by effects that were not included in the model: (1) near-ground inversion layers and cold air pools that occur mainly in flat terrain and lead to an increase of ammonia concentrations, and (2) the canalising effect of slopes in steep terrain inhibiting uphill dispersion.

In Southern Switzerland (region "orientation south" in Figure 27), the raw model clearly underestimates the measured concentrations, probably, because the import from the Po valley is underestimated; also, the warmer climate might be of importance. Therefore, the analysis of the residuals is done separately for that region (see Figure 29, lower diagram).

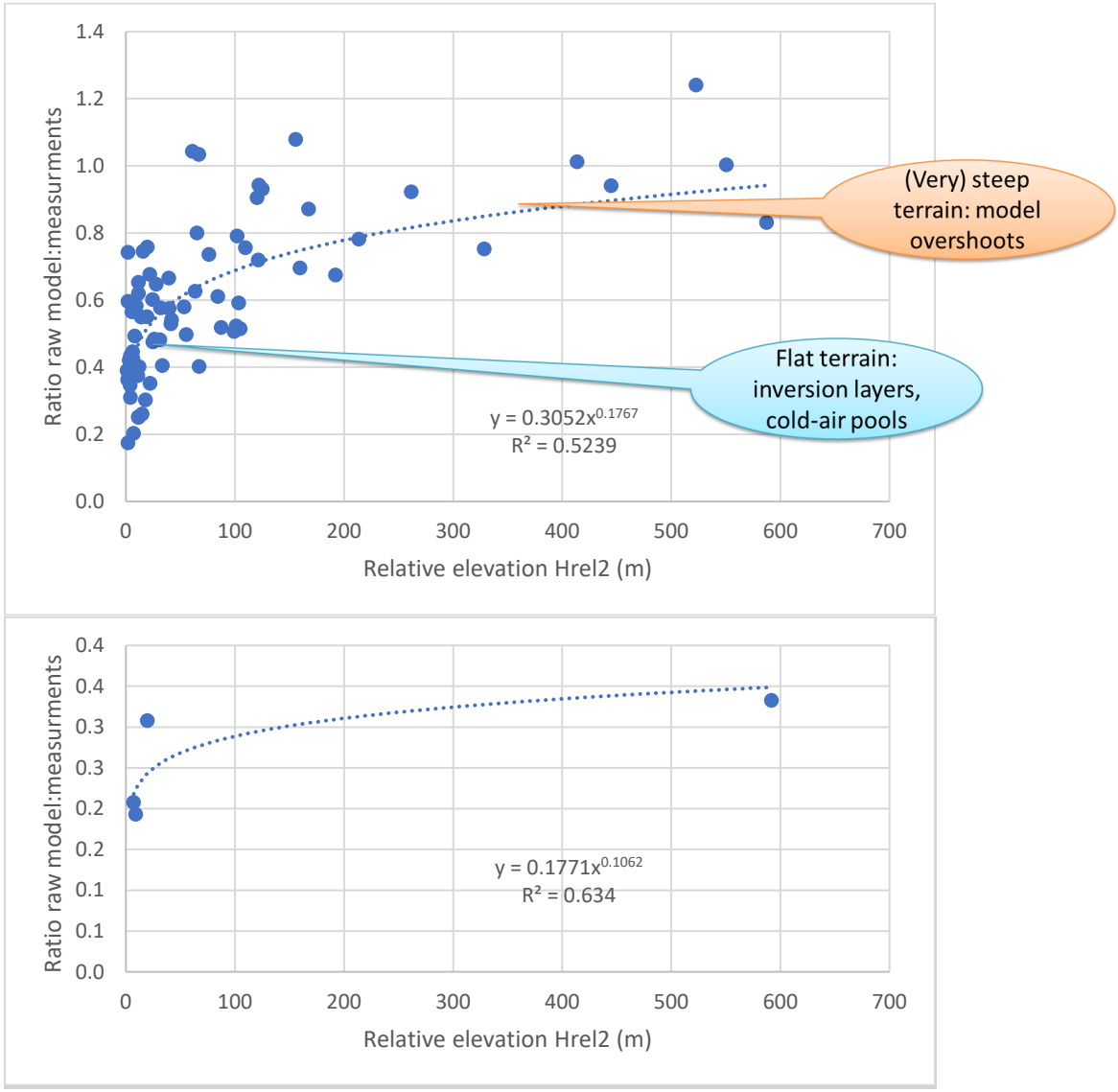

Figure 29: Relationship between the residuals (ratio raw model to measured ammonia concentrations) and the relative elevation (Hrel2), for Northern (upper diagram) and Southern (lower diagram) Switzerland.

A topographic correction factor was calculated for each raster cell using Hrel2 and the two regression functions shown in Figure 29. The factors were kept within the limits 0.3–1.1 and 0.2–0.4 for Northern and Southern Switzerland, respectively. The resulting map of ammonia concentrations in 2020 after these topographic corrections is shown in Figure 30 and the comparison with measurements in Figure 31. With the topographic corrections, R^2 of the linear regression improves from 0.49 (not shown) to 0.63 for the whole of Switzerland.

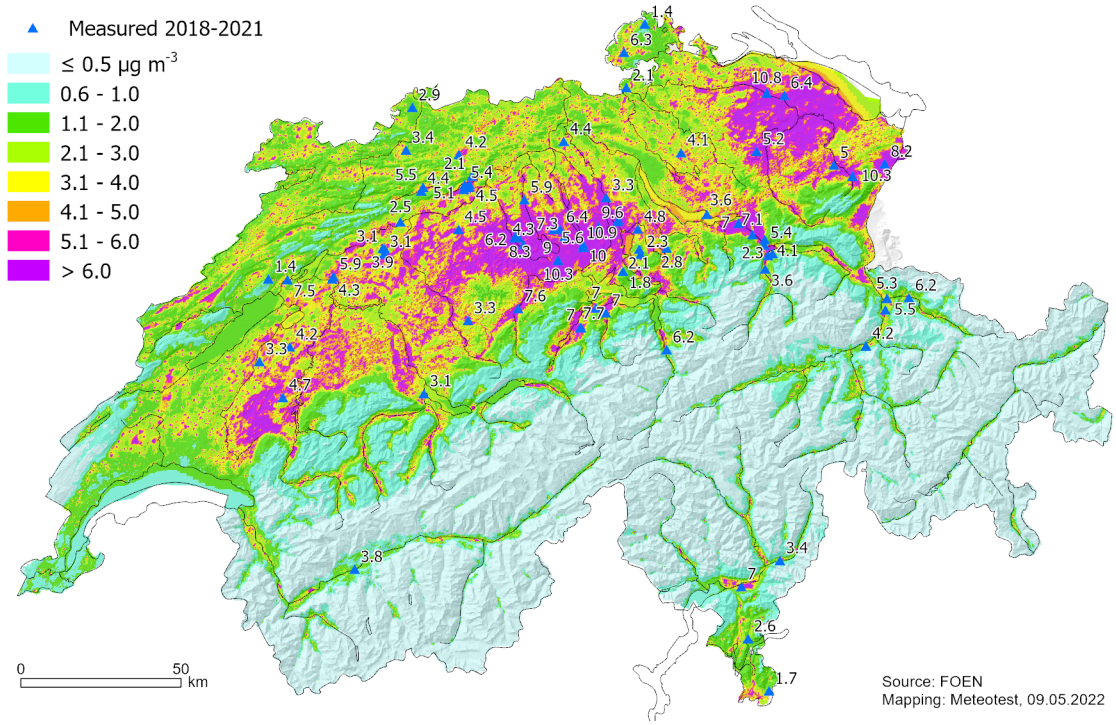

Figure 30: Map of NH_3 concentration in 2020 (100x100 m² raster) and monitoring sites (mean 2018–2021).

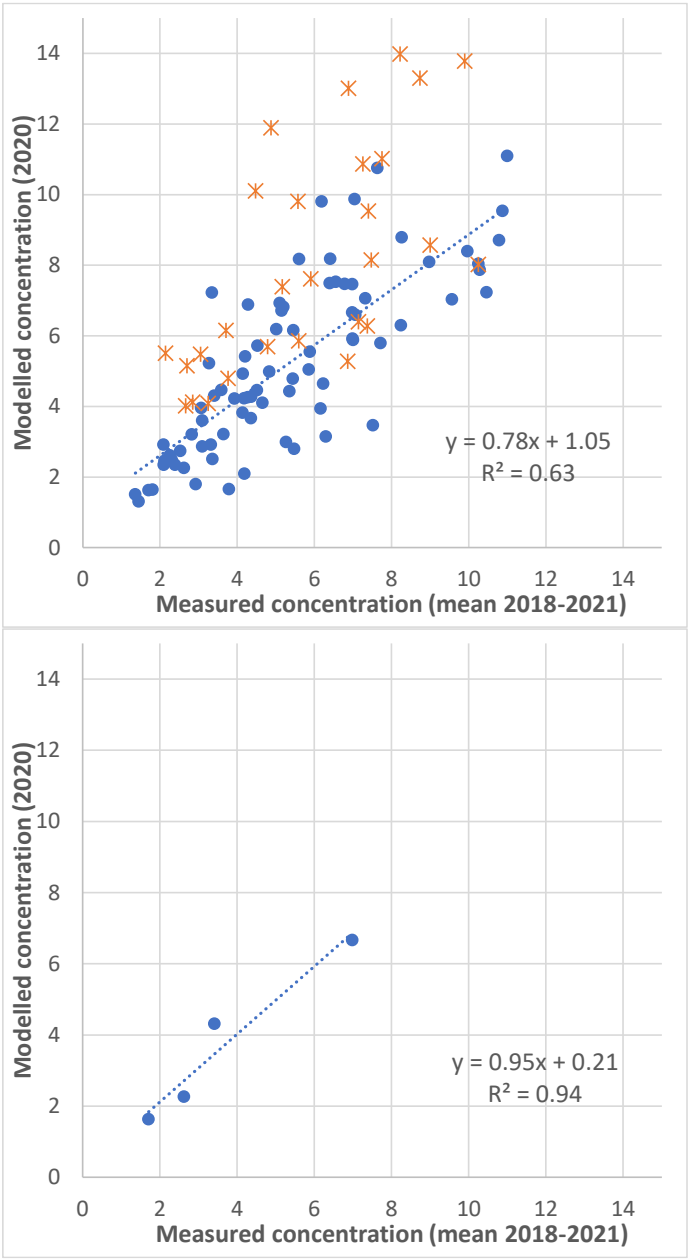

Figure 31: Upper diagram: Comparison of measured and modelled ammonia concentrations (µg m^{-3}), n=80 (blue markers); excluded monitoring sites are displayed with red markers. Lower diagram: comparison only with the four sites in Southern Switzerland.

3.6 Recalculation of the time series 1990–2015

Maps of nitrogen deposition and critical load exceedances had been produced for the years 1990, 2000, 2005, 2010 and 2015 by Rihm & Künzle (2019). In order to improve the homogeneity of the time series 1990–2020, the former maps were recalculated using the methods of 2020 where possible:

- The same land-use map was used for all years (SFSO 2021, survey 2014/2018, hectare raster), see chapter 3.3.
- The critical load data presented in chapters 2.2 and 2.3 were used for all years to calculate exceedances.
- The updated deposition velocities for gases (chapter 3.3) were applied for all years.
- The new map of HNO_3-concentrations (chapter 3.3) was used for all years. According to Seitler et al. (2021), the concentrations measured in 2014 and 2019 were quite similar and previous measurements in the years 1993–1998 and 2001–2002 (Thöni & Seitler 2010) were at the same level as well.
- Nitrate concentrations in rain in Southern Switzerland were recalculated 1990–2015 by applying a smooth transition from the southern to the northern region as shown in chapter 3.2.
- Ammonium concentrations in rain in Northern Switzerland were recalculated for 1990 by correcting an inconsistency in the west-east gradient.
- Concentrations of ammonia and nitrate in aerosols (PM10) were recalculated for 1990–2015: The concentration maps for 2020 (chapter 3.4) were adjusted to previous years by applying the scaling factors shown in Table 12. The factors were derived from measurements of the chemical composition of PM10 in the periods 1998–1999, 2008–2009 and 2018–2019 by Hüglin & Grange (2021).
- Previous maps of NO_2- and NH_3-concentrations for 1990-2015 have not been changed.

Table 12: Scaling factors for the concentrations of ammonium and nitrate in PM10 1990–2015 in relation to 2020.

	1990	2000	2005	2010	2015	2020
Ammonium	1.81	1.81	1.65	1.48	1.24	1.00
Nitrate	1.30	1.30	1.39	1.48	1.24	1.00

The following inconsistencies remain in the time series:

- The NH_3-emissions from livestock in 1990 were calculated with a simplified method as only the livestock units (LSU, *Grossvieheinheiten*) per farm were available as geo-referenced data (instead of animal categories).
- Due to lacking data, manure transport and summering of livestock could not be considered 1990–2010 for the mapping of NH_3-emissions.

4 Results

4.1 Critical Loads of Nitrogen

The spatial distributions of critical loads are displayed separately for the empirical method and for the SMB method on the maps in Figure 32 and Figure 33, respectively. The critical loads of nitrogen for forests ($CL_{nut}N$) calculated with the Simple Mass Balance (SMB) were not revised in this study.

The map in Figure 32 is a combination of all selected ecosystems as described in chapter 2.2.3. Only (semi-)natural ecosystems with high conservation importance were included. For each cell of the 1x1 km^2 raster, the critical load value of the most sensitive ecosystem existing in the cell was selected. The map in Figure 34 combines the results of the empirical method and SMB method showing the minimum critical load of both. Figure 35 presents the critical loads as cumulative frequency distributions.

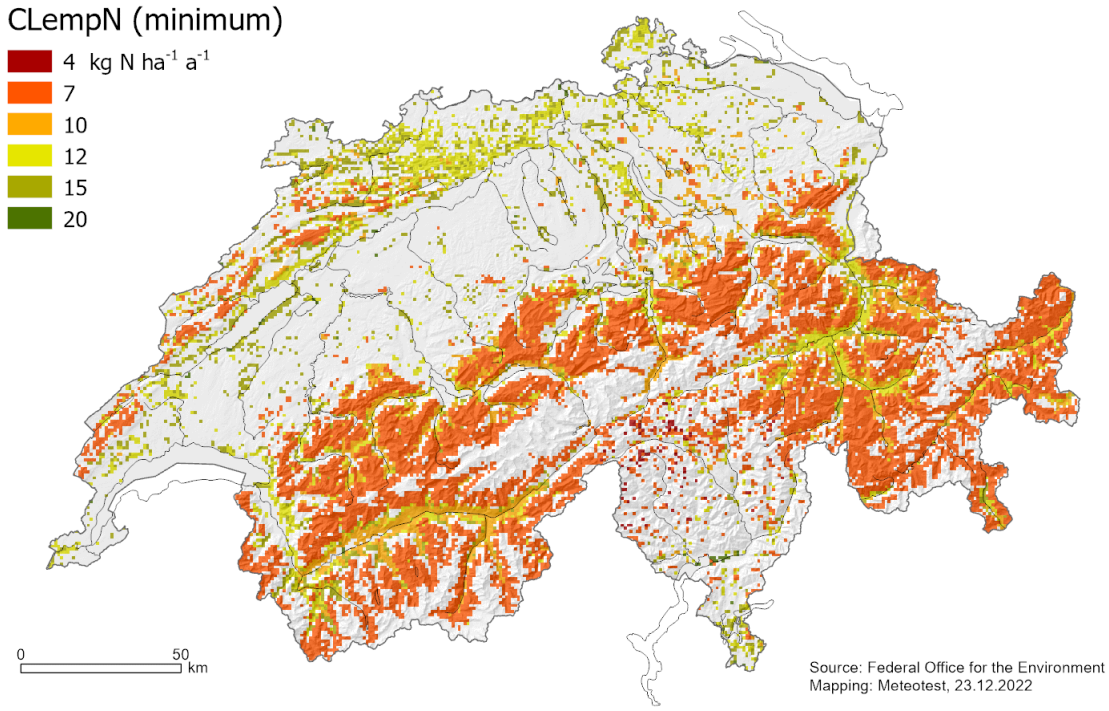

Figure 32: Empirical critical loads of nutrient nitrogen for (semi-)natural ecosystems, $CL_{emp}N$, minimum per km^2.

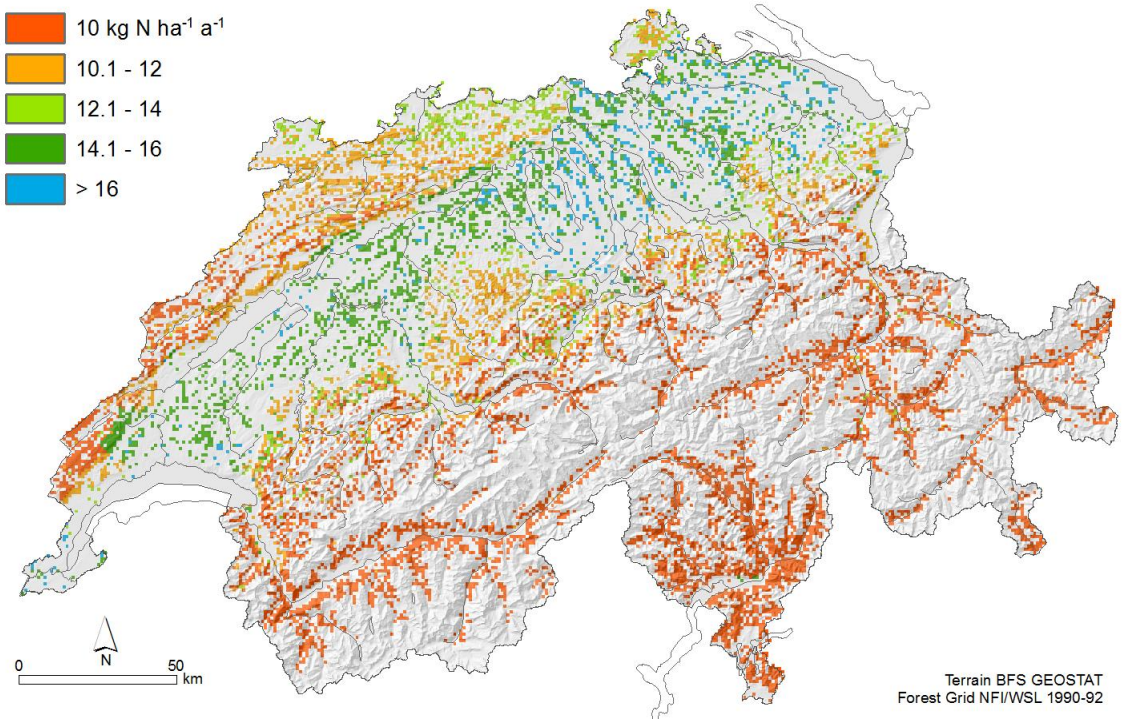

Figure 33: Critical loads of nutrient nitrogen for forests, $CL_{nut}N$.

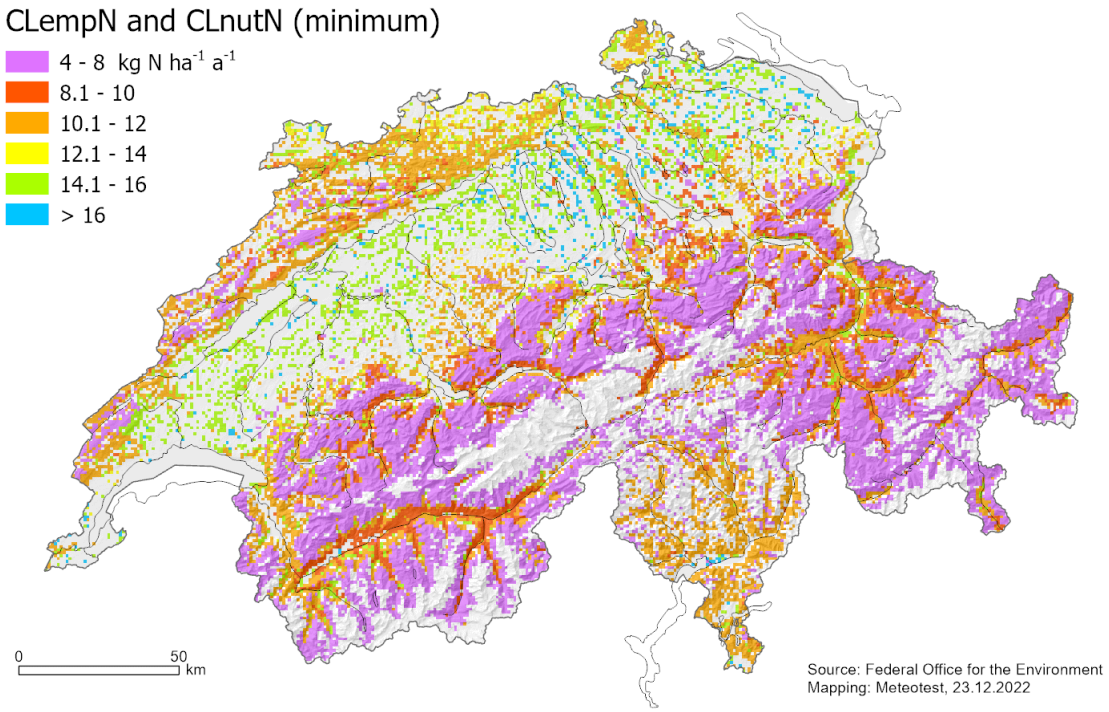

Figure 34: Combined critical loads of nutrient nitrogen, minimum of $CL_{nut}N$ and $CL_{emp}N$ per km^2.

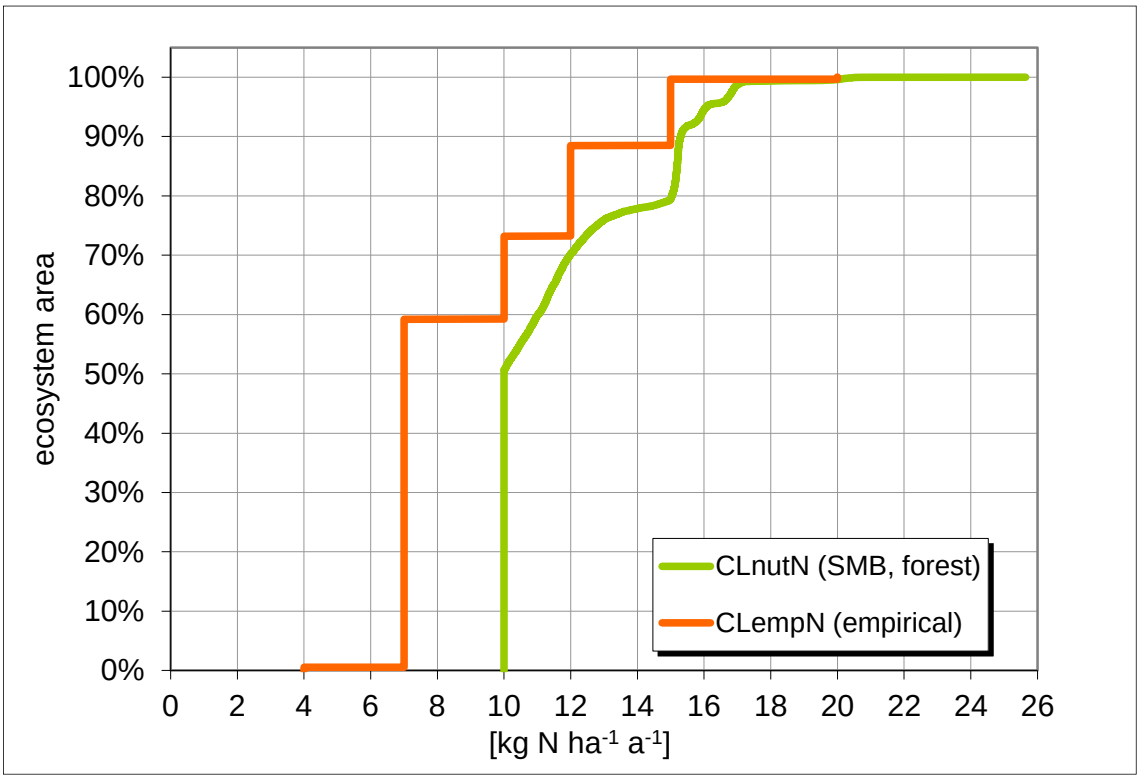

Figure 35: Cumulative frequency distributions of critical loads of nitrogen for Switzerland. The SMB method was applied to forests, the empirical method to different (semi-)natural ecosystems.

The critical loads for natural and semi-natural ecosystems ($CL_{emp}N$, empirical method, chapter 2.2) are in the range from 4 to 20 kg N ha^{-1} a^{-1} covering a total sensitive area of 17'532 km^2. The most sensitive ecosystems are alpine lakes, raised bogs, Littorellion, (sub-)alpine scrub habitats and (sub-)alpine grassland (4–10 kg N kg N ha^{-1} a^{-1}). The largest part of these sensitive areas is covered by (sub-)alpine grassland and scrub habitats; these poorly managed pastures and meadows represent a very important part of the Alpine vegetation. Because of their short vegetation period, the low temperatures and the relatively poor soils, their natural nitrogen demand, and consequently their critical load, is low. Critical loads between 10 and 20 kg N ha^{-1} a^{-1} were assigned to selected species-rich montane and sub-alpine grassland, fens and poorly managed forests with especially rich ground-florae.

In the Swiss Plateau, between the Alps and the Jura mountains, relatively few sensitive areas can be found on Figure 32. This can be explained by the fact that in this region a large part of the (semi-)natural ecosystems has disappeared due to intense land use and agricultural management (e.g. mountain hay meadows, see Bosshard 2015). Two main reasons can be mentioned for the poor occurrence of (semi-)natural ecosystems in the Central and Southern Alps: (1) Acidic alpine grasslands such as *caricion curvulae/sempervirentis* have not been included (no critical loads available), and (2) large areas south of the Alps are covered by forest, which was included in the SMB method.

The critical loads for productive and managed forests ($CL_{nut}N$), calculated with the SMB method (see chapter 2.3) are in the range from 10 to 25 kg N ha^{-1} a^{-1} covering a total sensitive area of 10'632 km^2 (Figure 33). As described in Chapter 2.3.1, the lower range of 10 kg N ha^{-1} a^{-1} was set with intent to avoid implausibly low values. The variation of the critical loads is mainly due to the removal of nitrogen by harvesting and denitrification losses. The average harvesting rates in the mountainous regions and south of the Alps are lower than in the Plateau (Figure 7). The denitrification rates depend on the percolation conditions of the soils. The highest denitrification rates and consequently the highest critical loads are found on wet soils of the lower Alps and in north-eastern Switzerland (Figure 9).

4.2 Deposition of Nitrogen

The modelled nitrogen depositions in 2020 are displayed in Figure 36. In general, the depositions are higher in the lowlands and valleys, where the pollutant concentrations are higher. This is the case for NH_3 due to animal husbandry and for NO_2 due to intense traffic and settlements. The atmospheric deposition of gaseous NH_3 is strongly correlated with the spatial distribution of NH_3 emissions (see Chapter 3.5). Intense animal husbandry and subsequent high NH_3 emissions occur mainly in central and eastern Switzerland. The highest depositions are calculated on forest stands in these high emission regions. In mountainous regions the density of livestock and NH_3 emissions is much lower.

As shown in Table 13, the resulting total nitrogen deposition in Switzerland for the year 2020 amounts to 59.2 kt N a^{-1} (14.3 kg ha^{-1} a^{-1}) to which gaseous NH_3 contributes 40%, wet NH_4^+ 28%, wet NO_3^- 14%, gaseous NO_2 9%, gaseous HNO_3 6%, dry NH_4^+ 2%, and dry NO_3^- 1%. The share of reduced nitrogen compounds (NH_y-N) is 70%.

Table 13: Total deposition of N compounds in Switzerland 2020. Units: kt N a^{-1} (*italic*: kg N ha^{-1} a^{-1}).

Receptors / **Compounds**	**Forest** 12'426 km²		**Non-forest** 28'716 km²		**Total** 41'142 km²	
Wet: NH_4^+	5.7	*4.6*	10.7	*3.7*	16.4	*4.0*
Dry: NH_4^+ aerosol	0.6	*0.5*	0.6	*0.2*	1.2	*0.3*
NH_3 gas	10.3	*8.3*	13.6	*4.7*	23.9	*5.8*
Total NH_y-N:	16.6	*13.4*	24.9	*8.6*	41.5	*10.1*
Wet: NO_3^-	2.9	*2.3*	5.3	*1.8*	8.2	*2.0*
Dry: NO_3^- aerosol	0.5	*0.4*	0.4	*0.1*	0.9	*0.2*
NO_2 gas	2.8	*2.2*	2.5	*0.9*	5.3	*1.3*
HNO_3 gas	1.4	*1.1*	1.9	*0.7*	3.3	*0.8*
Total NO_y-N:	7.6	*6.0*	10.1	*3.5*	17.7	*4.3*
Total N	24.2	*19.4*	35.0	*12.2*	59.2	*14.4*

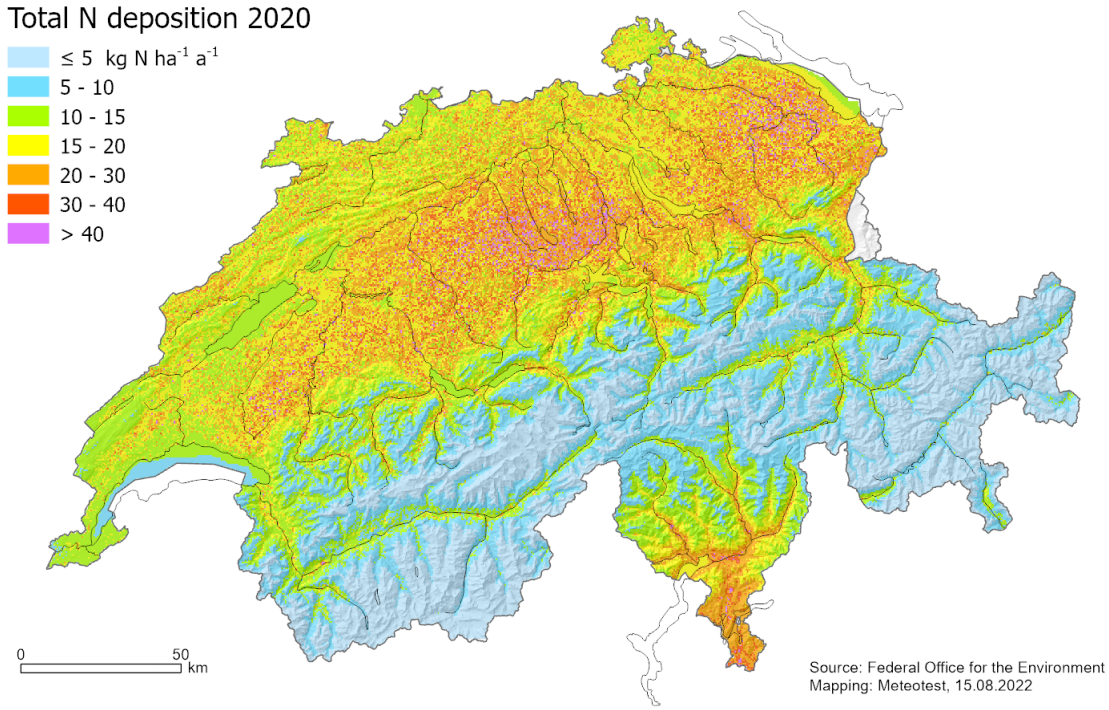

Figure 36: Total deposition of nitrogen in 2020, calculated on a 500x500 m² raster.

Table 14 and Figure 37 give an overview of the deposition development 1990–2020: In this period total N deposition in Switzerland decreased by 26%. In general, a more or less pronounced decrease is observed for most of the compounds. Based on available monitoring data (see chapter 3.6), the deposition of HNO_3 is kept constant over the whole period.

However, there is an increase of NH_3 deposition due to an overall increase of NH_3 concentrations from 2015 to 2020. According to the monitoring results by Seitler & Meier (2022), the years 2018–2020 were among the highest since measurements were started in 2000. For modelling the 2020 NH_3 concentrations, the average measured concentrations of the period 2018–2021 were used (see chapter 3.5.2) leading to higher modelled concentrations and deposition of NH_3 than in the previous years. Seitler & Meier (2022) noticed that in warm years generally higher concentrations are measured. A possible reason for this might be that the emissions from animal husbandry increase with temperature. A second reason for the general increase of gaseous NH_3 may be altered conditions in atmospheric chemistry (Butler et al. 2016). Grange et al. (2023) evaluated this phenomenon in Switzerland for the period 2004–2021 and concluded that the decrease of nitric acid and sulfuric acid in the atmosphere slowed down the transformation from NH_3 to NH_4^+. As a consequence, the NH_3 concentrations as well as the local deposition of NH_3 increases, while the long-range transport of NH_4^+ decreases.

Table 14: Total deposition of N compounds in Switzerland; years 1990–2020. Units: kt N a^{-1}.

kt N/yr	1990	2000	2005	2010	2015	2020	
NH_4^+ wet	24.2	21.3	19.4	17.3	16.1	16.4	*28%*
NH_4^+ aerosol	2.2	2.2	2.0	1.8	1.5	1.2	*2%*
NH_3 gas	21.6	19.3	19.3	19.0	18.3	23.9	*40%*
NO_3^- wet	18.2	14.5	12.4	11.9	10.4	8.2	*14%*
NO_3^- aerosol	1.1	1.1	1.2	1.3	1.1	0.9	*1%*
NO_2 gas	9.0	7.3	7.1	6.8	6.1	5.3	*9%*
HNO_3 gas	3.3	3.3	3.3	3.3	3.3	3.3	*6%*
NH_y total	47.9	42.8	40.8	38.1	35.8	41.5	*70%*
NO_y total	31.5	26.2	24.0	23.3	20.8	17.7	*30%*
N total	79.5	69.0	64.7	61.4	56.7	59.2	*100%*
Difference to 1990	---	*-13%*	*-19%*	*-23%*	*-29%*	*-26%*	

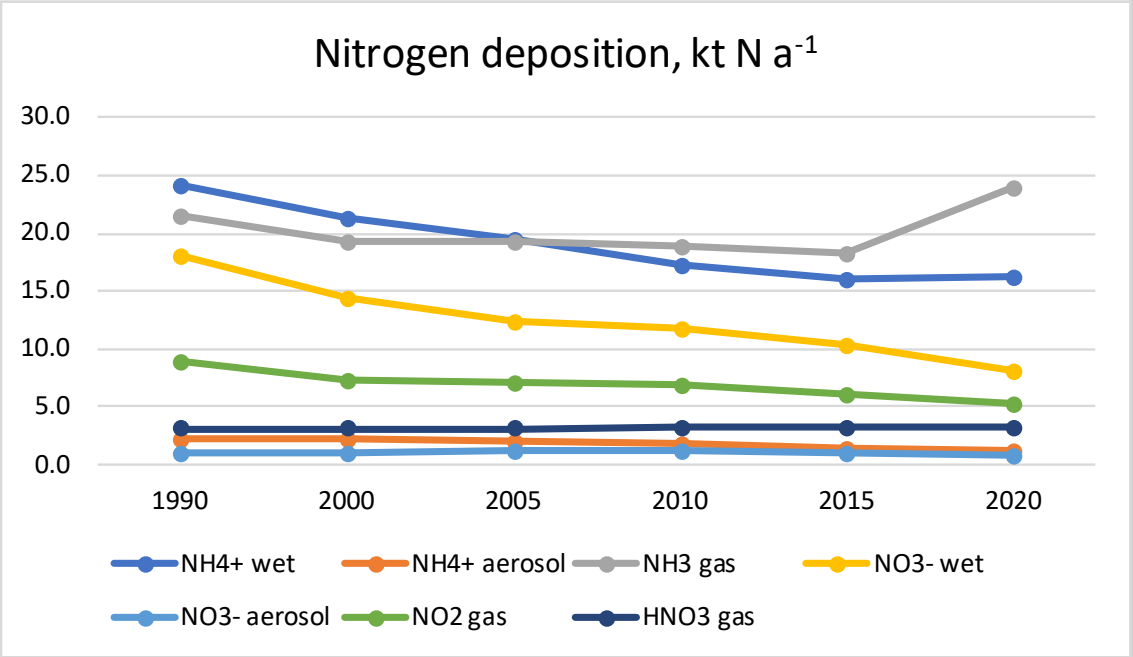

Figure 37: Total deposition of N compounds 1990–2020 in Switzerland, calculated by the national model (1x1 km^2).

4.3 Exceedances of Critical Loads of Nitrogen

Exceedances are calculated as deposition minus critical load. If deposition is lower than the critical load, there is no exceedance. Exceedance of critical loads indicates a long-term risk of adverse effects in the ecosystems (see chapter 2.1) due to increased nitrogen deposition.

The map in Figure 38 displays the exceedances of empirical critical loads in 2020. It shows the exceedance of the most sensitive (semi-)natural ecosystem type occurring in each 1x1 km² raster cell. Figure 39 shows the exceedances of critical loads for productive forests in 2020 calculated with the SMB method. The map in Figure 40 combines the exceedance of the critical loads for (semi-)natural ecosystems and forests showing the maximum exceedance per 1x1 km² raster cell.

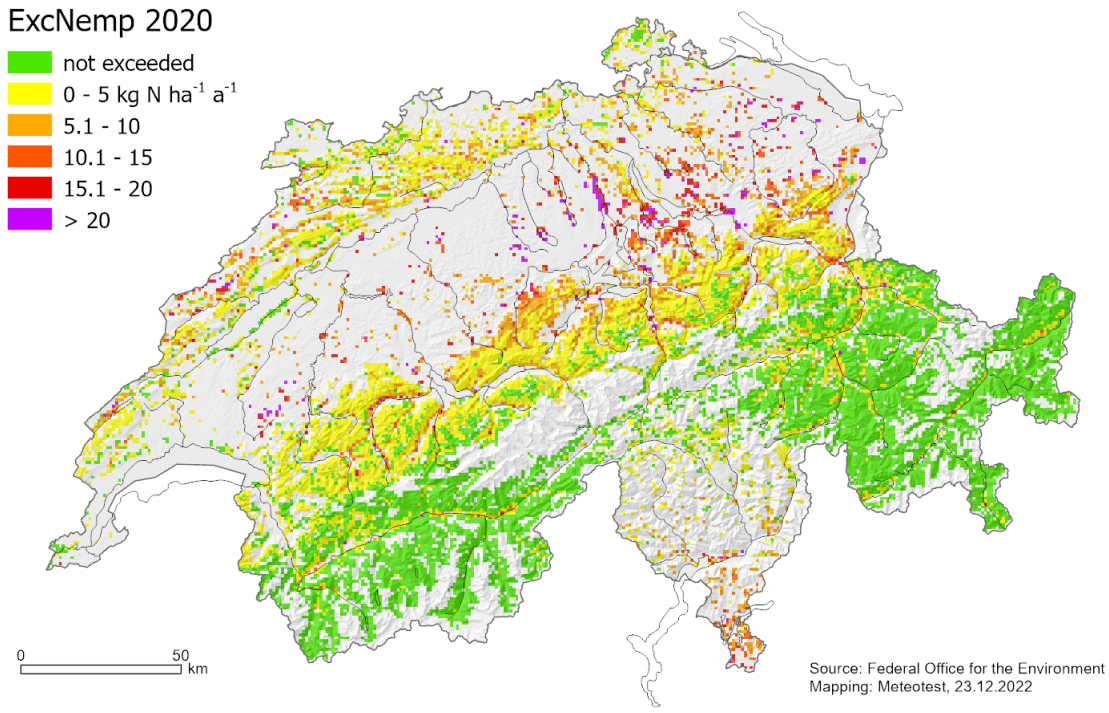

Figure 38: Exceedance of critical loads for (semi-)natural ecosystems ($CL_{emp}N$) by nitrogen depositions in 2020.

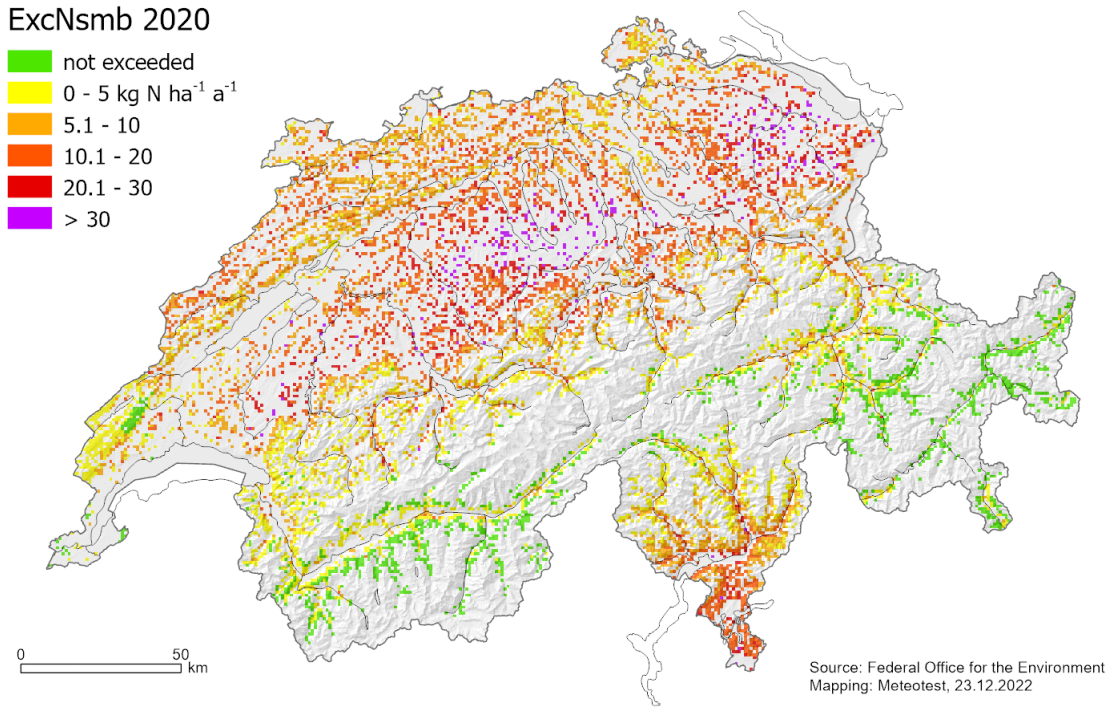

Figure 39: Exceedance of critical loads for productive forests ($CL_{nut}N$) by nitrogen depositions in 2020. Forest grid: WSL 1990/92.

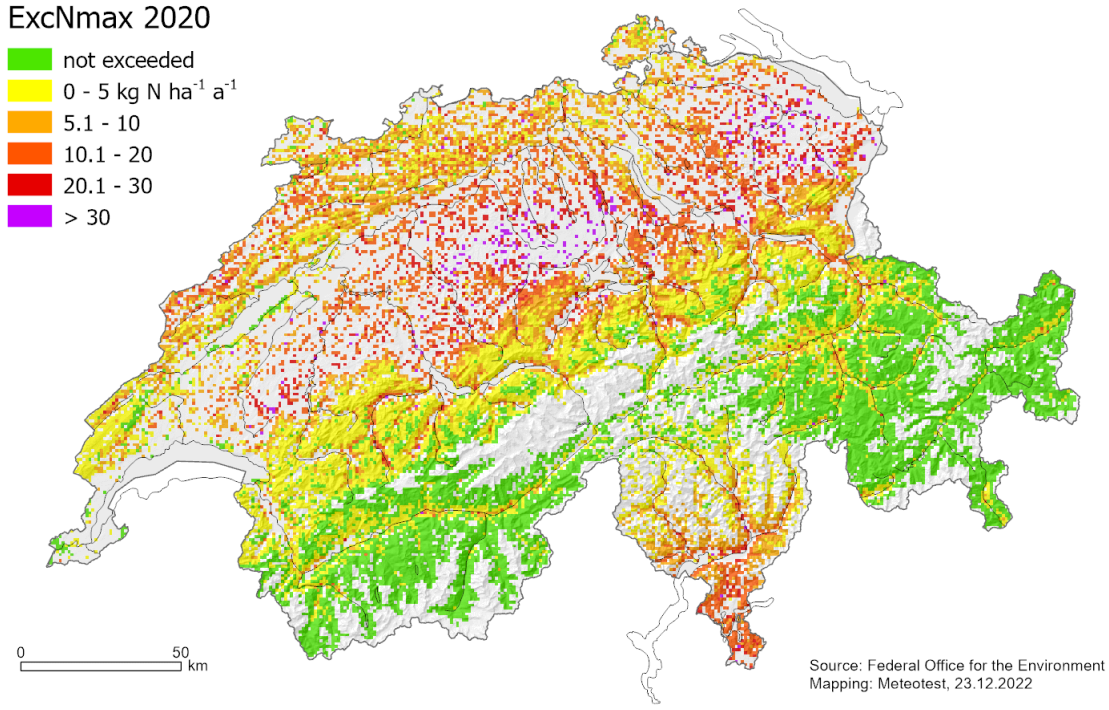

Figure 40: Combined map showing the maximum exceedance of critical loads for forests ($CL_{nut}N$) and (semi-)natural ecosystems ($CL_{emp}N$) by nitrogen depositions in 2020 per 1x1 km² raster cell.

Table 15 shows the percentages of the exceeded ecosystem areas for forests, (semi-)natural ecosystems and the combined exceedance. They were calculated on the 1x1 km² raster for the whole period 1990–2020. Overall, a reduction of the exceeded area can be observed between 1990 and 2005 which continues between 2010 and 2015. However, the percentage of exceeded area remains high. Between 2015 and 2020 the share of exceeded area slightly grows due to increased NH_3 depositions (chapter 4.2).

Table 15 shows also the average accumulated exceedance (AAE, expressed in kg N ha^{-1} a^{-1}), which is calculated as an area-weighted average of the exceedances of the critical loads (see Hettelingh et al. 2017). The decrease of the AAE between 1990 and 2015 is more pronounced than the decrease of the percentage of exceeded ecosystem areas. This means, that also the magnitude of the exceedances lessened on the areas that are still exceeded.

Table 15: Exceedance of critical loads on the 1x1 km² raster expressed as percent of the ecosystem area and as average accumulated exceedance (AAE).

	[a]Area (km^2)	1990	2000	2005	2010	2015	2020
Percentage of area exceeded							
Exceedance of CLempN, (semi-) natural ecosystems	17'359	78%	69%	61%	60%	52%	54%
Exceedance of CLsmbN, productive forest	10'461	96%	93%	89%	89%	85%	87%
Maximal (combined) exceedance per km^2	23'090	85%	78%	72%	72%	66%	67%
Average accumulated exceedance (kg N ha^{-1} a^{-1})							
Exceedance of CLempN, (semi-) natural ecosystems	17'359	6.0	4.2	3.6	3.0	2.4	2.7
Exceedance of CLsmbN, productive forest	10'461	14.5	11.4	10.2	9.1	7.7	8.7
Maximal (combined) exceedance per km^2	23'090	9.6	7.3	6.5	5.7	4.7	5.4

[a] area of raster cells containing (semi-) natural ecosystems and productive forests, this does not mean that the surface is entirely covered by these ecosystems.

In 2020, the critical loads for natural and semi-natural ecosystems calculated with the empirical method are exceeded on 54% of the mapped area. The highest exceedances (more than 10 kg N ha^{-1} a^{-1}) occur in raised bogs and species-rich grassland in the lower Alps and in the Jura mountains, where low critical loads and relatively high depositions coincide. No exceedances or low exceedances (less than 5 kg N ha^{-1} a^{-1}) occur on species-rich grassland and alpine scrub habitats in the inner-alpine valleys, which are relatively dry regions (low wet deposition) and remote from the main sources of emissions.

In the calculation of exceedances for forest ecosystems included in the empirical method (Table 2), deposition for open field conditions was used, because a part of these systems are open forests with a lower "filtering effect" in comparison to

closed forests. Generally, the exceedance in these unproductive forest ecosystems is underestimated by such an approach.

The critical loads for productive forests calculated with the SMB method are exceeded on 87% of the mapped area in the year 2020 (Figure 39). The exceedances are higher than those for the (semi-)natural ecosystems (Figure 38, the colour scheme in the two maps differs). This can be explained by the observation that the dry deposition is higher in forest stands than on open land, as the high surface roughness of forest canopies intensifies the dry deposition processes (chapters 3.3, 3.4, 4.2). The spatial distribution of the exceedances is determined to a large extent by present nitrogen deposition and not by critical loads. Again, the inner-alpine valleys (Valais, Engadin) have the lowest exceedances.

Figure 41 presents cumulative frequency distributions of exceeded area for sensitive ecosystems in Switzerland. The critical loads (according to chapter 2.2.2), nitrogen deposition and the resulting exceedance were calculated on a 100x100 m^2 raster for raised bogs, fens and dry grassland. For forests, the exceedance was calculated on the 1x1 km^2 sampling points of the initial national forest inventory (WSL 1990/92) (shown in Figure 39).

In 2020, the critical loads were exceeded on 94%, 74%, 42% and 87% of the area of raised bogs, fens, dry grassland and forests, respectively. The lowest exceedance was calculated for dry grassland (TWW) as these conservation areas are generally situated in dry regions and remote from strong sources of nitrogen emissions.

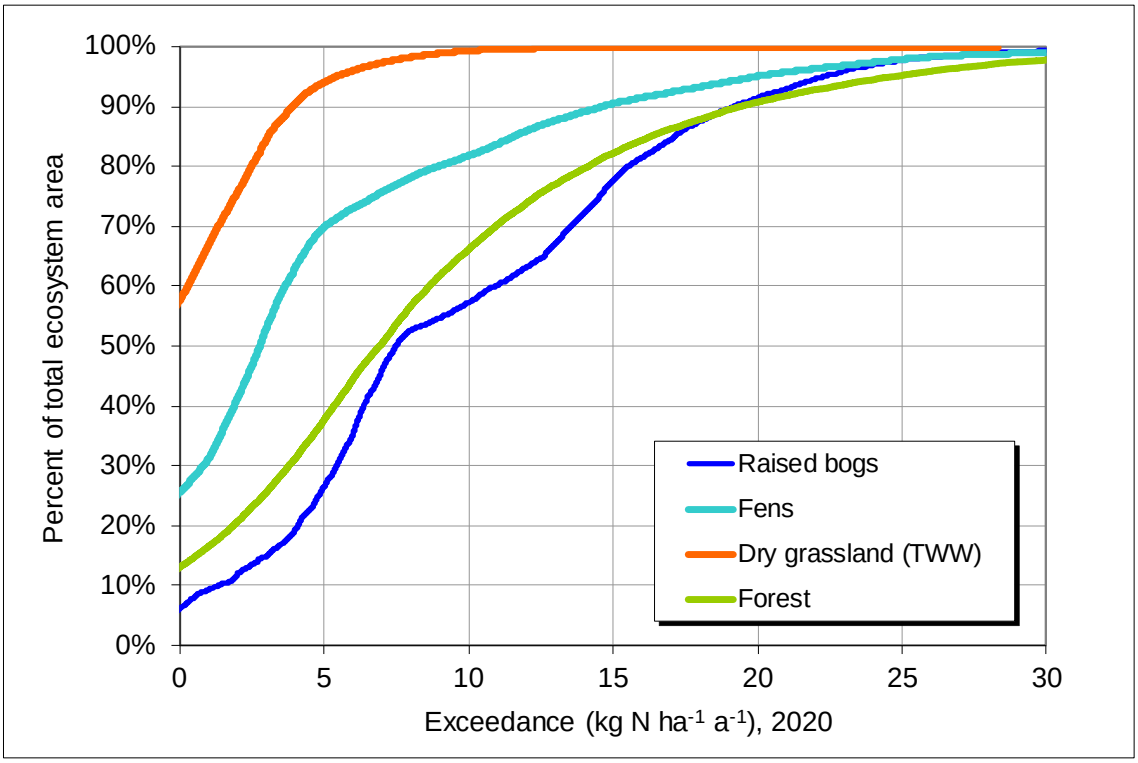

Figure 41: Cumulative frequency distribution of the exceedances of critical loads of nutrient nitrogen for different protected ecosystems. Units: percent of total ecosystem area. Nitrogen deposition: year 2020.

4.4 Reliability of the Results

Uncertainties in the computation of critical loads and depositions involve associated uncertainty in the exceedance of critical loads. It is a challenging task to quantify that uncertainty as the relevant processes take place in open, interacting (eco)systems. As explicated by de Vries et al. (2015, chapter 25), the critical load approach meets precautionary principles to support environmental sustainability; it aims at "preventing damage caused by deposition even when scientific proof would not be conclusive". However, for supporting air pollution policies, information about the reliability of the critical load exceedances is needed. Therefore, a straight-forward sensitivity analysis was carried out and presented in this chapter.

For empirical critical loads, the range of $CL_{emp}N$ given in the mapping manual partially reflects the uncertainty of the critical load (see chapter 2.2.1). E.g. for deciduous forest the range is 10–15 kg N ha^{-1} a^{-1}. Thus, assuming a critical load value of 12 kg N ha^{-1} a^{-1}, the range corresponds to an uncertainty of approximately ±25%. Uncertainty assessments of critical loads calculated with the SMB method ($CL_{nut}N$) are quite rare (de Vries et al. 2015, chapter 25). Therefore, a general uncertainty of ±30% is used in this sensitivity analysis. This assumption is also supported by a former sensitivity analysis of FOEFL (1996) where the influence of single input parameters to the SMB was analysed.

The local error of modelled depositions can be quite large. However, the influence of these uncertainties on the reliability of the exceedance is limited when moving from site-specific calculations to regional applications as it was done here for the Swiss territory.

Keeping these uncertainty ranges in mind, the following scenarios were defined in the sensitivity analysis:

- Standard run: These are the results presented in chapter 4.3 for the year 2020; those maps are considered as "best available" maps reflecting the current state of knowledge.
- CLN+30: All critical load values are increased by 30%.
- CLN-30: All critical load values are decreased by 30%.
- Dep-30: All deposition values are decreased by 30%.
- Dep+30: All deposition values are increased by 30%.

The outcome of the sensitivity analysis (expressed as percentage of exceeded ecosystem area) is shown in Table 16: For raised bogs and forests, the range of the exceedances is quite narrow in all scenarios (63%–100%), i.e. the magnitude of the exceedance is generally higher than the supposed uncertainties and therefore the reliability of the exceedance maps is very high. The range for dry grassland (TWW) is much wider (12%–76%), i.e. the prediction of exceedances is less reliable for this ecosystem. Nevertheless, a relevant part of the protected dry grasslands still exhibits an exceedance in scenario Dep-30 (minus 30% deposition). For fens, the range of exceedance is in between (33%–88%).

Table 16: Exceedance of critical loads of nutrient nitrogen for the standard run and four scenarios of the sensitivity analysis. Units: percent of total ecosystem area.

Ecosystem	CLN +30%	Standard 2020	CLN -30%
Raised bogs	88%	94%	100%
Fens	45%	74%	88%
Dry grassland (TWW)	20%	42%	76%
Forest	72%	87%	96%
Ecosystem	**Deposition -30%**	**Standard 2020**	**Deposition +30%**
Raised bogs	85%	94%	99%
Fens	33%	74%	85%
Dry grassland (TWW)	12%	42%	68%
Forest	63%	87%	94%

The reliability of the deposition model results was shown by independent deposition measurements. In 1992/1993 Neftel & Wanner (1994) carried out comprehensive field measurements on a meadow at Merenschwand (rural area of the Swiss Central Plateau) and found a total N deposition of 27–30 kg N ha^{-1} a^{-1} (depending on the measurement method for NH_3). This is in agreement with the temporally interpolated result of the deposition models 1990 and 2000 for the same site (30 kg N ha^{-1} a^{-1}).

The modelled depositions (version by Rihm & Künzle 2019) were also compared at 17 forest sites with independent throughfall measurements by Thimonier et al. (2019). They showed that the total N deposition modelled for forest stands produced similar results as the canopy budget model, which was based on the throughfall values.

4.5 Maps for the time series 1990–2020

For the years 1990, 2000, 2005, 2010 and 2015 updated maps of ammonia concentration, total N deposition and (maximum) exceedances of critical loads per raster cell (1x1 km^2) were produced, see Annex D. They were published together with the new maps for 2020 on the internet [13].

[13] https://www.bafu.admin.ch/bafu/en/home/topics/air/state/data/historical-data/maps-of-annual-values.html [29.03.2023]

5 Conclusions

This report provides an overall view of atmospheric nitrogen deposition in Switzerland. Maps of critical loads of nitrogen and their exceedances were produced for whole Switzerland by combining data on the sensitivity of ecosystems and on atmospheric nitrogen deposition, consequently applying the critical load concept and the mapping methods proposed by the ICP Modelling & Mapping under the UNECE Convention on Long-range Transboundary Air Pollution (CLRTAP 2017). Since the last report on critical loads (Rihm & Künzle 2019) the reliability of critical loads, modelled nitrogen depositions and critical load exceedances was improved, mainly by refining empirical critical loads under the Convention, and by updating the deposition model for all nitrogen compounds.

In 2020, the atmospheric nitrogen deposition ranged from 2 kg N ha^{-1} a^{-1} (1 percentile) to 43 kg N ha^{-1} a^{-1} (99 percentile) with an overall average of 14.4 kg N ha^{-1} a^{-1}. Compared to the natural deposition, which is estimated to be around 1–2 kg N ha^{-1} a^{-1} (Pardo et al. 2011, Bertills & Näsholm 2000), present deposition loads are almost one order of magnitude higher. This causes the exceedance of the critical loads for nitrogen for most forested areas and many (semi-)natural ecosystems in Switzerland. Hence, the present nitrogen depositions do not meet the target of sustainability in large areas, as they are beyond the ecologically safe limit. The situation is better for (sub-)alpine grassland, alpine scrub habitats and forests in the inner-alpine valleys (Valais, Grisons), where the critical loads are not exceeded or where the areas with exceedance have diminished since 1990.

In the long term, the exceedances of critical loads indicate potential risks for forests such as changes in nutrient conditions, growth disturbances, increased susceptibility to gales, drought, insect pests and pathogens and decreased biodiversity of the ground flora. For (semi-)natural ecosystems, exceedances indicate primarily a potential risk for changes in competitive relationships between species, resulting in loss of biodiversity. The critical load approach does not allow precise quantification of those risks, but one can say that they are potentially more severe the higher the exceedance is and the longer it lasts. Harmful effects on sensitive ecosystems are manifold and have been shown by various studies based on experiments and field observations (Bobbink et al. 2022), also in Switzerland, for example: Mitchel et al. 2002, Bassin et al. 2013, Roth et al. 2013, Roth et al. 2015, Waldner et al. 2015, de Witte et al. 2017, Braun et al. 2020a, Braun et al. 2020b, Roth et al. 2021.

In order to improve the situation, it is necessary to further reduce the emissions of air pollutants from agricultural activities (NH_3) and from combustion processes (NO_x). As the transboundary fluxes of nitrogen compounds are substantial, the control strategies and targets must continuously be coordinated among the European countries under the UNECE Convention on Long-Range Transboundary Air Pollution. In addition, critical loads (and critical levels) can also be applied in local evaluations to assess compliance of projects in the context of national legislation,

cantonal air pollution control action plans (BAFU 2020) or environmental impact studies.

A References

Achermann B., Bobbink R. (eds.), 2003: Empirical Critical Loads for Nitrogen, Expert Workshop Berne, 11-13 November 2002. Published by: Swiss Agency for the Environment, Forests and Landscape (SAEFL), Environmental Documentation No. 164, Air. Berne. https://www.bafu.admin.ch/bafu/en/home/topics/air/publications-studies/publications/empirical-critical-loads-for-nitrogen.html [19.08.2022]

Achermann B., Rihm B., Kurz D., 2007: National Focal Centre Report – Switzerland. In: Slootweg et al. 2007 (CCE Progress Report). p. 174-179. https://www.umweltbundesamt.de/en/cce-status-reports [20.09.2022]

Achermann B., Meier R., Rihm B., Kurz D., Braun S., Kohli L., Roth T., 2015: National Focal Centre Report – Switzerland. In: Slootweg et al. 2015 (CCE Status Report). p. 141-153. https://www.umweltbundesamt.de/en/cce-status-reports [24.08.2022]

Aksoyoglu, S., Tinguely M., 2018: Deposition velocities of nitrogen compounds in Switzerland. BAFU Project: 06.9115.PZ/0464-1294, internal report. Paul Scherrer Institute PSI, Villigen, Switzerland.

Alveteg M., Kurz D., Becker R. (2002) Incorporating nutrient content elasticity in the MAKEDEP model. Sustainable Forestry in Temperate Regions – Proceedings from the SUFOR International Workshop, April 7-9, 2002, Lund, Sweden. Reports in Ecology and Environmental Engineering 1:2002: 52-67.

Asman W.A.H. and van Jaarsveld H.A., 1990: A Variable-resolution Statistical Transport Model Applied for Ammonia and Ammonium, National Institute of Public Health and Environmental Protection (RIVM), Bilthoven, The Netherlands.

Asman W.A.H. and van Jaarsveld H.A., 1992: A variable-resolution transport model applied for NHx in Europe. Atmospheric Environment Vol. 26A, No. 3, 445-464.

BAFU (Hrsg.) 2020: Übermässigkeit von Stickstoff-Einträgen und Ammoniak-Immissionen. Bewertung anhand von Critical Loads und Critical Levels insbesondere im Hinblick auf einen kantonalen Massnahmenplan Luftreinhaltung. Bundesamt für Umwelt, Bern. Umwelt-Vollzug Nr. 2003: 23 S. http://www.bafu.admin.ch/uv-2003-d [14.03.2023]

BAFU, 2022: NABEL – Luftqualität 2021. Messresultate des Nationalen Beobachtungsnetzes für Luftfremdstoffe (NABEL) [Results of the National Air Pollution Monitoring Network]. Bundesamt für Umwelt, Bern. Umwelt-Zustand Nr. 2114. http://www.bafu.admin.ch/uz-2114-d [06.01.2023]

BAFU/WSL, 2021: Waldmischungsgrad LFI (Forest mix rate NFI). Raster data set with 10 m resolution. https://data.geo.admin.ch/ch.bafu.landesforstinventar-waldmischungsgrad [19.12.2022]

Barbieri A., and Pozzi S., 2001: Acidifying deposition, Southern Switzerland. Environmental Documentation - Air, Vol. 134, Swiss Agency for the Environment, Forests and Landscape (SAEFL), Bern, 113 p.

Bassin S., Volk M., Fuhrer J., 2013: Species composition of subalpine grassland is sensitive to nitrogen deposition, but not to ozone, after seven years of treatment. Ecosystems. 16, (6), 2013, 1105-1117. http://link.springer.com/article/10.1007%2Fs10021-013-9670-3 [28.03.2023]

Bertills U., Näsholm T. (eds.), 2000: Effects of Nitrogen Deposition on Forest Ecosystems. Swedish Environmental Protection Agency. Report 5067.

Bobbink R., Hettelingh J.-P. (eds.), 2011: Review and revision of empirical critical loads and dose-response relationships. Proceedings of an expert workshop held from 23-25 June 2010 in Noordwijkerhout, The Netherlands. Coordination Centre for Effects, National Institute for Public Health and the Environment (RIVM), Bilthoven, The Netherlands. RIVM report 680359002. ISBN 978-90-6960-251-6. https://www.umweltbundesamt.de/en/further-cce-reports [19.08.2022]

Bobbink R., Loran C., Tomassen H., (eds.) 2022: Review and revision of empirical critical loads of nitrogen for Europe. Results of the UNECE expert workshop on empirical critical loads in Berne, Switzerland, 26-28 October 2021. On behalf of the German Environment Agency / Coordination Centre for Effects (CCE). https://www.umweltbundesamt.de/publikationen/review-revision-of-empirical-critical-loads-of [06.12.2022]

Bonjour C., Kupper T. 2017: Stratified emission factors for 24 animal categories, emission stages and farm classes; results from the Agrammon-project. Pers. comm. Cyrill Bonjour and Thomas Kupper, HAFL Zollikofen, 20.11.2017.

Bosshard A., 2015: Rückgang der Fromentalwiesen und die Auswirkungen auf die Biodiversität. Agrarforschung Schweiz 6 (1): 20–27. http://www.agrarforschungschweiz.ch/artikel/2015_01_2033.pdf [23.12.2022]

Braun S., Tresch S., Augustin S., 2020a: Soil solution in Swiss forest stands: A 20 year's time series, PLoS ONE 15(7): e0227530. https://doi.org/10.1371/journal.pone.0227530

Braun S., Schindler C., Rihm B., 2020b: Foliar nutrient concentrations of European Beech in Switzerland: relations with nitrogen deposition, ozone, climate and soil chemistry. Front. For. Glob. Change 3:33. https://www.frontiersin.org/articles/10.3389/ffgc.2020.00033/full [28.03.2023]

Brümmer C., Schrader F., Wintjen P., Zöll U., and Schaap M., 2020: FORESTFLUX – Improvement of assessment tools for policy advice through local validation of atmospheric pollution modelling, in German, UBA Texte 40/2020, Umweltbundesamt, Dessau-Roßlau. https://www.umweltbundesamt.de/publikationen/forestflux-standoertliche-validierung-der

Brümmer C., Rüffer J.J., Delorme J.-P., Wintjen P., Schrader F., Beudert B., Schaap M., Ammann C., 2022: Reactive nitrogen fluxes over peatland and forest ecosystems using micrometeorological measurement techniques. Earth Syst. Sci. Data, 14, 743–761. https://doi.org/10.5194/essd-14-743-2022

Butler T., Vermeylen F., Lehmann C.M, Likens G.E., Puchalski M., 2016: Increasing ammonia concentration trends in large regions of the USA derived from the NADP/AMoN network. Atmospheric Environment 146 (2016) 132–140. https://doi.org/10.1016/j.atmosenv.2016.06.033

Chytry M. et al., 2020: EUNIS Habitat Classification: Expert system, characteristic species combinations and distribution maps of European habitats. https://doi.org/10.21256/zhaw-20531 [19.08.2022]

CLRTAP, 2017. Manual on methodologies and criteria for modelling and mapping critical loads and levels and air pollution effects, risks and trends. UNECE Convention on Long-range Transboundary Air Pollution; accessed [18.08.2022] at http://www.icpmapping.org [14.03.2023]

Delarze R., Gonseth Y., Galland P., 2008: Lebensräume der Schweiz. Ott Verlag, Bern. 424 p.

De Vries W., Hettelingh J.-P., Posch M. (eds), 2015: Critical Loads and Dynamic Risk Assessments: Nitrogen, Acidity and Metals in Terrestrial and Aquatic Ecosystems. Environmental Pollution Series Vol. 25, Springer Science+Business Media, Dordrecht, xxviii+662 pp.; ISBN 978-94-017-9507-4; DOI: 10.1007/978-94-017-9508-1 http://www.springer.com/environment/pollution+and+remediation/book/978-94-017-9507-4 [01.03.2023]

De Witte L.C., Rosenstock N.P., van der Linde S., Braun S., 2017: Nitrogen deposition changes ectomycorrhizal communities in Swiss beech forests, Science of the Total Environment 605-606 (2017) 1083-1096. https://pubmed.ncbi.nlm.nih.gov/28715856 [28.03.2023]

Duyzer J.H., Fowler D., 1994: Modelling land atmosphere exchange of gaseous oxides of nitrogen in Europe. Tellus 46B, 353-372.

Duyzer J.H., 1994: Dry deposition of ammonia and ammonium aerosols over heathland. Journal of Geophysical Research 991 No D9, 18757-18764.

EAFV, 1988: Schweizerisches Landesforstinventar, Ergebnisse der Erstaufnahme 1982-1986 [Swiss National Forest Inventory]. Eidgenössische Anstalt für das forstliche Versuchswesen (today WSL), Bericht Nr. 305, Birmensdorf. http://www.lfi.ch/index-en.php [20.09.2022]

Eggenberg S., Dalang T., Dipner M., Mayer C., 2001: Kartierung und Bewertung der Trockenwiesen und –weiden von nationaler Bedeutung. Technischer Bericht. Herausgegeben vom Bundesamt für Umwelt, Wald und Landschaft (BUWAL), Bern. Schriftenreihe Umwelt Nr. 325. https://www.bafu.admin.ch/bafu/de/home/themen/biodiversitaet/publikationen-studien/publikationen/kartierung-und-bewertung-trockenwiesen.html [24.08.2022]

EKL, 2014: Ammoniak-Immissionen und Stickstoffeinträge, Abklärungen der EKL zur Beurteilung der Übermässigkeit. Eidgenössische Kommission für Lufthygiene EKL. https://www.ekl.admin.ch/de/dokumentation/publikationen [22.12.2022]

Fangmeier A., Hadwiger-Fangmeier A., Van der Erden L., Jäger H.-J., 1994: Effects of Atmospheric Ammonia on Vegetation – a Review. Environmental Pollution 86, 43-82.

Flechard C. R., Nemitz E., Smith R. I., Fowler D., Vermeulen A. T., Bleeker A., Erisman J. W., Simpson D., Zhang L., Tang Y. S., Sutton M. A., 2011: Dry deposition of reactive nitrogen to European ecosystems: a comparison of inferential models across the NitroEurope network. Atmos. Chem. Phys., 11, 2703–2728. https://doi.org/10.5194/acp-11-2703-2011 [22.09.2022]

Flechard C. R., Ibrom A., Skiba U. M., de Vries W., van Oijen M., Cameron D. R., Dise N. B., Korhonen J. F. J., Buchmann N., Legout A., Simpson D., Sanz M. J., Aubinet M., Loustau D., Montagnani L., Neirynck J., Janssens I. A., Pihlatie M., Kiese R., Siemens J., Francez A.-J., Augustin J., Varlagin A., Olejnik J., Juszczak R., Aurela M., Berveiller D., Chojnicki B. H., Dämmgen U., Delpierre N., Djuricic V., Drewer J., Dufrêne E., Eugster W., Fauvel Y., Fowler D., Frumau A., Granier A., Gross P., Hamon Y., Helfter C., Hensen A., Horváth L., Kitzler B., Kruijt B., Kutsch W. L., Lobo-do-Vale R., Lohila A., Longdoz B., Marek M. V., Matteucci G., Mitosinkova M., Moreaux V., Neftel A., Ourcival J.-M., Pilegaard K., Pita G., Sanz F., Schjoerring J. K., Sebastià M.-T., Tang Y. S., Uggerud H., Urbaniak M., van Dijk N., Vesala T., Vidic S., Vincke C., Weidinger T., Zechmeister-Boltenstern S., Butterbach-Bahl K., Nemitz E., and Sutton M. A., 2020: Carbon–nitrogen interactions in European forests and semi-natural vegetation – Part 1: Fluxes and budgets of carbon, nitrogen and greenhouse gases from ecosystem monitoring and modelling. Biogeosciences, 17, 1583–1620, 2020, https://doi.org/10.5194/bg-17-1583-2020

FOAG 2017a: Anonymized delivery receipts for the manure shipments in 2015; extract from the HODUFLU database. Federal Office for Agriculture (FOAG), Bern. https://www.blw.admin.ch/blw/de/home/politik/datenmanagement/agate/hoduflu.html [21.12.2022]

FOAG 2017b: Location of alpine summering farms in 2015; extract from the AGIS-database. Federal Office for Agriculture (FOAG), Bern. https://www.blw.admin.ch/blw/de/home/instrumente/direktzahlungen/voraussetzungen-begriffe/soemmerungsbetriebe.html [21.12.2022]

FOAG 2021: Boundaries of agricultural zones in Switzerland. Federal Office for Agriculture (FOAG), Bern. https://www.blw.admin.ch/blw/de/home/politik/datenmanagement/geografisches-informationssystem-gis/landiwirtschaftliche-zonengrenzen.html [20.12.2022]

FOEFL, 1996: Critical Loads of Nitrogen and their Exceedances - Eutrophying Atmospheric Deposition. Federal Office of Environment, Forests and Landscape (FOEFL), Berne. Environmental Series Air No. 275. 84p. Out of print.

FOEN, 2011: NO2 ambient concentrations in Switzerland. Modelling results for 2005, 2010, 2015. Federal Office for the Environment, Bern. Environmental studies no. 1123: 68 pp. http://www.bafu.admin.ch/publikationen/publikation/01634/index.html?lang=en [20.11.2016]

FOEN 2013: Jahrbuch Wald und Holz 2013. Umwelt-Zustand Nr. 1332. [Annuals Forest and Wood 2013]. Federal Office for the Environment, Bern. http://www.bafu.admin.ch/publikationen/publikation/01743/index.html?lang=de&show_kat=/publikationen [20.09.2022]

FOEN, 2013: PM10 and PM2.5 ambient concentrations in Switzerland. Modelling results for 2005, 2010 and 2020. Federal Office for the Environment, Bern. Environmental studies no. 1304: 83 pp. https://www.bafu.admin.ch/bafu/en/home/topics/air/publications-studies/publications/pm10-and-pm2-5-ambient-concentrations-in-switzerland.html [22.12.2022]

FOEN, 2017: National Focal Centre Report – Switzerland. In: Hettelingh et al. 2017 (CCE Final Report). p. 177-190. https://www.umweltbundesamt.de/en/cce-status-reports [24.08.2022]

FOEN (ed.) 2017b: Switzerland's Informative Inventory Report 2017 (IIR) – Submission under the UNECE Convention on Long-range Transboundary Air Pollution. https://www.ceip.at/status-of-reporting-and-review-results/2017-submissions [22.12.2022]

FOEN, 2021: Switzerland's Informative Inventory Report 2021 (IIR), Submission under the UNECE Convention on Long-range Transboundary Air Pollution, Submission of March 2021 to the United Nations ECE Secretariat. Federal Office for the Environment, Bern. https://t1p.de/FOEN2021b [19.08.2022]

Franzaring J., Kösler J., 2022: Review of internationally proposed critical levels for ammonia. Proceedings of an Expert Workshop held in Dessau and online on 28/29 March 2022, prepared by the CCE and the German Environment Agency (UBA). Conference Background Document, final draft. https://www.umweltbundesamt.de/sites/default/files/medien/4038/dokumente/review_of_critical_levels_for_nh3.pdf [10.03.2023]

Grange S.K., Sintermann J., Hueglin C., 2023 (submitted): Sensitivity of atmospheric ammonia (NH_3) trends on meteorology and secondary particulate matter. Environmental Science and Technology.

Hegg O., Béguin C., Zoller H., 1993: Atlas schutzwürdiger Vegetationstypen der Schweiz [Atlas of Vegetation Types Worthy of Protection in Switzerland]. Edited by Federal Office of Environment, Forests and Landscape (BUWAL), Berne.

Heldstab J., Schäppi B., Künzle T., 2020: Immissionen Schweiz und Liechtenstein, Modellresultate NO_2, PM10, PM2.5 für 2015, 2020, 2030. INFRAS und Meteotest im Auftrag des Bundesamtes für Umwelt (BAFU). https://www.bafu.admin.ch/dam/bafu/de/dokumente/luft/externe-studien-berichte/no2-pm10-pm2-5-immissionen-schweiz-liechtenstein-aktualisierung-des-pollumap-modells-fuer-2015-2020-und-2030.pdf.download.pdf/PolluMap_Technischer-Bericht.pdf, https://www.bafu.admin.ch/dam/bafu/de/dokumente/luft/externe-studien-berichte/immissionen-schweiz-und-liechtenstein-modellresultate-no2-pm10-pm2-5-2015-2020-2030.pdf.download.pdf/PolluMap-Resultate-Bericht.pdf [23.03.2023]

Heldstab J., Schäppi B., Künzle T., 2021: Emissionskataster Schweiz 2015; Treibhausgase und Luftschadstoffe. INFRAS und Meteotest im Auftrag des Bundesamtes für Umwelt (BAFU). https://www.bafu.admin.ch/dam/bafu/de/dokumente/klima/externe-studien-berichte/emissionskataster-schweiz-2015-treibhausgase-und-luftschadstoffe.pdf.download.pdf/Emissionskataster-Treibhausgase_Infras.pdf [23.03.2023]

Hertel O., Skjøth C. A., Løfstrøm P. et al., 2006: Modelling nitrogen deposition on a local scale: a review of the current state of the art. Environmental Chemistry, 3, 317–337.

Hesterberg R., Blatter M., Fahrni M., Rosset M., Neftel A., Eugster W., Wanner H., 1996: Deposition of Nitrogen-containing Compounds to an Extensively Managed Grassland in Central Switzerland. Environmental Pollution Vol. 91, No. 1, 21-34.

Hettelingh J.-P., Posch M., Slootweg J. (eds.), 2017: European critical loads: database, biodiversity and ecosystems at risk, CCE Final Report 2017, Coordination Centre for Effects, RIVM Report 2017-0155, Bilthoven, Netherlands. https://www.umweltbundesamt.de/en/cce-status-reports [24.08.2022]

Hornung M., Sutton M.A., Wilson R.B. (eds.), 1995: Mapping and modelling of critical loads for nitrogen. Report of a workshop held at Grange-over-Sands, Cumbria, UK under the auspices of the UN-ECE Convention on Long Range Transboundary Air Pollution, Working Group for Effects, 24–26 October 1994. Organised by the UK Department of Environment and hosted by the Institute of Terrestrial Ecology (Merlewood). 207p.

Hüglin C., Grange S.K., 2021: Chemical characterisation and source identification of PM10 and PM2.5 in Switzerland. Project Report, Swiss Federal Laboratories for Materials Science and Technology (Empa), Dübendorf, on behalf of the Federal Office for the Environment (FOEN). https://www.bafu.admin.ch/dam/bafu/de/dokumente/luft/externe-studien-berichte/chemical-characterisation-and-source-identification-of-pm-in-switzerland.pdf.download.pdf/Characterisation-source-identification-PM.pdf [23.03.2023]

Hunziker C., 2022: Digital data of the Federal Inventories of Fenlands and of Dry Grassland of National Importance, including vegetation data. Pers. comm., on behalf of the Federal Office for the Environment (FOEN).

Hürdler J., Prasuhn V., Spiess E., 2015: Abschätzung diffuser Stickstoff- und Phosphoreinträge in die Gewässer der Schweiz – MODIFFUS 3.0. Agroscope, im Auftrag des Bundesamtes für Umwelt (BAFU). https://www.agroscope.admin.ch/agroscope/en/home/topics/environment-resources/soil-bodies-water-nutrients/landwirtschaftlicher-gewaesserschutz/modiffus.html [20.12.2022]

Hutchings C., 2021: Net nitrogen fluxes per zip-code caused by manure transport in 2020; calculations based on the HODUFLU data base of the Federal Office for Agriculture FOAG. Pers. comm. by Catherine Hutchings (Agroscope) to Beat Rihm (Meteotest AG), 21.12.2021.

Hutchings C., Spiess E., Prasuhn V., 2023: Abschätzung diffuser Stickstoff- und Phosphoreinträge in die Gewässer der Schweiz mit MODIFFUS 3.1, Stand 2020. Agroscope Science (in Vorbereitung).

INFRAS 2017: Swiss ammonia emissions 2015 from transportation, results of a link-based traffic model. Pers. comm. by B. Notter, 31.08.2017.

Kupper T., Bonjour C., Achermann B., Rihm B., Zaucker F., Menzi H., 2013: Ammoniakemissionen in der Schweiz 1990-2010 und Prognose bis 2020. Hochschule für Agrar-, Forst- und Lebensmittelwissenschaften (HAFL), im Auftrag des Bundesamts für Umwelt (BAFU), Mai 2013.

Kupper T., Häni C., 2021: Stratified emission factors for 24 animal categories, emission stages and 40 farm classes; results from the Agrammon-project. Pers. comm. Thomas Kupper, HAFL Zollikofen, 26.11.2021.

Kupper T., Häni C., Bretscher D., Zaucker F. 2022: Ammoniakemissionen der schweizerischen Landwirtschaft 1990 bis 2020. Bericht im Auftrag des BAFU. https://agrammon.ch/de/downloads/ [19.12.2022]

Kurz D., Posch M., 2015: Revising Critical Loads of Acidity for Forsts in Switzerland for the Call for Data 2014/15. Interim Report, EKG Geo-Science (Bern) and Coordination Centre for Effects (RIVM, Bilthoven/NL).

Loubet B., Asman W.A.H., Theobald M.R., Hertel O., Tang Y.S., Robin P., Hassouna M., Dämmgen U., Genermont S., Cellier P., Sutton M.A., 2009: Ammonia Deposition Near Hot Spots: Processes, Models and Monitoring Methods. In: Atmospheric Ammonia. Detecting Emissions Changes and Environmental Impacts, edited by: Sutton, M. A., Reis, S., and Baker, S. M., Springer, Dordrecht, the Netherlands, 205–267, https://doi.org/10.1007/978-1-4020-9121-6_15

Lövblad G. and Erisman J.W., 1992: Deposition of Nitrogen in Europe. In: Grennfelt P. and Thörnelöf E. (eds.): Critical Loads for Nitrogen – report from a workshop held in Lökeberg, Sweden, 6-10 April 1992. Organized by the Nordic Council of Ministers in collaboration with the Convention on Long-range Transboundary Air Pollution. Nord 1992:41. 430pp.

Lövblad G., Erisman J.W., Fowler D., 1993: Models and Methods for the Quantification of Atmospheric Input to Ecosystems. ISBN 92 9120 2533, Nordic Council of Ministers, Store Strandstraede 18, DK-1255 Copenhagen.

MeteoSwiss 2022: Supply of annual precipitation maps 2018–2021, 1x1 km^2 resolution. https://www.meteoswiss.admin.ch/home/services-and-publications/produkte.subpage.html/en/data/products/2014/raeumliche-daten-niederschlag.html [22.09.2022]

Mitchell E.A.D., Buttler A., Grosveriner P., Rydin H., Siegenthaler A., Gobat J-M., 2002: Contrasted effects of increased N and CO2 supply on two keystone species in peatland restoration and implications for global change, Journal of Ecology 90, issue 3, 529-533. https://besjournals.onlinelibrary.wiley.com/doi/full/10.1046/j.1365-2745.2002.00679.x [28.03.2023]

NABEL 2022: Supply of annual pollutant concentration and deposition in precipitation 2000–2021 from the National Air Pollution Monitoring Network for (NABEL). Pers. comm.

17.06.2022, Federal Office for the Environment, Bern. https://www.bafu.admin.ch/bafu/en/home/topics/air/state/data/national-air-pollution-monitoring-network--nabel-.html [22.09.2022]

Neftel A., Wanner H., 1994: Stickstoffeintrag aus der Luft in ein Naturschutzgebiet. Ed.: Bundesamt für Umwelt, Wald und Landschaft (BUWAL), Umwelt-Materialien Nr. 28. Bern.

Nilsson, J., and Grennfelt, P. (eds.) 1988. Critical loads for sulphur and nitrogen. Report from a workshop held at Skokloster, Sweden, 19-24 March 1988. Miljørapport 15, Nordic Council of Ministers, Copenhagen, 418p.

Nussbaum M., Burgos S. 2021: Soil organic carbon stocks in forests of Switzerland: Update of soil organic carbon stock estimation for the national greenhouse gas inventory. Bern University of Applied Sciences, School for Agricultural, Forestry and Food Sciences (BFH-HAFL), Zollikofen. Commissioned by the Federal Office for the Environment FOEN, Bern. http://www.climatereporting.ch

Pardo L.H., Fenn M.E., Goodale C.L., Geiser L.H. et al., 2011: Effects of nitrogen deposition and empirical nitrogen critical loads for ecoregions of the United States. Ecological Applications 21(8), 3049-3082.

Posch M., Eggenberger U., Kurz D., Rihm B., 2007: Critical Loads of Acidity for Alpine Lakes. A weathering rate calculation model and the generalized First-order Acidity Balance (FAB) model applied to Alpine Lake catchments. Environmental studies no. 0709. Federal Office for the Environment, Berne. 69 p. https://www.bafu.admin.ch/bafu/de/home/themen/wasser/publikationen-studien/publikationen-wasser/critical-loads-of-acidity-for-alpine-lakes.html [24.08.2022]

Reiss D., Rihm B., Thöni C., Faller M., 2004: Mapping Stock at Risk and Release of Zinc and Copper in Switzerland – Dose Response Functions for Runoff Rates derived from Corrosion Rate Data. Water, Air, and Soil Pollution, 159, 101-113.

Riedmann A., Hertz J., 1991: Ergänzende Betrachtungen zum Gesamteintrag von Schadstoffen in den Wald des Kantons Zürich. Forschungsstelle für Umweltbeobachtung, WSL, Birmensdorf.

Rihm B., Kurz D., 2001: Deposition and Critical Loads of Nitrogen in Switzerland. Water, Air and Soil Pollution, 130, 1223-1228.

Rihm B., Achermann B. 2016: Critical Loads of Nitrogen and their Exceedances. Swiss contribution to the effects-oriented work under the Convention on Long-range Transboundary Air Pollution (UNECE). Federal Office for the Environment, Bern. Environmental Studies no. 1642: 78p. https://www.bafu.admin.ch/bafu/en/home/topics/air/publications-studies/publications/Critical-Loads-of-Nitrogen-and-their-Exceedances.html [22.12.2022]

Rihm B., Künzle T., 2019: Mapping Nitrogen Deposition 2015 for Switzerland. Technical Report on the Update of Critical Loads and Exceedance, including the years 1990, 2000,

2005 and 2010. Meteotest, Bern, commissioned by the Federal Office for the Environment (FOEN). https://www.bafu.admin.ch/bafu/en/home/topics/air/publications-studies/studies.html [22.09.2022]

Roth T., Kohli L., Rihm B., Achermann B., 2013: Nitrogen deposition is negatively related to species richness and species composition of vascular plants and bryophytes in Swiss mountain grassland. Agriculture, Ecosystems & Environment, 178, 121–126. https://doi.org/10.1016/j.agee.2013.07.002

Roth T., Kohli L., Rihm B., Amrhein V., Achermann B., 2015: Nitrogen deposition and multi-dimensional plant diversity at the landscape scale. Royal Society Open Science 2: 150017. http://dx.doi.org/10.1098/rsos.150017

Roth T., Kohli L., Rihm B., Meier R., Amrhein V.: 2021, Negative effects of nitrogen deposition on Swiss butterflies, Conservation Biology 2021;1–11. https://doi.org/10.1111/cobi.13744

Schöpp W, Posch M, Mylona S, Johansson M. 2003. Long-term development of acid deposition (1880–2030) in sensitive freshwater regions in Europe. Hydrol. Earth. Syst. Sci. 7, 436–446. https://sci-hub.se/10.5194/hess-7-436-2003 [19.08.2022]

Schrader F., Brümmer C., 2014: Land Use Specific Ammonia Deposition Velocities: a Review of Recent Studies (2004–2013). Water Air Soil Pollut (2014) 225:2114. DOI 10.1007/s11270-014-2114-7

Seitler E., Thöni L., Meier M., 2016: Atmosphärische Stickstoff-Deposition in der Schweiz, 2000 bis 2014. FUB – Forschungsstelle für Umweltbeobachtung, Rapperswil. https://www.bafu.admin.ch/bafu/de/home/themen/luft/publikationen-studien/studien.html [22.09.2022]

Seitler E., Meier M., Ehrenmann Z., 2021: Atmosphärische Stickstoff-Deposition in der Schweiz 2000 bis 2019. FUB – Forschungsstelle für Umweltbeobachtung, Rapperswil. 131 S. https://www.bafu.admin.ch/bafu/de/home/themen/luft/publikationen-studien/studien.html [22.09.2022]

Seitler E. 2022: Ammonia concentrations measured with passive samplers in Switzerland, 2018–2021. Pers. comm. by Eva Seitler, Forschungsstelle für Umweltbeobachtung (FUB, Rapperswil) to Beat Rihm (Meteotest, Bern), 25.3.2022.

Seitler E., Meier M., 2022. Ammoniak-Immissionsmessungen in der Schweiz 2000 bis 2021, Messbericht. Forschungsstelle für Umweltbeobachtung (FUB). Im Auftrag des Bundesamtes für Umwelt (BAFU), der OSTLUFT (AI, AR, GL, GR, SG, SH, TG, ZH, FL), der inNET (LU, NW, OW, SZ, UR, ZG), und der Kantone AG, BE, BL/BS, FR, NE, SO. https://www.bafu.admin.ch/bafu/de/home/themen/luft/publikationen-studien/studien.html [19.08.2022]

SFSO, 2000: Digital soil map 1:200'000 ("Bodeneignungskarte", BEK). Swiss Federal Statistical Office, GEOSTAT, Neuchâtel. https://www.bfs.admin.ch/bfs/de/home/dienstleistungen/geostat/geodaten-bundesstatistik/boden-nutzung-

bedeckung-eignung/abgeleitete-und-andere-daten/bodeneignungskarte-schweiz.html [20.09.2022]

SFSO 2004: Forest composition in Switzerland; mixing ratio of coniferous and deciduous trees, hectare raster (Waldmischungsgrad). Swiss Federal Statistical Office, GEOSTAT, Neuchâtel. https://www.bfs.admin.ch/bfs/en/home/services/geostat/swiss-federal-statistics-geodata/land-use-cover-suitability/derivative-complementary-data/forest-composition-in-switzerland.html [19.12.2022]

SFSO 2017: Livestock statistics of individual farms for 2015; database extract (Landwirtschaftliche Betriebszählungen). Swiss Federal Statistical Office (SFSO), Neuchâtel. https://www.bfs.admin.ch/bfs/de/home/statistiken/kataloge-datenbanken/medienmitteilungen.assetdetail.40797.html [22.12.2022]

SFSO 2021: Swiss Land-Use Statistics (Arealstatistik), hectare raster with 72 basic categories. Swiss Federal Statistical Office (SFSO), Neuchâtel. https://www.bfs.admin.ch/bfs/en/home/services/geostat/swiss-federal-statistics-geodata/land-use-cover-suitability/swiss-land-use-statistics.html [19.12.2022]

SFSO 2021b: Livestock statistics of individual farms; database extract from the farm structure census 2020 (Landwirtschaftliche Strukturerhebung). Swiss Federal Statistical Office (SFSO), Neuchâtel. https://www.bfs.admin.ch/bfs/en/home/statistics/catalogues-databases/press-releases.assetdetail.16984919.html [19.12.2022]

Staelens J., Wuyts K., Adriaenssens S., Van Avermaet P., Buysse H., Van den Bril B., Roekens E., Ottoy J.-P., Verheyen K., Thas O., & Deschepper E., 2012: Trends in atmospheric nitrogen and sulphur deposition in northern Belgium. Atmospheric Environment, 49, 186–196. http://dx.doi.org/10.1016/j.atmosenv.2011.11.065

Steingruber S. 2018, Acidifying Deposition in Southern Switzerland - Monitoring, maps and trends 1983-2017, Cantone Ticino, Ufficio dell'aria, del clima e delle energie rinnovabili. https://www4.ti.ch/fileadmin/DT/temi/aria/monitoraggio/Acidifying_Deposition_Southern_Switzerland_1983-2017.pdf [22.09.2022]

Steingruber S. 2022: Equations for calculating nitrogen concentration in precipitation in the Canton Ticino, 2018-2021. Pers. comm. 23.06.2022.

Sutton M.A., Asman W.A.H., Schjorring J.K., 1994: Dry deposition of reduced nitrogen. Tellus 46B, 255–273.

Swiss Confederation, 1991: Verordnung über den Schutz der Hoch- und Übergangsmoore von nationaler Bedeutung (Hochmoorverordnung) vom 21. Januar 1991 (Stand am 1. November 2017). [Ordinance on the Protection of Raised and Transitional Bogs of National Importance]. https://www.fedlex.admin.ch/eli/cc/1991/270_270_270/de [23.08.2022]

Swiss Confederation 1994: Verordnung über den Schutz der Flachmoore von nationaler Bedeutung (Flachmoorverordnung) vom 7. September 1994 (Stand am 1. Juli 2021). [Ordinance on the Protection of Fenlands of National Importance] https://www.fedlex.admin.ch/eli/cc/1994/2092_2092_2092/de [24.08.2022]

swisstopo, 2006: swissBOUNDARIES3D, administrative units and national boundaries of Switzerland and the Principality of Liechtenstein in vector form. https://www.swisstopo.admin.ch/en/geodata/landscape/boundaries3d.html [20.12.2022]

Thimonier, A., Kosonen, Z., Braun, S., Rihm, B., Schleppi, P., Schmitt, M., Seitler, E., Waldner, P., and Thöni, L., 2019: Total deposition of nitrogen in Swiss forests: Comparison of assessment methods and evaluation of changes over two decades, Atmos. Environ., 198, 335–350, https://doi.org/10.1016/j.atmosenv.2018.10.051

Thöni L., Seitler E., 2010: Stickstoff- & Elementdeposition OSTLUFT 2000 bis 2008. Forschungsstelle für Umweltbeobachtung (FUB), Rapperswil, im Auftrag von OSTLUFT. https://www.ostluft.ch/index.php?id=80 [23.12.2022]

UNECE, 2005: Technical Report of ICP Materials. UNECE Working Group on Effects, EB.AIR/WG.1/2005/7. http://www.unece.org/index.php?id=5189 - / https://unece.org/fileadmin/DAM/env/documents/2005/eb/wg1/EB.AIR.WG.1.2005.7.e.pdf [22.09.2022]

UNECE 2010: Report of the Working Group on Effects on its twenty-ninth session, Geneva, 22-24 September 2010. Executive Body for the Convention on Long-range Transboundary Air Pollution (UNECE), Working Group on Effects. ECE/EB.AIR/WG.1/2010/2.

UNECE, 2012: 1999 Protocol to Abate Acidification, Eutrophication and Ground-level Ozone to the Convention on Long-range Transboundary Air Pollution, as amended on 4 May 2012. Economic Commission for Europe, Executive Body for the Convention on Long-range Transboundary Air Pollution. ECE/EB.Air/114

van Zanten M.C., Sauter F.J., Wichink Kruit R.J., van Jaarsveld J.A., van Pul W.A.J., 2010: Description of the DEPAC module - Dry deposition modelling with DEPAC_GCN2010. RIVM Report 680180001/2010, Bilthoven, the Netherlands.

Waldner P., Thimonier A., Graf Pannatier E., and 40 more authors, Minaya M., 2015: Exceedance of critical loads and of critical limits impacts tree nutrition across Europe. Annals of Forest Science (2015) 72:929–939. https://literatur.thuenen.de/digbib_extern/dn055317.pdf [28.03.2023]

Wesley M.L. and Hicks B.B., 2000: A review of the current status of knowledge on dry deposition. Atmospheric Environment 34, 2261–2282.

WSL 1990/92: Swiss National Forest Inventory (NFI), data extracts 30 May 1990 and 8 December 1992. Swiss Federal Institute for Forest, Snow and Landscape Research, Birmensdorf. http://www.lfi.ch/index-en.php [20.09.2022]

WSL 2013: Swiss National Forest Inventory NFI, data extract 30.8.2013. Markus Huber, Swiss Federal Institute for Forest, Snow and Landscape Research (WSL), Birmensdorf. http://www.lfi.ch/index-en.php [20.09.2022]

B Glossary

Ammonia: NH_3

Ammonium: NH_4^+

Base cations: Ca^{2+}, Mg^{2+}, K^+ and Na^+.

Critical levels: "Concentrations of pollutants in the atmosphere above which adverse effects on receptors, such as human beings, plants, ecosystems or materials, may occur according to present knowledge" (CLRTAP 2017). Pollutants are in particular SO_2, NO_x (NO and NO_2), O_3 and NH_3.

Critical load: "A quantitative estimate of an exposure to one or more pollutants below which significant harmful effects on specified sensitive elements of the environment do not occur according to present knowledge" (CLRTAP 2017).

Deposition: A quantitative estimate of atmospheric input of pollutants to specified elements of the environment.

Exceedance of critical loads: (atmospheric) deposition minus critical load.

Load: atmospheric deposition of chemical compounds.
Units e.g. kg ha^{-1} a^{-1}.

Level: Concentration of chemical compounds in the atmosphere. Units e.g. µg m^{-3}.

Nitrate: NO_3^-

Nitric acid: HNO_3

Nitrogen dioxide: NO_2

Nitrogen saturation: situation in an ecosystem where the availability of inorganic nitrogen is in excess of the total combined plant and microbial nutritional demand.

C Abbreviations

AAE average accumulated exceedance

a year

a.s.l. above sea level

BDM Biodiversity Monitoring Switzerland

CCE Coordination Centre for Effects (until 2018 at RIVM, Bilthoven NL, now at Umweltbundesamt, Dessau D)

$CL_{emp}N$ Empirical critical loads of (nutrient) nitrogen

$CL_{nut}N$ Critical loads of nutrient nitrogen calculated with the SMB method

EMEP Co-operative Programme for Monitoring and Evaluation of the Long-range Transmission of Air Pollutants in Europe

f_{de} Denitrification fraction

FOEN Federal Office for the Environment, Berne

FUB Forschungsstelle für Umweltbeobachtung, Rapperswil, Switzerland

GVE livestock unit corresponding to one milk cow (Grossvieheinheit)

ha hectare

IAP Institut für angewandte Pflanzenbiologie, Witterswil, Switzerland

ICP International Cooperative Programme (under LRTAP)

ICP M&M ICP Modelling and Mapping

kt kiloton

LRTAP (Convention on) Long-range Transboundary Air Pollution

eq equivalents (=mol of charges)

NABEL Nationales Beobachtungsnetz für Luftfremdstoffe (national air pollution monitoring network)

NFC National Focal Centres for mapping activities under the Convention on LRTAP

NFI National Forest Inventory

NH_3 ammonia (gas)

NH_x reduced nitrogen compounds: NH_3 and NH_4^+

NO_y oxidised nitrogen compounds: NO_2, NO_3^- and HNO_3

N_i acceptable immobilization rate of N in soil organic matter

$N_{le(acc)}$ acceptable nitrogen leaching rate from the soil to the groundwater

N_u net nitrogen uptake by vegetation

PM10 particulate aerosols below 10 µm diameter

SFSO Swiss Federal Statistical Office

SMB Simple Mass Balance, method for calculating critical loads of nutrient nitrogen and critical loads of acidity

TWW Dry Grasslands of National Importance, National Inventory

UNECE United Nations Economic Commission for Europe

V_{dep} Effective deposition velocity, in mm s^{-1}

WGE Working Group on Effects (Convention on LRTAP)

WHO World Health Organisation, Regional Office for Europe

WSL Eidgenössische Forschungsanstalt für Wald, Schnee und Landschaft (Swiss Federal Institute for Forest, Snow and Landscape Research), Birmensdorf

µg microgram

D Annex: Time series maps

The following overview maps are shown for the years 1990, 2000, 2005, 2010, 2015 and 2020:

- Ammonia concentrations

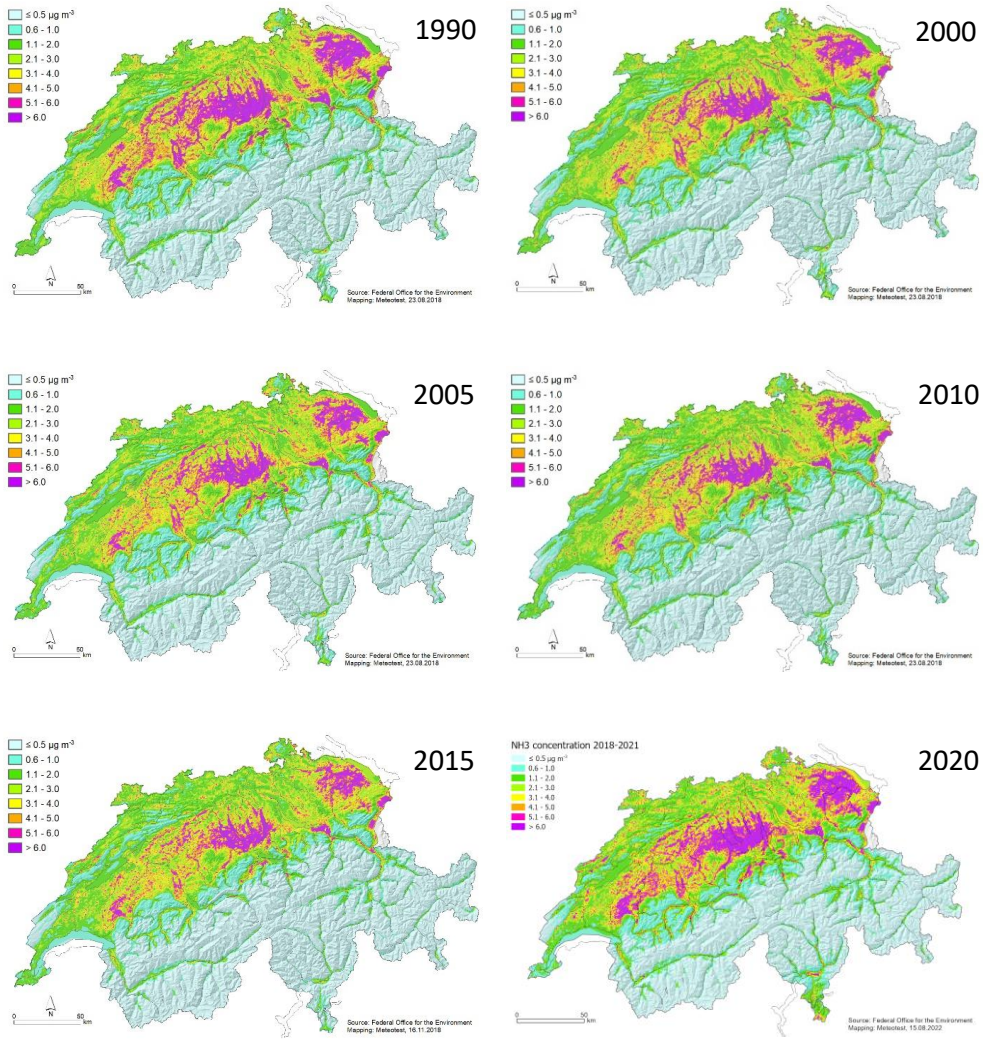

Ammonia concentration

- ≤ 0.5 µg m^{-3}
- 0.6 - 1.0
- 1.1 - 2.0
- 2.1 - 3.0
- 3.1 - 4.0
- 4.1 - 5.0
- 5.1 - 6.0
- > 6.0

- Total atmospheric nitrogen deposition

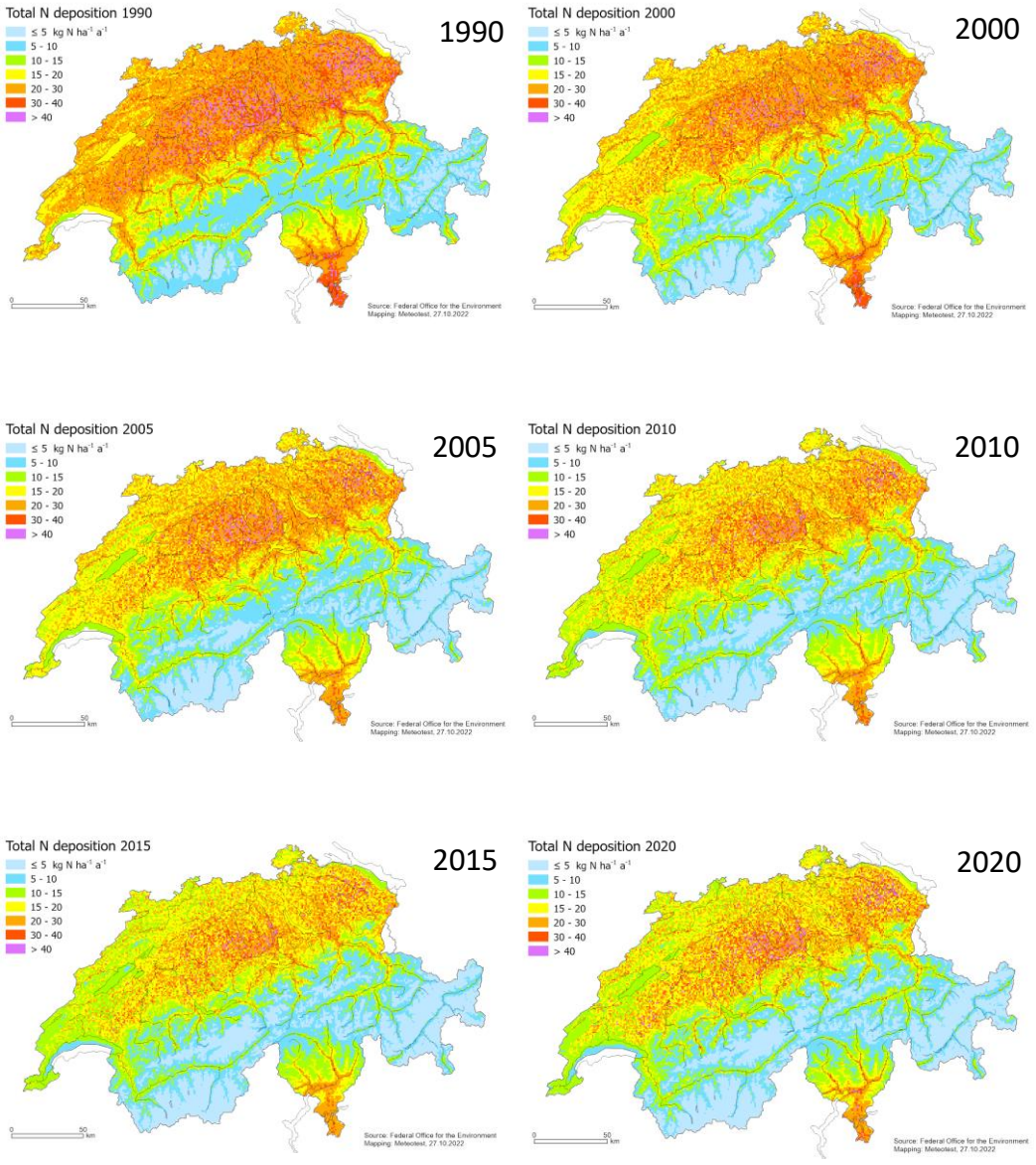

Total deposition of nitrogen

- ≤ 10 kg N ha^{-1} a^{-1}
- 10 - 15
- 15 - 20
- 20 - 30
- 30 - 40
- > 40

- Maximum exceedance of critical loads per raster cell (1x1 km^2)